Primary Driving Force in Wood Vacuum Drying

by

Zhangjing Chen

Dissertation submitted to the Faculty of the
Virginia Polytechnic Institute and State University
in partial fulfillment of the requirements for the degree of

Doctor of Philosophy

in

Wood Science and Forest Products

Approved:

Fred M. Lamb, Chairman
Frederick A. Kamke
Douglas J. Nelson
Christian Skaar
Marshall S. White

Keywords: driving force, wood vacuum drying, boiling front, room temperature drying, end grain drying

December 2, 1997
Blacksburg, Virginia

Primary Driving Force in Wood Vacuum Drying

by

Zhangjing Chen

Committee Chairman: Fred M. Lamb

(Abstract)

The objective of this research based on both the theory and experimentation was to prove that the total pressure difference is the primary driving force during the vacuum drying. The theoretical drying rates of diffusion, free water bulk flow and water vapor bulk flow were calculated and compared. The concept of equilibrium moisture content under the vacuum was developed. The theoretical maximum moisture content drop in one cycle was calculated using energy balance. The model was developed for the vacuum drying to understand the mechanism of the vacuum drying including the boiling front and its movement.

To evaluate the effect of the sample size on the drying rate, four different thicknesses (1, 1.5, 2, 2.5 inches) and three different lengths (5, 10, 15 inches) were used. In the cyclic drying, the specimens were heated to the 60°C. The vacuum was pulled to about 18 mm Hg. The vacuum pump was kept running for 140 minutes. It was found that in cyclic vacuum drying, drying rate was not affected by the thickness. However, it was affected by the length. The cyclic drying curve consisted of two distinct parts. The fast drying period lasted about 10 to 20 minutes. The slow drying period occurred next when the pressure inside wood got close to the ambient pressure.

In end grain vacuum drying, the specimens were coated with wax, wrapped in the plastic film and inserted into a rubber tube to prevent the moisture loss from the side surfaces during drying. The specimen size was 1×1×10 inches. Red oak and white oak were sealed and dried in both cyclic and continuous vacuum drying. The results showed that sealed specimens dried almost as fast as unsealed specimen. There was little moisture loss from the side surfaces. There was a moisture gradient along the length in both cyclic drying and continuous vacuum drying.

Red oak specimens of 2.5×1.5×10 inches were used to study the boiling front in the vacuum drying. In order to detect the boiling phenomenon, the saturation pressures were calculated and were

compared with the pressures at the same time and the same location. Boiling occurred during drying and the boiling front retreated to the center of wood as drying proceeded. The retreating speed depended on the heat supply and the permeability.

Vacuum drying at room temperature was investigated. The specimens were dried at 20°C and pressure near 18 mm Hg. The results showed that wood can be vacuum dried at room temperature with little or no degrade at a reasonable drying rate.

All experimental results support the objective of this study that the primary driving force is the total pressure difference.

Acknowledgment

I would like to express my deepest appreciation to my major advisor, Dr. Fred M. Lamb, for his encouragement, patience, guidance and expertise during this research. Without him, I could not have completed my education in the United States. His technical and moral supports are deeply acknowledged. My gratitude is also given to the other members of my committee, Dr. Frederick A. Kamke, Dr. Douglas J. Nelson, Dr. Christian Skaar, and Dr. Marshall S. White for their helpful suggestions and assistance with this dissertation.

I am grateful to Dr. Geza Ifju, Department head, for providing me with the opportunity to study at Virginia Tech. I would like to acknowledge the assistance of Kenneth L. Albert and Carlile H. Price for preparing samples, and the assistance of Harrison Sizemore and Robert S. Wright for setting up the experimental equipment. I appreciate the help of the many staff members at the Thomas M. Brooks Forest Products Center, especially Angela G. Riegal and Sharon C. Daley, for their exceptional assistance over the past seven years.

I am especially indebted to my wife, Haiping, for her understanding and support in this study. My thanks also are given to my parents and parent-in-laws for their caring and to my daughter, Susan, for her much joy.

Table of Contents

List of Figures

List of Tables

1. Introduction

Current vacuum drying technology has its beginning in 1962. Recently, it has gained a renewed interest in both industry and research. An increase in vacuum drying is expected in the near future, especially in Europe and Asia. In vacuum drying, lumber is placed in a tight drying chamber, and the vacuum system pulls a vacuum on the lumber. Wood is theoretically dried with moisture evaporation at low boiling temperatures (usually about 40°C). In cyclic vacuum drying, the lumber is heated intermittently by hot air convection. After the wood has reached the required temperature, a vacuum is pulled on the lumber. The drying continues until the drying rate is very small, at which time the cycle is repeated.

Many studies have been conducted on vacuum drying, from which it has been found that vacuum drying significantly shortens the drying time, especially for thick lumber, and the drying quality is usually good. Vacuum drying is often used for high valued species or for a large dimension lumber. However, little work has been done on the theoretical aspects of vacuum drying. Lack of technical information and operating procedures has reduced the utilization of this drying technology.

Bulk flow and diffusion are two forms of water transportation inside the wood. Generally, it is recognized that free water bulk flow (FWBF) controls moisture movement at moisture content (MC) above fiber saturation point (FSP) and diffusion controls the moisture movement at MC below FSP. Little is known about water vapor bulk flow (WVBF) which is driven by the total pressure difference. WVBF strongly depends on the gas permeability of wood. In vacuum drying, there is a total pressure difference within the wood. This causes mass flow of water vapor from the center to the surface. It is essential to study WVBF in vacuum drying when water movement is no longer entirely diffusion controlled. It is well documented that permeability affects the vacuum drying rate, and that wood is much more permeable in the longitudinal than in transverse directions. However, the effect of anisotropy of wood permeability on the vacuum drying has not been studied in detail. It is expected that there is a significant difference in the moisture transport between the longitudinal

and transverse directions since the ratio of hardwood longitudinal permeability to transverse permeability is usually more than 30,000. Also, there is some controversy on various issues, such as, whether water is boiling inside the wood. It is still uncertain whether most moisture is transferred in steam (vapor) or liquid form and what role the total pressure difference plays as a drying force in vacuum drying.

Drying involves the water removal and heat supply to the wood, both of which affect the vacuum drying rate. It is important to know how they function in vacuum drying. This will help understand the influence of the thickness and length of specimen on the drying rate. It is unknown how much of water is transferred longitudinally and removed from the end grain surface during vacuum drying. Vacuum drying is fast and the drying rate is determined by the heat supply which in turn is controlled by the ambient temperature. The higher the ambient temperature is, the higher is the drying rate. The evaporation rate from the wood surface is large even at room temperatures. It is interesting to observe the vacuum drying rate when the ambient temperature is reduced to room temperature.

Although vacuum drying can significantly shorten the drying time, the checking (surface checks and internal checks) remains a major problem. Also, the moisture gradient along the thickness is generally quite steep in vacuum drying, even higher than in conventional drying (Kanagawa and Yisujima 1993). The mechanism of vacuum drying needs to be investigated in order to understand the cause of defects such as checking.

Oaks (*Quercus* spp.) are the most important and most abundant hardwoods in the North Temperate Zone. They constitute about 40% of the hardwood volume in the U.S. Lumber and veneers made from oaks have excellent quality and outstanding beauty. Oaks account for nearly 30% of all hardwood lumber used in the furniture industry and are used extensively in both residential and industrial flooring. White oak has lower permeability than red oak because of the presence of tyloses in white oak. Due to the importance of oaks and the difference between the permeability of white oak and red oak, they are chosen as the woods for this research.

2. Hypothesis and Objective

2.1. Hypothesis

Vacuum drying of wood is based on the fact that the boiling point of water is substantially lowered when the atmospheric pressure over it is lowered. By lowering the atmospheric pressure, a pressure gradient inside the wood develops. As the wood temperature approaches or exceeds the boiling point of water, water vapor is rapidly generated and hydrodynamic bulk flow results from the pressure gradient. Under this condition, the wood permeability may be the dominant factor controlling moisture movement. The two hypotheses are,

(1) If permeability is an important factor, the anisotropy of permeability should reveal that moisture transferred in the longitudinal direction will be much larger than in the transverse direction.

(2) If a boiling front (transition location which separates boiling and non-boiling regions) exists in vacuum drying, then, from the boiling front to the surface, the total pressure difference is a major driving force. The moisture transferred in the boiling region is in steam form by WVBF, and Darcy's law is applicable. From the boiling front to the center, the drying mechanism is the same as in conventional kiln drying.

2.2. Objectives

The overall goal is to investigate the mechanism of vacuum drying. Detailed understanding of moisture transport during vacuum drying can lead to a method to monitor and control the drying rate in order to improve the vacuum drying process. The objectives of this study are to show, based on measurement of the pressures and temperatures at different locations inside the lumber together with the assumed permeability values, that:

(1) Total pressure difference is the major driving force which controls the vacuum drying rate.

(2) Moisture is removed mainly in the longitudinal direction and moisture moves in steam form.

(3) Boiling occurs inside the wood. There is a boiling front and the boiling front moves toward the center of the lumber as drying proceeds.

3. Literature Review

3.1. Mechanism of Moisture Movement

3.1.1. Energy State of Moisture in Wood

Kinetic and potential energies are the two principle forms of energy. Kinetic energy is proportional to the velocity squared. Since the movement of water in wood is quite slow, the kinetic potential is generally negligible (Siau 1984). On the other hand, the potential energy, which is due to position or internal condition, is of primary importance in determining the state and movement of water in wood. Water moves constantly in the direction of decreasing potential energy.

The rate of decrease of potential energy with distance is the moving force which causes moisture flow. The forces involved in the wood moisture movement include gravitational force, capillary force and hygroscopic force (Hillel 1971).

The total water potential in the wood can be defined as the amount of work that must be done per unit quantity of pure water in order to transport reversibly and isothermally water from a pool of pure water at a specified elevation at atmospheric pressure to the wood water (Zimmerman 1983, Kozlowski and Pallardy 1997). The total water potential of the wood water can be the sum of the separate contributions of several components:

$$E = E_g + E_p + E_v + E_o + \text{.....} 3.1$$

where E is the total potential; E_g is the gravitational potential; E_p is the pressure potential; E_v is the chemical potential; and E_o is the osmotic potential.

The liquid movement inside the wood due to gravity is often neglected, typically when the pore dimensions are very small (Siau 1984). The chemical potential which is due to partial vapor pressure difference is significant in diffusion that occurs in the conventional drying (Walker 1993).

It is interesting to discuss the pressure potential which is the driving force for bulk flow including FWBF and WVBF. Bulk flow (liquid or vapor flow) due to the total pressure difference can be caused by external pressure, shrinkage, high temperatures and capillarity (Waananen and Okos

1989). Discussion of bulk flow can be found in several sources (Hillel 1971, Salisbury and Ross 1992, Zimmermann 1983, Kozlowski and Pallardy 1997). The following information can be drawn from them. When wood is completely saturated (the theoretical maximum MC), its water is at a hydrostatic pressure equal to atmospheric pressure. In unsaturated wood, the water is constrained by capillary and adsorptive forces, hence its energy potential is generally negative. Under normal conditions, wood is generally unsaturated and the wood water potential is negative (suction).

A negative pressure potential has often been termed capillary potential and more recently matric potential in wood science (Siau 1984). This potential of water in wood results from the capillary and adsorptive forces due to the wood matrix. These forces attract and bind water in the wood and lower its potential energy below that of bulk water. The flow caused by capillary force or adsorptive force can not easily be separated since capillary menisci are at a state of internal equilibrium with the adsorptive films. None can be changed without affecting the others (Hillel 1971).

3.1.2. Free Water Bulk flow (Movement of Liquid Water)

Moisture exists in wood as bound water within the cell wall, capillary water in liquid form and water vapor in gas form in the voids of wood (Haygreen and Bowyer 1996). Capillary water bulk flow refers to the flow of liquid through the interconnected voids and over the surface of a solid due to molecular attraction between the liquid and the solid (Haygreen and Bowyer 1996).

In saturated wood, wood is in the equilibrium with capillary water at the same elevation. The actual pressure is atmospheric and the suction is zero. Water in unsaturated wood is subject to a subatmospheric pressure or suction, which is equivalent to a negative pressure potential. Water loss may occur until the suction increases to a certain critical value at which the largest pore begins to empty. This critical suction is called the air entry suction in soil science (Hillel 1971). As suction is further increased, more water is drawn out of the wood. The relatively large pores which can not retain water against the suction applied will empty out. A gradual increase in suction will result in the emptying of progressively smaller pores. Until at high suction values, only the very narrow pores retain water. Similarly an increase in wood water suction is associated with a decreasing thickness

of the hydration films covering the wood partial surfaces. Water flows from a zone where the hydration films (water films) are thicker to where they are thinner and it flows from where matric suction is lower to where it is higher. When suction is uniform, there is no moving force (Hillel 1971).

An understanding of free water movement in the gross capillary structure of wood requires a knowledge of capillary pressure. Capillary pressure and matric potential play a central role in the description of liquid flow in porous media (Eaton and Hale 1993).

3.1.3. Water Vapor Bulk Flow

At temperatures approaching and exceeding the boiling point of water, rapid vapor generation may produce significant total pressure gradients in addition to partial vapor pressure gradients (Waananen and Okos 1989). Water vapor will be moved from a high pressure to a low pressure regions under total pressure difference. This is similar to free water bulk flow. Gas permeability is considered in water vapor bulk flow (Tesoro et al. 1974, Bolton and Petty 1978, Walker 1993). Although the density of water vapor is small, the volume flow rate is large under the certain pressure differences. A significant amount of moisture may be transferred by water vapor bulk flow. In vacuum drying, total pressure differences within wood causes water vapor bulk flow. There is a continuous water vapor supply in the boiling region because of water evaporation (Waananen and Okos 1989).

3.1.4. Diffusion

Unlike free water bulk flow due to capillary forces (matric potential), diffusion is the transfer of a material by essentially random molecular motion of single molecules in response to concentration gradients (Hougen et al. 1940). Water and other small molecules can migrate across cell walls even when wood is impermeable and there is not a pressure gradient (Walker 1993).

In Fickian diffusion (Massey 1986), all water molecules are free to migrate. They generally diffuse from a region of high moisture content to a region of low moisture content, which reduces the moisture gradient and equalizes the moisture content. The rate of diffusion increased with temperature, increasing about 37 times when temperature is raised from 25 to 100°C (Walker 1993).

The principle reason for drying wood at higher temperatures is because the rate of diffusion increases with the temperature. Diffusion plays an important role in the drying of lumber, at all moisture content with impermeable timbers and in permeable timber wherever the moisture content is too low for hydrodynamic flow of water through the lumens (Walker 1993).

Diffusion in wood occurs in the hygroscopic range (Walker 1993, Perre and Mosnier 1995). According to Siau (1984), there are two types of diffusion occurring in the wood, intergas diffusion and bound water diffusion. Intergas diffusion is the transfer of water vapor through air in the lumens of the cells. Bound water diffusion is water transfer within the cell wall of wood.

3.2. Vacuum Drying

3.2.1. Definition of Vacuum Drying

In vacuum drying, the lumber is placed in a tight drying chamber. The vacuum drying system pulls a vacuum on the lumber so that the water in wood is boiling and is drawn out of the wood (Simpson 1984). Vacuum drying is actually based on the fact that the boiling point of water is substantially lowered when the atmospheric pressure over the wood is lowered.

The relation between the saturation pressure and temperature from 0 to 100°C is expressed as (Siau 1984):

$$P_o = 8.75 \times 10^7 Exp(-\frac{10400}{RT}) \quad \text{.....3.2}$$

where P_o is saturated pressure, cm Hg; R is gas constant, 1.987 cal/molK and T is Kelvin temperature.

This relation is graphically presented in Figure 3.1.

3.2.2. History of the Vacuum Drying

The history of the vacuum drying of wood can be traced back to early 1920's and a patent on the vacuum drying system of wood was registered in 1922 in Sweden (Ressel 1994).

In 1962, the first industrial vacuum dryer using cyclic technology was built (Pagnozzi 1983).

In 1964, a small dryer was made with the electric resistance plates working under a continuous vacuum. In 1975, a dryer with hot air heating was developed for the first time. The first radio frequency vacuum dryer was built in the early 1970's (Koppleman 1976).

3.2.3. Types of Vacuum Drying Systems

Vacuum drying systems can be separated based on the method of heat transfer to the wood, into four type. There are: conduction by direct contact with a hot plate or electric heating blanket; convection using superheated steam at high temperature; convection using hot air as in cyclic systems and radio-frequency dielectric heating (Chen and Lamb 1995b). Cyclic vacuum drying is a discontinuous vacuum drying system. The others are continuous systems.

In cyclic drying, the latent heat of evaporation is essential for drying. As soon as the latent heat provided by the residual heat in the wood is used up, the drying stops. There is no easy way to convey heat to the lumber under vacuum. In absence of air, convection is almost absent and radiant heat around the wood only can heat the outside of the stack (Simpson 1984).

In radio-frequency vacuum drying (RFV), the wood dielectric is placed between metal plates or electrodes (Hamano and Nishio 1986). When an RF electric current is applied, the molecules change their directions cyclically, resulting in a rapid vibration of molecules, and heat is generated. Radio-frequency generated heat produces high temperature inside the wood in very short time (Avramidis et al. 1994).

In hot platen vacuum dryer, the stacks of wood are laid out between aluminum heating plates. Hot water flows through the plates and hot plates heat the lumber to the required temperatures (Kanagawa and Yasujima 1993).

3.2.4. Vacuum Drying Rate

Both research and practical experience agree that vacuum drying of lumber is fast. Voigt et al. (1940) and Avramidis et al. (1994) concluded that the vacuum drying rate is inversely proportional to ambient partial air pressure, and that it is comparable with the drying rates obtained by high temperature drying above 100°C. For vacuum drying 8/4 red oak 8-foot long, it took about 88 hours

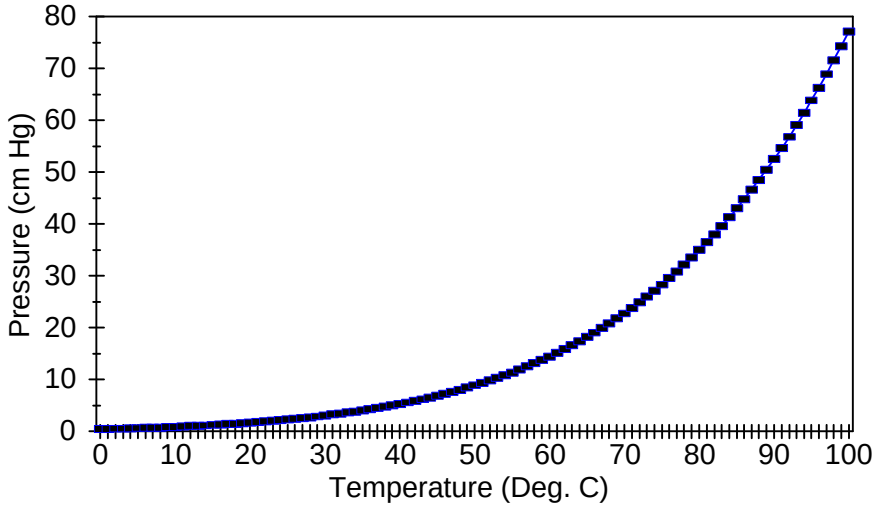

Figure 3.1 Relationship between Saturated Vapor Pressure and Temperature

to dry from an initial MC of 67% to final MC of 7%. Whereas with conventional kiln drying, for the same size lumber, it took 63 days to dry to 8% MC (Harris and Taras 1984). The speed of radio-frequency vacuum drying is almost seventeen times that of conventional drying (Harris and Taras 1984). They also dried 5/4 mixed oak species from green to 8% MC in 65 hours as compared to 42 days for conventional kiln drying. In cyclic vacuum drying of hornbeam, drying time was by 25-30% when compared with conventional drying (Trebula and Dekret 1984). For drying softwoods, such as pine, Moldrup and Moldrup (1992) found that vacuum drying was three times faster than conventional kiln drying with the same drying quality.

Drying speed is related to the species, especially the permeability of the species (Kanagawa and Yasujima 1993). In the RFV, high permeable woods, such as Apitong, dried 13 times faster than with conventional kiln drying. The vacuum drying rate of low permeable woods, like Matoa and Wester red cedar are only 2.6 and 1.4 times faster, respectively, when compared with conventional kiln drying (Kawabe and Mori 1984). Drying time in vacuum drying, especially using radio frequency heating is significantly shortened because the temperatures are higher in the lumber core than in the surface. Moyne and Martin (1982) concluded that the acceleration of drying rate is due to pressure driven flow occurring under vacuum conditions.

3.2.5. Vacuum Drying Quality

The quality of the vacuum dried lumber is generally good. Usually lower degrade is found in vacuum drying than in conventional kiln drying (Wengert and Lamb 1982). With vacuum drying, lumber is similar in color after drying to the color before drying (Moldrup and Moldrup 1992). Also vacuum dried lumber has a lighter color than predried lumber (Wengert and Lamb 1982).

Drying stresses in vacuum drying are similar to those in conventional kiln drying. At the early stage of drying, the lumber surface is in tension and the core is in compression. As drying continues below FSP, stresses reverse (Harris and Taras 1984). Harris and Taras (1984) found that the residual stress was small after RFV drying. Smaller residual stresses and less degrade were found for lumber that was cyclic vacuum dried compared to lumber that was RFV dried.

Wengert and Lamb (1982) evaluated several methods for drying 5/4 and 8/4 red oak lumber.

They recorded number of the drying checks in lumber dried by RFV, cyclic vacuum drying and predrying followed by kiln drying. Vacuum drying had substantially low checks including end, surface and internal checks. They also found that RFV has less crook (36% less than predried). Simpson (1987) dried red oak of 4/4 and 10/4 thicknesses using a heating blanket vacuum system and reported no surface checking and low (2 to 2.2%) honeycombing. No internal and surface checks were found in RFV by Avramidis et al. (1994).

In vacuum drying, a steep moisture gradient occurs in the surface layer of a sample because it does not move sufficient moisture from the center to the surface. This steep moisture gradient is developed even at the early stages of drying (Kanagawa and Yisujima 1993, Avramidis et al. 1994). Vacuum drying systems also show a large variation in the final MC between and within board especially in RFV which has an uneven heating temperature (Lamb and Wengert 1993). Conventional kiln drying maintains a lower moisture gradient through the board thickness than does RFV. The variation among boards ranges from 2 to 28% MC for RFV compared with 7 to 11% MC for conventional drying as reported by Trofatter et al. (1986).

3.2.6. Property Change in Vacuum Drying

It is reported that the shrinkage of red oak lumber dried by RFV is approximately 30% less than that dried by conventional kiln drying (Harris and Taras 1984). For RFV, red oak was dried from green to 5.5% MC with an average shrinkage of 4.1% radially and 7.5% tangentially. By comparison, for conventional drying, red oak dried from green to 7.8% MC, had shrinkage values of 5.6% and 10.3% in the radial and tangential direction respectively.

The equilibrium moisture content (EMC) is significantly lower in vacuum drying than in conventional drying (Lee and Harris 1984). Taniguchi and Nishio (1991) reported that lumber dried by RFV had an EMC of 0.7 to 1% lower than that dried by conventional kiln drying.

In comparison with dehumidification drying and conventional kiln drying, lumber dried by RFV has slightly lower compressive strength, bending stiffness, bending strength, shear strength, and hardness. However this difference is statistically insignificant except for the compressive strength (Taniguchi and Nishio 1991, Lee and Harris 1984). There was no difference in hardness or toughness

between oak lumber dried by RFV and by conventional kiln drying according to Wengert and Lamb (1982).

3.3. Wood Drying Models

3.3.1. Model Development

Development of mathematical models to describe wood drying has been a topic of research for many decades (Salin 1991). Since Tuttle (1925) presented the first mathematical theory for wood drying, numerous models have been developed. Basically these model can be classified into three categories (Kamke and Vanek 1994, 1996): empirical curve-fitting equations, moisture diffusion equations, and fundamental heat and mass transfer equations. Most of the wood drying models fall into the category of fundamental heat and mass transfer equations. Generally, one dimensional heat and mass transfer is assumed (Plumb et al. 1985, Stanish et al. 1986, Liu et al. 1990). Recently, two-dimensional models have been suggested (Furguson and Turner 1994, Perre and Mosnier 1995).

Several mechanisms of internal mass transfer have been proposed in the drying literature including liquid diffusion, vapor diffusion, surface diffusion, and bulk flow (Waananen et al. 1993). Diffusion-controlled transport below FSP and the capillary pressure controlled transport above FSP are frequently used in describing conventional wood drying. The key characteristics of the drying models discussed include controlling process resistances, internal mechanisms of moisture movement, structural and thermodynamic assumptions, methods of material property measurement, model solution, and model validation.

Model developments have been based on approaches in which the descriptions of transfer phenomena have been derived from either Fourier's and Fick's laws or the principles of irreversible thermodynamics and entropy production (Bramhall 1979a, 1979b, Thomas et al. 1980, Benet and Jouanna 1983, Plumb et al. 1984, Stanish et al. 1986, Adesanya et al. 1988, Liu 1990). Traditionally moisture content gradients have been employed as the driving forces for diffusion (Droin et al. 1988, Droin et al. 1989a, 1989b, Vergnaud 1991). In addition, gradients of chemical potential, water potential, and spreading pressures have also been used (Siau 1983, Nelson 1986a, 1986b, 1986c,

Cloutier et al 1992). Thermally induced mass transfer (Soret effect) is also taken into account (Degroot and Mazar 1962, Siau 1983)

The main difficulty in modeling wood drying is the fact that wood is an anisotropic medium. Modeling is also complicated because more than one mechanism may contribute to the total flow and the contribution of different mechanisms may change as the drying process proceeds (Bruin and Luyben 1980).

A diffusion mechanism for internal mass transfer has been assumed in many modeling studies. Distinction can be made between liquid diffusion, vapor diffusion, and surface diffusion of adsorbed molecules. Phenomenological laws such as Fourier's law, Fick's law, and Ohm's law are based on the proportion between a flux and a driving force. When more than one driving force is present in a process, cross effects can occur. In coupled heat and mass diffusion, a gradient in temperature can cause mass transfer (Soret effect) and a gradient in mass concentration can cause heat flow (Defour effect). Whitaker (1988) performed a detailed analysis of the Soret and Dufour effects for heat and mass transfer in a porous medium. He concluded that the effects are negligible when compared with coupling effects caused by classic equilibrium thermodynamic considerations. Fortes and Okos (1981) developed a drying model for food using an irreversible thermodynamics framework. They observed that the cross-effect terms were small compared to direct terms. Based on this analysis, it does not appear practical to utilize irreversible thermodynamics for development of drying models for porous solids.

Internal mass transfer due to a gradient in total pressure has been postulated in drying materials such as wood and food (Moyne and Degiovanni 1985, and Waanenan et al. 1993). At temperatures approaching and exceeding the boiling point of water, rapid vapor generation may produce significant total pressure gradients in addition to partial vapor pressure gradients (Moyne and Degiovanni 1985). Total pressure driven flow may also occur in moderate temperature vacuum drying and in high temperature convective and contact drying (Moyne and Degiovanni 1985). Moyne and Degiovanni (1985) derived a one dimensional drying model which accounts for total pressure driven flow. Theoretical predictions were compared qualitatively with experimental results obtained

for the drying of light concrete slabs in superheated steam. Predicted and experimental curves were shown to have similar shapes. Cross et al. (1979) studied the theoretical development of pressure gradients within iron ore pellets during drying. Based on the results from their model, the porosity of the body was shown to be a significant factor in determining the maximum pressure gradient.

3.3.2. Methods of Model Solution

Combination of flux equations with mass and energy balance equations gives rise to a system of nonlinear partial differential equations. Numerical techniques are usually used to solve these systems of equations. Sidiropoulos and Tzimopoulos (1983) presented several approaches to heat and mass transfer equations. Finite difference and finite element methods are frequently employed to solve the second degree partial equations. Stanish et al. (1986) solved a set of equations using an adaptive mesh finite difference method. Patankar (1991), Fortes and Okos (1981) and Vergnaud (1992) also used finite difference techniques to solve heat and mass transfer equations.

3.3.3. Model Validation

In some cases, only theoretical drying models are developed with no attempt to apply the models or assess their validity. Comparison of predicted drying curves with experimental curves gives one measure of model validity. Stanish et al. (1986) determined model coefficients from selected data and found that predictions using these coefficients were good over a broad range of conditions. In these cases, the theoretical basis of the models is indirectly supported.

Comparison of actual and predicted moisture profiles gives a second measure of model validity. Experimental measurement of moisture profiles in solid materials is difficult, and has limited the ability to validate drying models. There is high variability among results of various models. Most of the simulation results were not in close agreement with actual laboratory tests. The explanation for the difference can be found in the uncertain coefficients used in the models, different degrees of simplifications, and different ways of solving the heat and mass transfer equations (Kamke and Vanek 1994, 1996). They concluded that simple models will work as well as sophisticated models.

3.3.4. Modeling Vacuum Drying

An important group of problem in modeling is that water has transformation points at which

it changes from one phase to another with emission or absorption of heat, (such as, melting, freezing and evaporating). The problem of ice thickness was studied by Stefan and Jaeger (1959). They discussed the new feature of such a problem to be the existence of a moving surface of separation between any two water phases. Luikov (1975) also studied steady state heat and mass transfer between a capillary porous medium and an external gas steam during drying. He concluded that evaporation takes place inside the body at a certain depth and that the deepening of the evaporation front has an appreciable effect on the heat transfer. The moving evaporation front divides the system into two regions. While the moisture in one region is in vapor form only, in the other region, it is as a mixed vapor and liquid. The moisture in vapor form moves out to the surface without removing any appreciable amount of heat from the system. The problem reduces to the simultaneous solution of a pure heat conduction problem in one region and an unsteady state coupled problem of heat and mass transfer with a moving boundary in the other region.

This unsteady state problem, characterized by a moving evaporation front in a porous medium and simultaneous transfer of heat and moisture, is called the generalized Stefan's problem. Gupta (1974) presented an approximate solution to this problem in which he assumed that the effect of the temperature gradient on the mass transfer is small and can be neglected. Cho (1975) gave the exact solution to this problem. For the problem of freezing of a humid porous medium, Mikhailov (1976) presented the exact solution. Lin (1982) presented the exact solution of coupled heat and mass transfer of the sublimation and desublimation problems in a porous medium, assuming that mass transfer was controlled by Fick's law alone. Coupled heat and mass transfer with moving interfaces, taking place in a porous medium when considering the effect of surface pressure and permeability on the sublimation rate, is exactly solved by Peng and Chen (1993).

In a model of wood vacuum drying, Guilmain et al. (1996) adds a third partial equation (pressure partial equation) to the classical models which consisted of only two equations: an energy equation and a mass transfer equation. With their simulation results they recognized the importance of moisture transport in a gaseous phase under the influence of a total pressure gradient in vacuum drying. They concluded that the boiling of water must be considered. However, they did not include

the evaporation phenomenon and different phase zones during vacuum drying. In porus materials, the drying rate increases with a lowering of the surrounding pressure below atmospheric pressure. Ressel (1994) mentioned that Stefan's problem occurs in wood vacuum drying. Stefan's problem is considered to be important factor in this research.

3.4. Wood Physical Properties Related to Vacuum Drying.

3.4.1. Permeability

Permeability refers to the capability of a solid substance to allow the passage of gases or liquids under pressure (Erickson 1970). Permeability assumes the mass movement of molecules in which the pressure or driving force may be supplied by such sources as mechanically applied pressure, vacuum, thermal expansion, gravity, or surface tension (Waanenen and Okos 1989). At temperatures above the boiling point and at MC above FSP, hydrodynamic bulk flow results from the pressure gradient arising from steam pressure within the wood (Waanenen and Okos 1989). Under this condition, the permeability of wood is the dominant factor controlling moisture movement (Waanenen and Okos 1989). Wood has a relatively large permeability due to its cellular structure, especially in the longitudinal direction.

3.4.1.1. Wood Permeability in Relation to its Anatomical Structure

The permeability of wood depends on its microscopic structure. Wood of a certain species may have a large void volume, but because of limitations of interconnections, the permeability may be low (Erickson 1970). Transverse permeability is dependent primarily upon the permeability of pits (Comstock and Cote 1968). Pit aspiration reduces the permeability (Comstock and Cote 1968).

Due to the complex structure of wood, permeability is an extremely variable property. The early research on gas permeability by Smith and Lee (1958) showed differences in longitudinal permeability of 5×10^6 times between permeable and impermeable hardwoods. A wide variation in permeability also occurs within one species. Smith and Lee (1958) observed permeability differences in different oak specimens up to three thousand to one.

Tesoro et al. (1974) concluded that permeability of sapwood was always higher than that of

heartwood. This is caused by the tyloses, pit aspiration and extractive content in heartwood (Cote 1963). In ring porous hardwoods, earlywood is frequently more permeable than latewood due to the large earlywood vessels (Cote 1963).

3.4.1.2. Anisotropy of Permeability

The arrangement, shape and size of the microscopic elements give wood the directional quality of an anisotropic porous medium. Permeability in wood shows marked differences depending on the direction of flow. The ratio of longitudinal to tangential permeability for softwood is large. For hardwood, it ranges from 30,000 to 4×10^8 (Siau 1984). On the average, the ratio of longitudinal to radial to tangential gas permeability in the oven dry condition for hardwoods is 21661:23.3:1 (Smith and Lee 1958). This high ratio in hardwoods may be explained by the number and distribution of open vessels. Vessels are responsible for the relatively high longitudinal permeability in hardwoods (Cote 1963). Tyloses greatly increase the resistance to flow along vessels, and they account for the low permeability of some species, such as, white oak (Walker 1993).

3.4.1.3. Relation between MC and Permeability

An increase in permeability with loss of moisture would be expected, since a loss of moisture would result in shrinkage of the fibrous strands in the pits and a corresponding increase in the size of openings in the pits (Siau 1984).

Wood above FSP would be expected to have very low gas permeability because high capillary pressures must be overcome to force air bubbles through the minute pit openings (Siau 1984). The ratio of gas permeability values between 0 and 20% MC is fairly constant for a given species, regardless of thickness or direction of flow (Choong and Tesoro 1974). The ratio of permeability at 0 MC to that at 20% MC was about 2 to 1 for the impermeable specimens, and for the permeable specimens it was about 1.35 to 1 (Choong and Tesoro 1974).

In softwoods, green lumber may have higher permeability, due to severe drying condition, and pit aspirations which may cause low permeability at low MC (Comstock and Cote 1968). Pit aspiration can be minimized by proper drying so that high earlywood permeability can be retained after drying (Bolton and Petty 1978).

3.4.1.4. Gas Permeability and Liquid Permeability

A high degree of correlation between gas and liquid permeability exists. The relationship between the logarithms of gas and liquid permeability values is nearly linear (Choong and Tesoro 1974). The ratio of gas to liquid permeability is shown to change more in those species that have lower permeability (Choong and Tesoro 1974).

3.4.2 Wood Thermal Properties

Wood thermal conductivity (K) is the ratio of the heat flux to the temperature gradient through a wood sample (Siau 1984). Wood has a relatively low thermal conductivity due to its porous structure, and cell wall properties. MacLean (1941) measured the thermal conductivities of various woods with a large range of MC and specific gravities (SG). He presented two empirical equations which gave the best agreement with his experimental data. The transverse thermal conductivity can be expressed as:

$$K=[SG\times(4.8+0.09\times MC)+0.57]\times 10^{(-4)}\frac{cal}{cm^{\circ}Cs}.....3.3$$

when moisture content of wood is below 40%.

$$K=[SG\times(4.8+0.125\times MC)+0.57]\times 10^{(-4)}\frac{cal}{cm^{\circ}Cs}.....3.4$$

when moisture content of wood is above 40%.

The free water in the cell lumens contributes more and more to the thermal conductivity when MC increases. The longitudinal thermal conductivity is about 2.5 times of that of transverse thermal conductivity (MacLean 1941).

The thermal conductivity of wood is affected by a number of factors;

a. density of wood,

b. moisture content of wood,

c. grain direction,

d. extractive and chemical substances in the wood,

e. earlywood and latewood,

f. defects such as checks, knots, etc.

Another thermal property of wood which affects the heat transfer is the specific heat (c). The specific heat of a material is defined as the ratio of its thermal capacity to that of water at 15°C. It can be calculated as the calories of heat required to raise a one-gram mass by 1°C (Skaar 1972). It depends on the temperature and MC of wood, however, it does not vary with the density or species. The specific heat of dry wood C_w increased linearly with the temperature over a limited temperature range. It can be expressed as:

$$c_w = 0.266 + 0.00116 \times T \quad \text{.....3.5}$$

where T is the temperature (°C), and the unit for specific heat is cal/g°C

Specific heat of moist wood is higher than that of dry wood. It can be calculated by:

$$c = \frac{c_w + 0.01 \times MC}{1 + 0.01 \times MC} + A \quad \text{.....3.6}$$

A is the additional specific heat due to the wood-water bond energy. For wood at 10% MC, A ranges from 0.02 to 0.04 at the temperature 30°C to 60°C and it ranges from 0.04 to 0.09 at 30% MC at the same temperature range (Wangaard 1981).

3.5. Mechanisms of Drying under Vacuum

Because Fick's law is not applicable in vacuum drying (Neumann et al. 1992), recently work has concentrated on the theoretical aspects of the driving force and moisture movement mechanisms during vacuum drying. Early studies did not consider the pressure influence on drying. By increasing the wood permeability using steam explosion, the vacuum drying rate of such treated wood was higher than the drying rate of a specimen without the such treatment at all moisture contents (Hayashi et al. 1993, 1995). The permeability of wood was found to be the dominant factor in controlling moisture movement in vacuum drying. In this case, bulk flow is thought to be the way most moisture is removed from the wood.

Total pressure changes in a vacuum dryer have recently been used to identify the importance of a bulk flow mass transfer mechanism in pasta at temperatures above the boiling point of water (Waananen and Okos 1989). Pressure driven flow becomes the dominant transport in moisture migration within heated concrete at elevated temperature (Moyanand Giovanni 1985). Drying rates for the bulk flow process were two to six times those observed for diffusion in concrete (Moyanand Giovanni 1985).

Knowing the importance of pressure effects in vacuum drying, Sasaki et al. (1987) measured the pressures inside wood during RFV. They drilled holes into the wood and inserted glass tubes that were connected to manometers. They measured the pressure distribution and found that there was a pressure difference along the length and width. However they did not measure temperatures so that they did not compare pressure with the saturation pressure.

Perre and Mosnier (1995) measured the pressures in wood during radiative heating vacuum drying. They defined a drying front in vacuum drying. Furthermore, they suggested the drying front is at that location where the MC in the wood is lower than FSP.

When the pressure is lower than the saturated pressure, water boils (Kanagawa and Yasujima 1993). Most studies support the concept that moisture is vaporized in the wood during drying as the boiling temperature is lowered by vacuum. In RFV, the temperature of the wood reaches the boiling point in a very short time (Avramidis et al. 1994). However, Neumann et al. (1992) simultaneously

measured the temperature and pressure at different depths of beech boards during convective vacuum drying in superheated steam at 2×10^4 Pa (0.2 bar). They found that pressures at different depths were always higher than the saturation pressures corresponding to the local temperatures. They concluded that water is not boiling in the wood and the fast drying in vacuum drying may not be attributed to the boiling phenomena as most studies indicate. Their measurements were done in the center of boards. However, this work did not exclude the possibility of boiling near the ends of the boards. If longitudinal moisture transportation is important, a boiling front may occur there.

The boiling front concept has been proposed by Chen and Lamb (1995a). They suggested that not only does boiling occur inside the wood, but also there is a boiling front. From the boiling front to the surface of the wood, the pressure is lower than the saturation pressure and moisture in this region evaporates. From the boiling front to the center of the wood, boiling does not occur because the pressure inside the wood is higher than the saturation pressure. The boiling front retreats from the surface toward the center as drying proceeds. The retreating speed depends on the heat supply and the properties of the wood, such as permeability and conductivity (Chen and Lamb 1995a).

Neumann et al. (1992) stated that the pressure at the surface dropped rapidly when vacuum drying began, while the pressure in the center decreased when the MC of the wood was below FSP. Not only is there a pressure gradient across the thickness or width, but also there is also one along the length (Neumann et al. 1992, Avramidis et al. 1994). Avramidis et al. (1994) found that the internal pressure gradient is also significant along the longitudinal direction during RFV. They concluded that this is a result of the large permeability in the longitudinal direction and that moisture evaporates from the end grain. This phenomenon also results in a large temperature gradient in the longitudinal direction. This may cause faster drying rates in vacuum drying. Under these conditions, Soret and Dufour effects can be neglected (Dayan and Gluekler 1982).

Sasaki et al. (1987) studied the change in pressure inside wood as drying proceeds. They found that the pressure verse time curves were divided into three periods. In the initial period, the pressure decreased rapidly depending on the permeability and location in the board. In the second

period, the pressure remained nearly constant. In the third period, after MC was below FSP, the pressure began to decrease again and approached the reduced pressure in the chamber.

In vacuum drying, the total pressure gradient inside wood is a more important drying force than diffusion, unlike the case in conventional kiln drying. Total pressure differences inside a porous medium have recently been used to identify the importance of a bulk flow mass transfer mechanism at temperatures above the boiling point of the water, during vacuum drying of other materials such as food (Waananen and Okos 1989). Their predicted results were in agreement with the experimental results. Noack (1965) found that moisture migrates during the vacuum drying in a gas state (steam) when wood dries below FSP. He concluded that the drying force is the pressure difference between the vapor pressure in the lumina and the ambient pressure. Moyne and Martin (1982) concluded that the acceleration of the drying rate due to pressure driven flow occurred during hot platen drying of wood under vacuum. The surface of wood exposed to lower pressure results in a significant heat release by evaporation of water held within the porous structure. Pressure driven flow becomes dominant at high temperatures (Moyne and Martin 1982).

4. Moisture Movement During Vacuum Drying

The objective of this phase of study is to compare the magnitudes of diffusion, FWBF and WVBF. Wood drying involves the movement of moisture from the interior to the surface of lumber and the evaporation of moisture from the surface to the environment. Two forms of moisture transport exist in wood: diffusion and bulk flow (FWBF and WVBF). These forms of transportation are a result of three kinds of mechanisms: vapor movement through cell lumens and pit cavities, bound water movement through the cell walls, and free water movement through cell lumens and pit cavities in liquid form.

4.1. Diffusion

There have been extensive studies of bound water diffusion and vapor movement in the past (Walker 1993). A diffusion is molecular mass flow under the influence of a concentration gradient. Therefore a total pressure difference is not necessary for diffusion to occur. Fick's law represents the relationship between the flux and the concentration gradient.

Fick's law defines unidirectional moisture diffusion as the rate of mass transfer per unit of cross sectional area (flux) J_d per unit change of concentration dC per unit of specimen length dx. For steady state conditions in wood where the flux and gradient (dC/dx) remain constant over time, Fick's law can be expressed as (Siau 1984):

$$J_D = -D \times \frac{dC}{dx} \quad \text{.....4.1}$$

where D is the diffusion coefficient of wood (cm^2/s).

This can be rewritten so that the concentration difference (dC) is expressed in terms of the moisture content difference(dMC):

$$J_d = -D \times \frac{G_m \rho_w \times dMC}{100 dx} \text{.....4.2}$$

where G_m is the nominal specific gravity at the moisture content MC and ρ_w is the density of water (g/cm^3), unity.

The equations that are used to explain diffusion for moisture movement in wood are a combination of vapor and bound water diffusion. They can be separated theoretically into the following equations for the transverse direction (Siau 1984).

An emperical equation for transverse bound water diffusion can be expressed as:

$$D_{bt} = 0.07 \times \exp\left(\frac{70 \times MC - 9200}{RT}\right) \text{.....4.3}$$

where R is the gas constant, 1.987 (cal/mol K); and T is the Kelvin temperature; MC is the moisture content (%); D_{bt} is the transverse bound water diffusion coefficient of wood (cm^2/s).

Vapor diffusion coefficient in the lumens can be expressed (Siau 1984) as:

$$D_v = \frac{0.016 P_o T^{0.75}}{RPG_m \rho_w} \times \frac{dH}{dMC} \text{.....4.4}$$

where D_v is the vapor diffusion coefficient (cm^2/s); P_o is the saturation vapor pressure at temperatrue T; P is the total pressure; H is the relative humidity (%).

These two values are then inserted into the equation below to calculate the theoretical gross wood diffusion coefficient in the transverse direction (Siau 1984):

$$D_{gt}=\frac{\sqrt{V_a}D_{bt}D_v}{(1-V_a)[\sqrt{V_a}D_{bt}+(1-\sqrt{V_a})D_v]}.....4.5$$

V_a is the porosity of wood, which can be calculated from the following equation (Siau 1984):

$$V_a=1-G\times(0.667+0.01\times MC).....4.6$$

G is specific gravity, 0.56 for red oak (Alder, 1995)

The longitudinal bound water diffusion coefficient of the cell wall is approximately three times that in the tangential direction and two times that in the radial direction. It is assumed that longitudinal cell wall bound water diffusion coefficient is 2.5 times the transverse direction (Siau 1984).

$$D_{bl}=2.5\times D_{bt}.....4.7$$

Vapor diffusion through the lumens is the same as in the transverse direction.

The gross wood longitudinal diffusion coefficient D_{gl} can be expressed as (Siau 1994):

$$\frac{1}{D_{gl}}=(1-V_a)[\frac{1}{D_vV_a+D_{bl}(1-V_a)}+\frac{(1-\sqrt{V_a})}{100D_{bl}V_a}].....4.8$$

In order to effectively compare the diffusion rate with transportation rates for bulk flow

(FWBF and WVBF), diffusion rates will be calculated at 30% MC and 10% MC using equation 4.8.

Table 4.1 shows the calculated diffusion coefficients for average MC of 30% and 10% at 60°C for red oak.

Table 4.1 Diffusion Coefficients at 30% and 10% MC for Red Oak at 60°C

MC (%)	30	10
D_v ($cm^2/s \times 10^5$)	2.7	15
D_{bt} ($cm^2/s \times 10^{7)}$	8.5	2
D_{bl} ($cm^2/s \times 10^7$)	21.3	5
V_a	0.458	0.57
D_{gt} ($cm^2/s \times 10^6$)	4.3	1.88
D_{gl} ($cm^2/s \times 10^6$)	23.8	117

At the different MC gradients, the diffusion rates (J_d) can be calculated at the average MCs of 30% and 10% (Table 4.2). They are graphically presented in Figure 4.1. Several moisture gradients are chosen since moisture gradient during the drying generally falls among them.

Moisture diffusion through wood is not affected by pressure, according to Kollmann and Cote (1968). Because diffusion rates increase with temperature, they may be even smaller in vacuum drying than in conventional kiln drying, since lower temperatures are used.

4.2. Water Vapor Bulk Flow (WVBF)

The movement of water vapor through wood under a total pressure difference can be assumed to follow Darcy's law. Although the density of water vapor is small, an appreciable certain amount of water is still transferred when the flow rate is large.

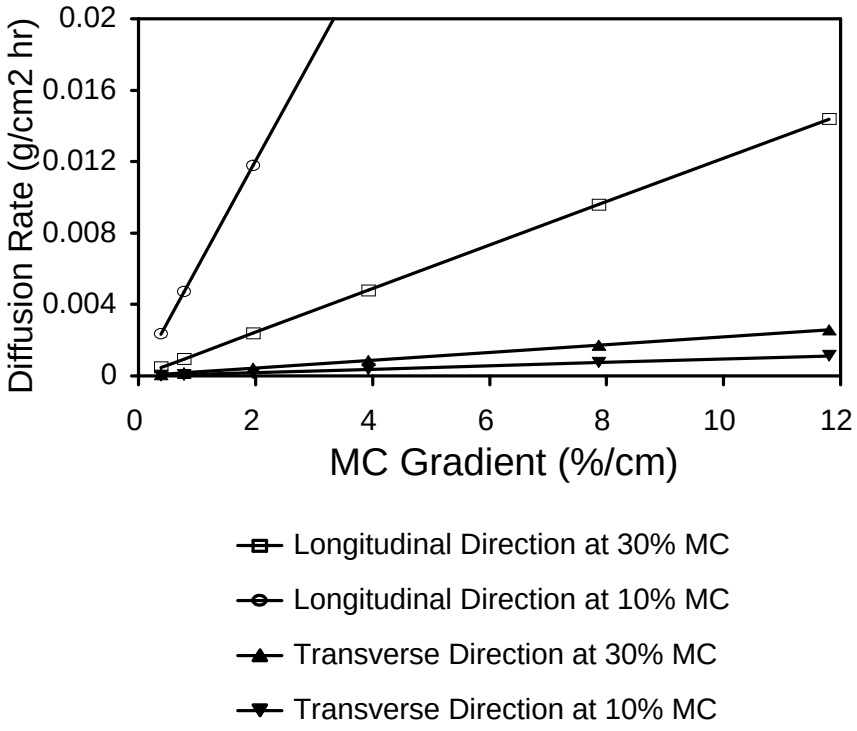

Figure 4.1 Calculated Moisture Diffusion Rate at Temperature of 60°C in Red Oak

Table 4.2 Diffusion Rates in Transverse and Longitudinal Directions for Red Oak

MC Difference within one inch	MC Gradient (%/cm)	Longitudinal Diffusion Rate $\times 10^4$ ($g/cm^2\,hr$)	Longitudinal Diffusion Rate $\times 10^4$ ($g/cm^2\,hr$)	Transverse Diffusion Rate $\times 10^4$ ($g/cm^2\,hr$)	Transverse Diffusion Rate $\times 10^4$ ($g/cm^2\,hr$)
		at 30%MC	at 10%MC	at 30%MC	at 10%MC
1	0.394	4.6	23.4	0.87	0.38
2	0.787	9.6	47.17	1.73	0.76
5	1.968	23.4	117.9	4.33	1.9
10	3.937	47.98	236	8.67	3.79
20	7.874	99.6	472	17.34	7.58
30	11.81	144	708	26.01	11.37

Darcy's law for gas (water vapor) can be written as (Siau 1984):

$$J_g = \rho_g \frac{K_g}{\eta_g} \frac{\overline{P} dP}{P dx} \quad .....4.9$$

where K_g is the gas specific permeability; dP/dx is the pressure gradient; P bar is the average pressure; η_g is the viscosity of vapor; ρ_g is the density of the steam at the pressure P.

The relative permeability of the solid to bulk gas flow is dependent on the relative saturation and on the permeability of the solid when no free water is present. For gas flow, the longitudinal permeability decreases with increasing relative saturation or MC (Choong and Tesoro 1974). When MC is above FSP, the relationship between the gas permeability and the MC can be expressed as (Choong and Tesoro 1974):

$$K_g = K_g^d \times \frac{V_a}{V_d} = K_g^d \times \frac{1 - G(0.667 + 0.01MC)}{(1 - 0.967G)} \quad \text{.....4.10}$$

where V_a is porosity at MC; V_d is the porosity at 30% MC; K_g^d is gas permeability of red oak at 30% MC, 43.18 darcy.

At MC below FSP, the gas permeability is constant and not affected by the MC. Due to the fact that the gas permeability is a function of the moisture content at MCs above FSP, we only can estimate the vapor bulk flow rate since the moisture distribution is unknown.

In the following calculation, the temperature is assumed to be 35°C, which is considered to be a low temperature for vacuum drying. The rate will be larger at higher temperature.

An approximate equation is,

$$\rho_g \frac{K_{green}}{\eta_g} \frac{\overline{P} dP}{P dx} \le \rho_g \frac{K_g}{\eta_g} \frac{\overline{P} dP}{P dx} \le \rho_g \frac{K_{10}}{\eta_g} \frac{\overline{P} dP}{P dx} \quad \text{.....4.11}$$

where K_{green} is the minimum gas permeability and K_{10} is the maximum gas permeability assuming the final MC is 10%, both calculated from equation 4.10.

Assuming the water vapor is saturated, there is a relationship between saturation pressure and temperature. Knowing temperature, WVBF rates calculated from above equation are shown in Table 4.3 and Figure 4.2.

Several temperature gradients were selected to represent the temperature gradient during drying.

4.3. Free Water Bulk Flow (FWBF)

The migration rate of the free water is assumed to follow Darcy's law for flow through porous media (Waananen and Okos 1989).

Darcy's law for liquid may be written as (Siau 1984):

$$J_l = -\rho_w \frac{K_l}{\eta_w} \frac{dP_l}{dx} \text{.....4.12}$$

where J_l is the free water bulk flow rate; P_l is the pressure within the free water; η_w is the viscosity of the water; ρ_w is the density of water, unity.

Table 4.3 Calculated Water Vapor Bulk Flow Rates in Red Oak

Temperature Difference within One Inch	Temperature Gradient (°C/cm)	Green MC (g/cm^2 hr)	MC=10% (g/cm^2 hr)
1	0.394	0.05234	0.1023
2	0.787	0.11085	0.2167
5	1.969	0.32286	0.6311
10	3.937	0.86127	1.6837
20	7.874	3.1143	6.0882
30	11.81	8.974	17.54
40	15.75	21.55	42.136

The viscosities and densities of the gases and liquids are functions of pressure, temperature and the composition of each phase. The pressures P_l and P are related by the capillary pressure P_c (Spolek and Plumb 1981):

$$P_l = P - P_c \text{.....4.13}$$

where P is the total pressure in the lumen.

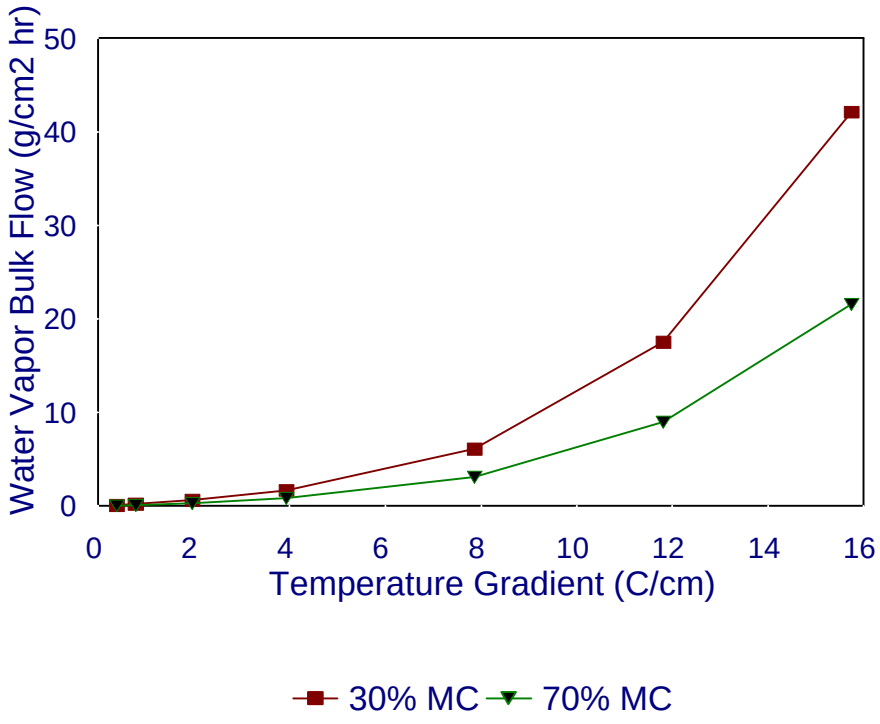

Figure 4.2 Calculated Water Vapor Bulk Flow Rate in Red Oak

The capillary pressure is related to saturation, pore size, pore shape, the angles at which fluid water air interface contacts the solid surface, the density difference between phases, temperature and radii of the curvature of the interface (Spolek and Plumb 1981).

The total pressure within the liquid phase is equal to the total local gas pressure minus the capillary pressure associated with the gas-liquid interface. Spolek and Plumb (1981) measured the relationship between capillary pressure and wood saturation. P_c (Pa) can be calculated by equation 4.14, which is the relationship between capillary pressure and the MC (Figure 4.3).

$$P_c = 10^4 \times \left(\frac{0.01 \times G \times MC - 0.3G}{1 - G \times 0.997}\right)^{0.61} \quad .....4.14$$

The relative permeability of the wood to liquid flow is dependent on the relative saturation and on the permeability of the wood when it is completely saturated.

The relationship between gas permeability K_g^d (when MC is at FSP) and liquid permeability K_f^s (when the wood is fully saturated) for hardwood species was reported by Choong and Tesoro (1974), to be:

$$LogK_g^d = 0.03 + 0.81 \times LogK_f^s \quad .....4.15$$

Liquid permeability is also related to MC (Figure 4.4). Below a certain critical relative saturation or irreducible saturation, liquid permeability falls to zero and liquid migration ceases due to a loss of continuity in the liquid phase. The MC at this critical relative saturation is the critical MC ($MC_{c)}$.

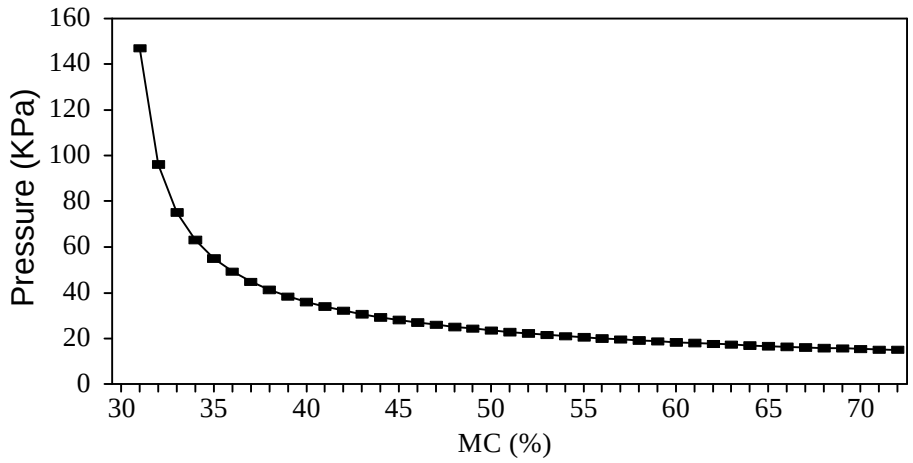

Figure 4.3 Calculated Relationship between Capillary Pressure and Moisture Content (equation 4.14)

According to Stanish et al. (1986), the equation is:

$$MC_c = S_{ir} \times \frac{100 \times V_d}{(MC - 30)} \text{.....4.16}$$

Assuming the specific gravity for red oak is 0.56 (Alder 1995) and S_{ir} is 0.1, the MC_c is 38.2%. This means that when MC of red oak is less than 38.2%, there is essentially no FWBF. Above this critical MC, the relation between the permeability K_l and MC is as follows (Stanish et al. 1986):

$$K_l = K_f^s [1 - \cos(\frac{\pi}{2} \times \frac{0.01 \times G \times (MC - 30)/V_d - S_{ir}}{1 - S_{ir}})] \text{.....4.17}$$

Continuing with our example for red oak, free water movement only occurs above 38.2% MC. The higher the MC, the larger the flow rate will be under the same conditions. Furthermore, moisture gradient is developed. As a result, there is a capillary pressure difference when the wood MC is above the critical MC (MC_c). It is impossible to calculate FWBF without knowing the MC distribution. The range of FWBF (maximum and minimum values) can only be estimated under certain conditions. Table 4.4 shows the calculated result for FWBF at a MC of 70% using Darcy's law (Figure 4.5). Several moisture gradients are chosen since moisture gradient during drying generally falls among them.

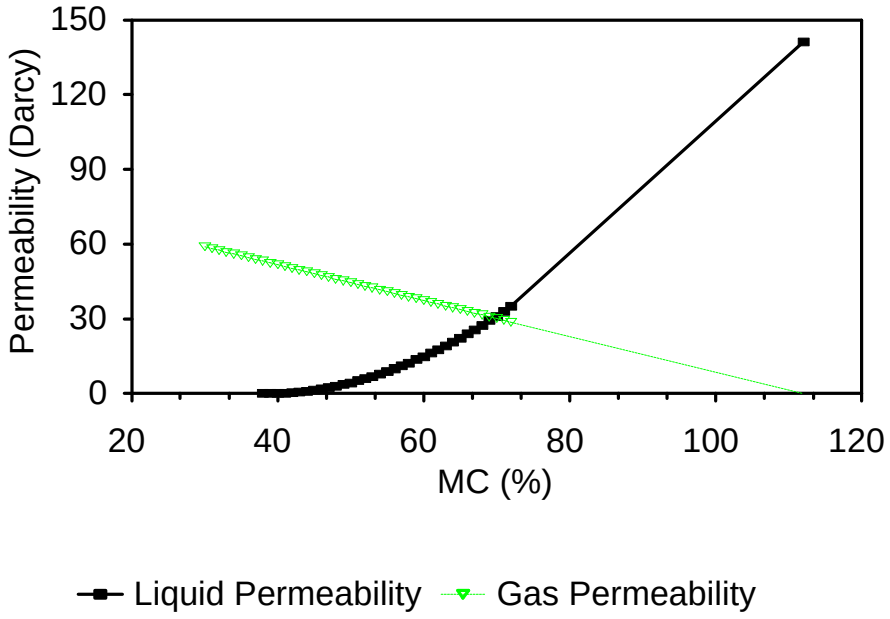

Figure 4.4 Calculated Relationship between Permeability and Moisture Content according to Equations 4.10 and 4.17

Table 4.4 Calculated Free Water Bulk Flow Rates in Red Oak

MC Difference in one inch	MC Gradient (%/cm)	Max. Flow Rate (g/cm^2 hr)	Min. Flow Rate (g/cm^2 hr)
1	0.394	104.8	98.78
2	0.787	214.1	189.3
5	1.969	571.6	411.4
10	3.937	1292	621.2
15	5.907	2236	643.5
20	7.874	3544	506.2
30	11.81	8954	30.26

Note: Maximum value is achieved at the maximum permeability when MC is equal to 70%. The minimum value is when the value of MC is at the lower end.

The transverse permeability of oak is very small. For red oak, it is found that in the longitudinal direction it is about 4.9×10^8 time the radial direction (Eaton and Hale 1993) and in the tangential it is about twice of the radial direction (Siau 1984). Since the vapor and free water flow rates are proportional to the permeability, the flow rate will be negligibly small in the transverse direction.

4.4. Moisture Evaporation in the Vacuum

In a perfect vacuum, water molecules escape from the solid interface without returning back to the solid, the evaporation rate can be computed from the Hertz-Knudson equation (Jones 1991):

$$J_e = 0.0583 \times P \times \sqrt{\frac{18}{T}} \quad \text{.....4.18}$$

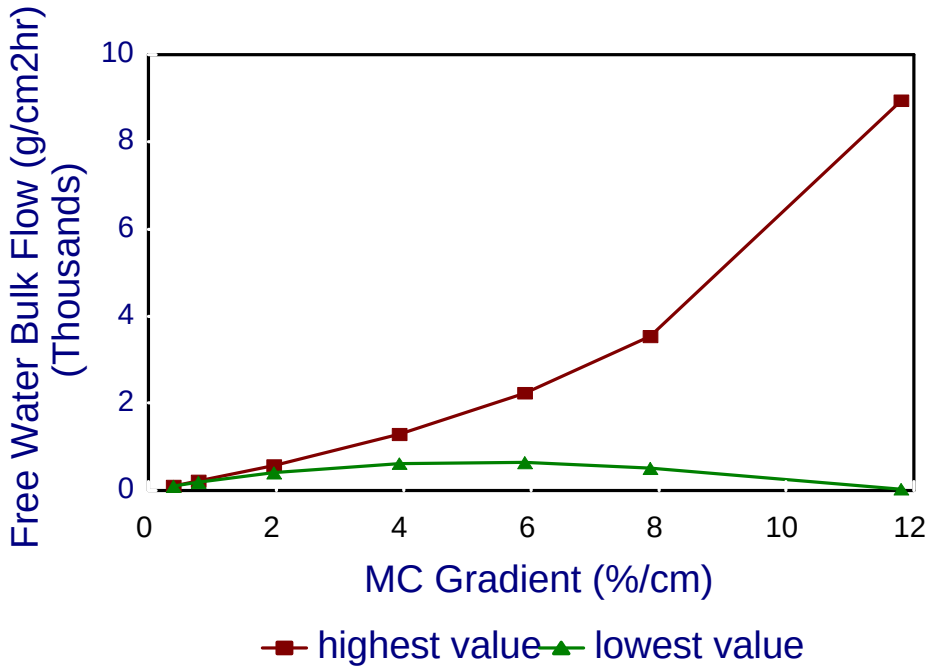

Figure 4.5 Calculated Free Water Bulk Flow Rate in Red Oak at MC of 70%

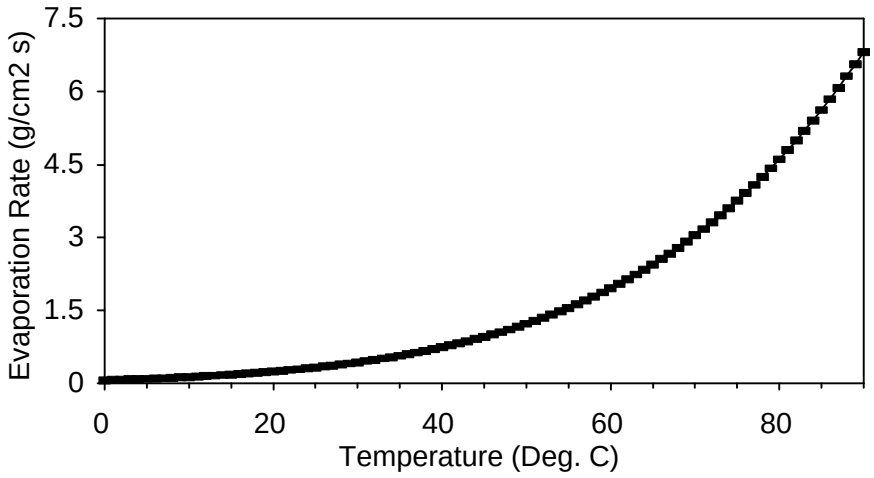

Figure 4.6 Calculated Relationship between Evaporation Rate of Water and Temperature in a Vacuum

where J_e is the evaporation rate, g/cm^2 s; P is the saturation vapor pressure of the water at the Kelvin temperature T, mm Hg.

The relationship between the evaporation rate and temperature is presented in Figure 4.6. This shows that evaporation in a perfect vacuum depends on the temperature only, the higher the temperature, the faster the evaporation rate.

4.5. Analysis of Moisture Movement During Drying

From the above calculations, we can see the magnitudes of several forms of moisture transportation. For a given moisture gradient in the longitudinal direction, generally speaking, moisture by FWBF is the largest, followed by WVBF and diffusion is the smallest (Figure 4.7). Surface evaporation is generally not a limitation in vacuum drying. Figure 4.8 and Figure 4.9 represent the moisture transportation in conventional kiln drying and in vacuum drying.

In conventional kiln drying, there is essentially no total pressure difference. Therefore, there is little or no WVBF. Furthermore, because surface evaporation at the beginning of drying is large, the surface MC drops below FSP, and there is no FWBF at the surface. In the inner layers, there is FWBF due to the MC gradient. Thus, diffusion occurs at or near the surface. Since the diffusion rate near the surface is much smaller than FWBF inside the wood, it controls the drying speed. Therefore the drying speed depends on diffusion rather than on FWBF in conventional kiln drying. In contrast, in vacuum drying WVBF near surface is larger than diffusion. However, it is still smaller than FWBF, and will control the drying speed in vacuum drying. It is necessary to point out that although longitudinal diffusion rates are not much larger than transverse diffusion rates, the difference in side surface area and end grain surface area in lumber are even greater. Therefore moisture removal from the side surface can not be neglected in conventional kiln drying. In contrast, for vacuum drying, WVBF controls the drying speed, because the ratio of longitudinal to transverse WVBF is much larger than the ratio of transverse to longitudinal surface area. Therefore, longitudinal moisture transport is dominant for common sizes of lumber in vacuum drying. This can be shown in the following example.

Assuming red oak lumber with the dimensions of 2 inches (5.08 cm) thick, 6 inches (15.24 cm) wide, and 8 feet (243.84 cm) long, the surface area of the end grain is 154.8 cm^2. The four side surface area is 9910 cm^2. The total area is 10065 cm^2. The volume is 18878 cm^3. Assuming the specific gravity of red oak is 0.56 (Alder 1995), so that the oven-dry weight of board is about 10572 grams. If the lumber is dried from green (71%) to 10% MC, the total water removed will be 6448 grams. If the diffusion rate at the moisture gradient of 10%/inch (3.94%/cm) for the transverse direction is 0.000867 g/cm^2 hr and for the longitudinal direction is 0.0048 g/cm^2 hr. According to this calculation, the drying rate will be 9.33 g/hr and it will take 691 hours (28.8 days) to dry to the final MC.

If WVBF at the temperature gradient of 5°C/inch (1.969°C/cm) is 0.323 g/cm^2 hr, then, the drying rate from the only end grain is 50 g/hr. Thus, it will take only 129 hours to dry the lumber to the final MC. Although the surface area available for diffusion is large, WVBF by the end grain is still 5.36 times faster.

From the above calculation, it is impossible that diffusion controls the vacuum drying process. Simpson (1987) stated it takes less than 10 days to dry wood under a vacuum. Many commercial processes take even less. Although the free water bulk flow rate is large, the surface evaporation is even higher. Very soon, there is not enough free water supply to the surface to evaporate, since surface MC is lower than critical MC. The vapor bulk flow from the end grain and the diffusion from the side face will control the drying process. In vacuum drying, diffusion is the same as in the conventional kiln drying or may be even smaller due to the lower temperature in vacuum drying (Kollmann and Cote 1968). Generally, WVBF plays a more important role than diffusion in the vacuum drying.

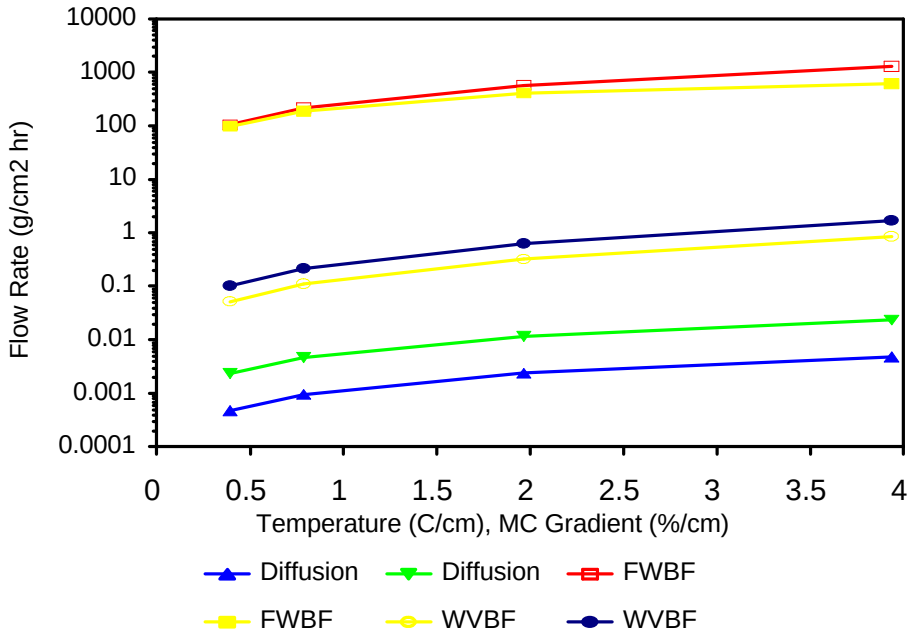

Figure 4.7 Comparison of Several Calculated Moisture Flow Rates in Red Oak

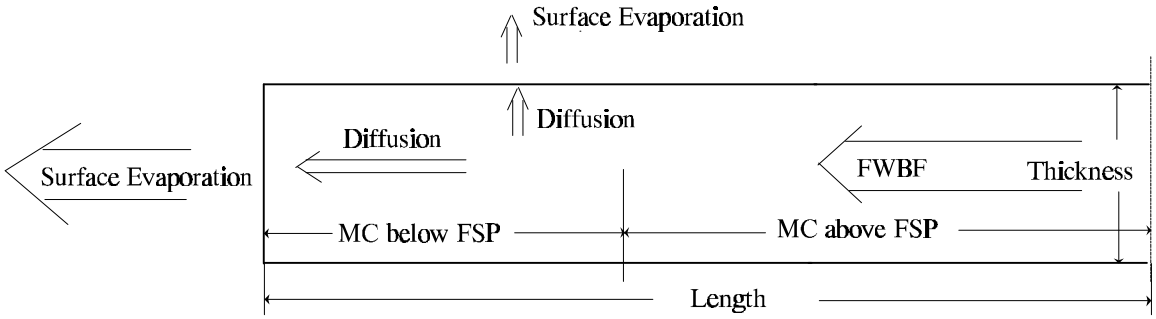

Figure 4.8 Diagram of Moisture Movement in Conventional Kiln Drying

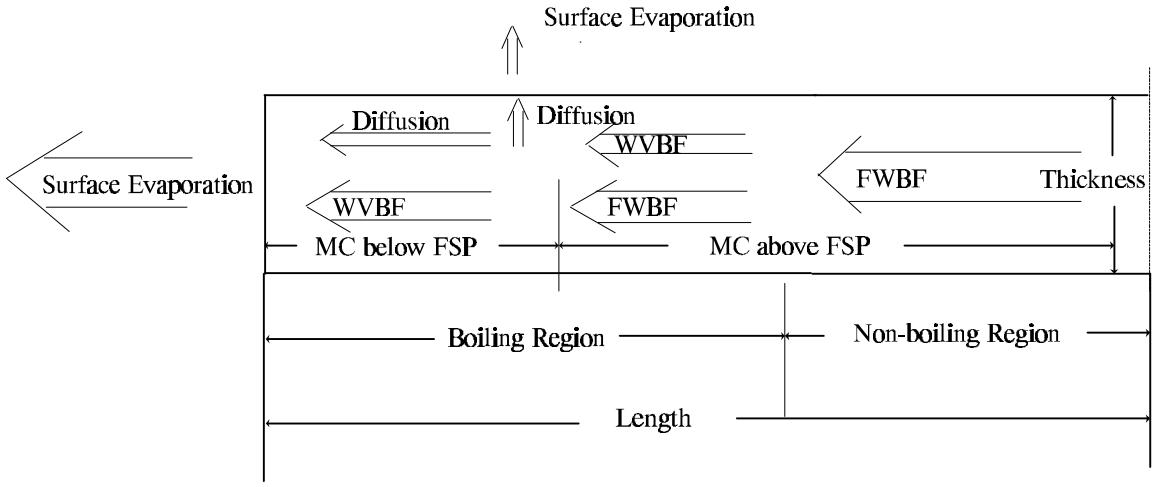

Figure 4.9 Diagram of Moisture Movement in Vacuum Drying

5. Wood as a Three-phase System

The three phases of ordinary water are represented in wood as follows: the solid phase consisting of the wood substance itself; the liquid phase consisting of free water; and the gaseous phase consisting of air and water vapor. It is important to analyze the proportion of these three phases inside the wood in order to better understand the mechanism of vacuum drying.

If shrinkage is not considered, then the volume of wood is equal to the sum of each phase (Skaar 1972):

$$V = V_w + V_a + V_m \text{.....5.1}$$

V is the total volume of wood; V_w is the volume of wood substance; V_a is the void volume; V_m is the volume of water or moisture in wood.

The wood substance fraction (v_w) can be calculated as (Skaar 1972):

$$v_w = \frac{V_w}{V} = \frac{W_w/d}{W_w/(Gd_m)} = \frac{Gd_m}{d} \text{.....5.2}$$

The water fraction (v_m) can be calculated as (Skaar 1972):

$$v_m = \frac{W_m/d_m}{W_w/(Gd_m)} = G \times MC/100 \text{.....5.3}$$

The air fraction (v_a) is the porosity (if water vapor not considered) which can be calculated (equation 4.6) as (Skaar 1972):

$$v_a = 1 - G \times (0.667 + MC/100) \text{.....} 5.4$$

where W_w and W_m are the weights of wood substance and moisture respectively; G is the specific gravity of the wood; d_m is the density of water, unity; MC is the moisture content of wood, (%); d is the density of wood substance, 1.5 g/cm^3 (Siau 1984).

The calculated results for the proportions of the three phases for red oak (G=0.56) are presented in Figure 5.1. It can be seen the percentage of wood substance does not change. The percentage of void increases as MC decreases. On the other hand, the percentage of water decreases as MC decreases.

Figure 5.2 and Figure 5.3 represent the proportion of the three phases at MC's of 30% and 60%. If the MC of red oak with SG of 0.56 is 60%, then the porosity of the wood is 0.29. The moisture volume fraction is about 0.336 and wood substance is about 0.374 which does not change with the MC if the wood is above FSP or if shrinking is not considered. This means that one cubic centimeter of red oak wood will contain 0.29 cm^3 void space, 0.374 cm^3 wood substance, and 0.336 cm^3 water. Water, in turn, consists of 0.168 cm^3 bound water and 0.168 cm^3 free water or 0.168 grams of free water and 0.168 grams of bound water.

In vacuum drying, the pressure inside the wood is larger than the environmental pressure. Thus, air in the environment can not enter the wood during drying. Instead, water evaporates into water vapor. Together, the water vapor and the air are removed by bulk flow driven by the total pressure difference. This is different from conventional kiln drying in which outside air enters the wood as MC decreases. The problem is what volume of air and water vapor will be removed during the vacuum drying process.

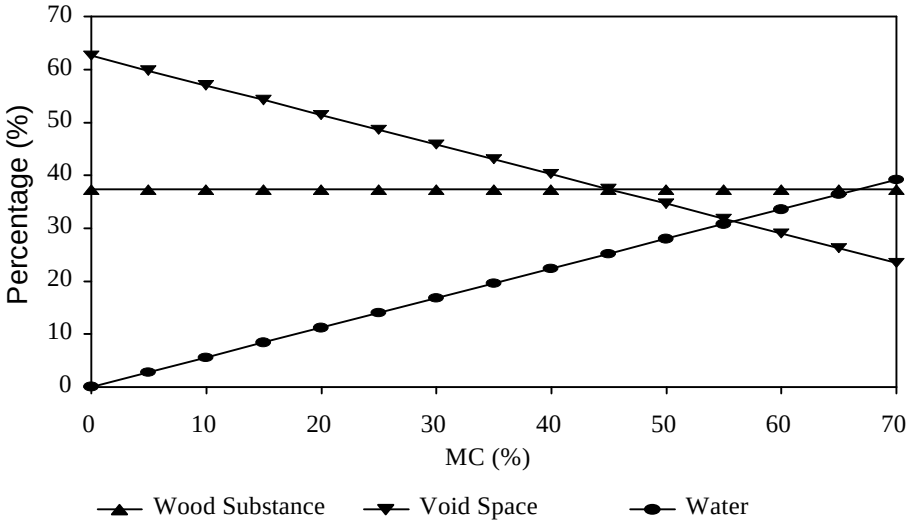

Figure 5.1 Calculated percentage of Three Phases in Wood in Relation to Moisture Content for Red Oak

For example, if 1 cm^3 red oak is dried from 60% to 10% final MC, the volume of air is 0.29 cm^3 at 60%MC. The moisture at 60% MC about 0.336 grams and at 10% MC is about 0.056 grams. Therefore, total moisture removed from 1 cm^3 wood is: 0.336-0.056=0.28 grams If this amount of water evaporates at the temperature of 50°C, the specific volume of saturated steam at this temperature is about 12032 cm^3/g (based on a steam table).

Then, the water vapor volume is: 0.28×12032=3369 cm^3. This is 11,617 times the volume of air inside wood. If only a small amount of the free water evaporates, its volume far exceeds the volume of air in the wood since the volume of air is decreasing. The water vapor volume increases significantly when evaporation takes place. If the evaporation takes place during vacuum drying, then gas bulk flow is dominated by the water vapor component. As a result, the volume of air inside the wood can be reasonably neglected.

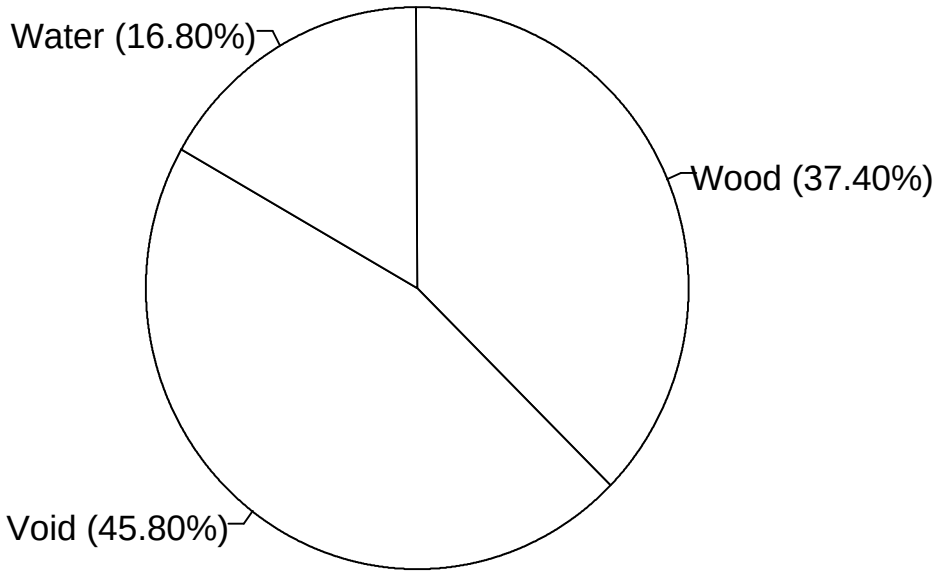

Figure 5.2 Calculated Volume Percentage of Three Phases in Wood at 30% MC for Red Oak

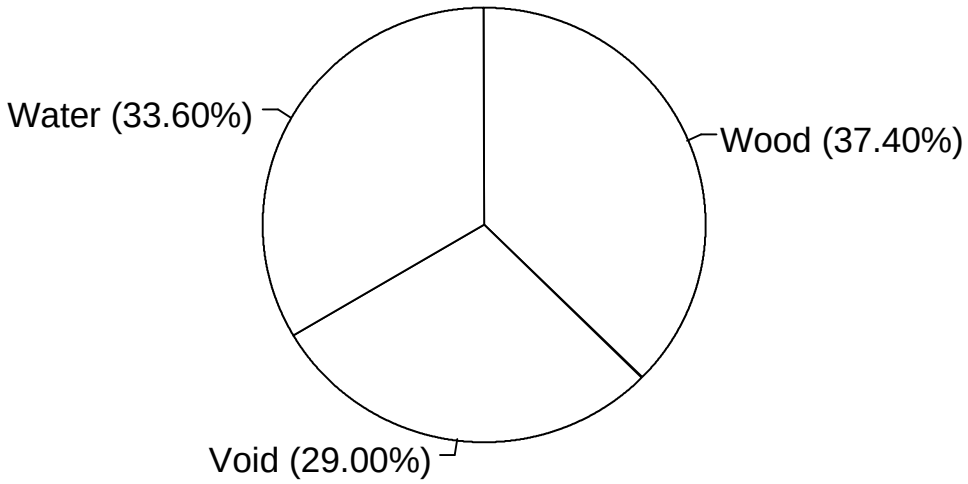

Figure 5.3 Calculated Volume Percentage of Three Phases in Wood at 60% MC for Red Oak

6. Equilibrium Moisture Content under Vacuum

The relationship of EMC with relative humidity and temperature of wood at the temperatures up to 100°C has been well established (Forest Product Lab. 1990). The relationship is based on Sitka. There are some EMC data above 100°C with the pure steam at atmospheric pressure (Simpson and Rosen 1981).

The knowledge of EMC under the vacuum is important for vacuum drying, since the water vapor pressure is closely related to the EMC at MCs below FSP. The Hailwood and Horrobin sorption theory has been applied to wood for many years. The sorption theory considers the wood as a polymer. Through calculation, Simpson (1971, 1973) derived the coefficients of the Hailwood and Horrobin model to estimate the EMC for Sitka spruce. He found the maximum deviation between the calculated values and EMC standard table is about 0.9% MC with the average standard deviation of 0.13% MC. Although based on Sitka spruce, it is suitable for other species (Simpson, 1973).

The Hailwood-Horrobin formulas to calculated EMC is (Simpson 1973):

$$MC=\left(\frac{K_1K_2h}{1+K_1K_2h}+\frac{K_2h}{1-K_2h}\right)\times\frac{1800}{W}\text{.....6.1}$$

where

$$K_1=4.737+0.04773T-0.00050123T^2\text{.....6.2}$$

$$K_2 = 0.70594 + 0.001698T - 0.0000055534T^2 .....6.3$$

$$W = 223.385 + 0.6942T + 0.018533T^2 .....6.4$$

where MC is equilibrium moisture content, (%); T is the Kelvin temperature; and h is the relative humidity, (%).

This model representing sorption isotherms are relatively simple analytically and gives excellent agreements with the experimental results in a broad range of relative humidity (Simpson 1973). Sorption isotherms are experimentally determined in the humid air at normal pressure. Voigt et al. (1940) proved this validity also for vacuum condition. Therefore, the Hailwood and Horrobin model which is used for normal atmospheric pressure can be applied to vacuum condition.

In atmospheric pressure, the relative humidity is defined as the ratio of the partial water vapor pressure in the air to the saturated water vapor pressure. Since there is no air in a vacuum, there is not partial air pressure. Thus, the absolute pressure in the system is the same as water vapor pressure. In such a vacuum drying system, there are two parameters: the absolute pressure and temperature. The relative humidity (h) in the vacuum system is defined as the ratio of the absolute pressure (p) in this system to the saturated vapor pressure (p_0) at a given temperature (T). The relative humidity in the vacuum is:

$$h = \frac{p}{p_0} \times 100\% .....6.5$$

With knowledge of relative humidity and wood temperature, the Hailwood and Horrobin model can be used to estimate the EMC of wood under vacuum. Figures 6.1 and 6.2 are the

calculated EMCs as function of temperature and water vapor pressure.

From the calculated results shown in these figures, the drying conditions in a cyclic vacuum drying system can be examined. When wood is heated to the required temperature, a vacuum is pulled to a given absolute pressure. During the drying, the pressure remains constant in the chamber. As a result, the relative humidity inside the chamber increases as moisture evaporates and wood cools. As the wood temperature decreases, the EMC of the system increases as drying continues. This is opposite to what happens in conventional kiln drying where the relative humidity is decreased by raising the dry bulb temperature in order to control the speed of drying. Whereas, the cyclic vacuum drying system actually is slowed because drying conditions become milder.

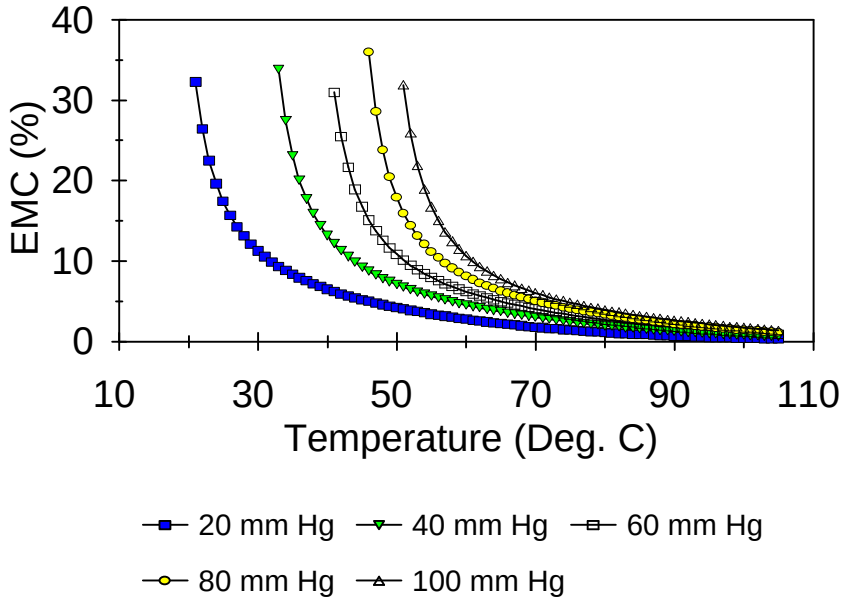

Figure 6.1 Calculated Equilibrium Moisture Content at Certain Pressures in Relationship to Temperatures

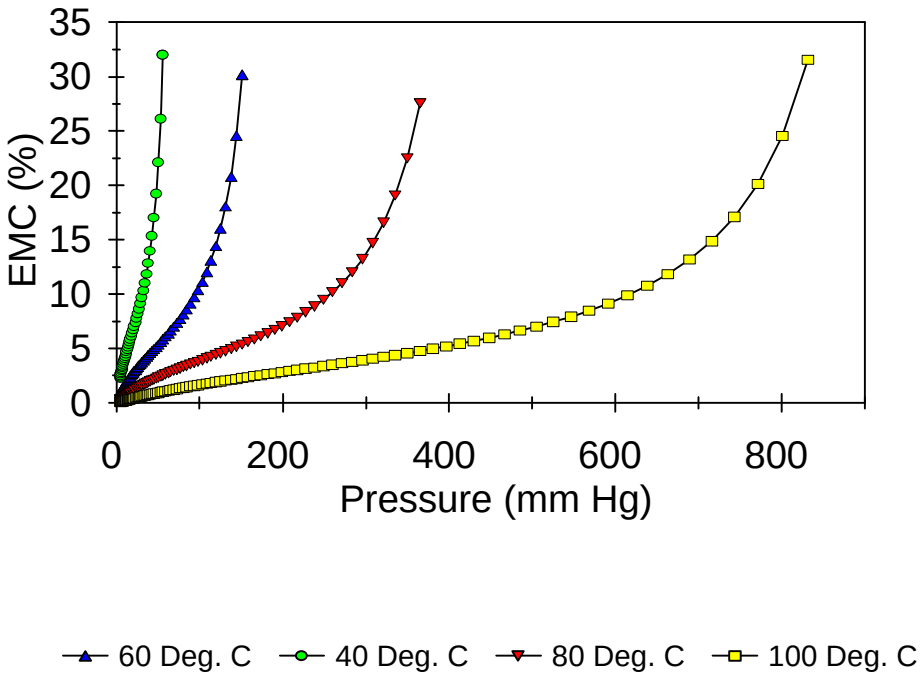

Figure 6.2 Calculated Equilibrium Moisture Content at Certain Temperature in Relationship to Pressures

7. Maximum Moisture Content Drop Per Cycle

The objective of this phase is to estimate the maximum moisture removal or the maximum moisture content drop per cycle in cyclic vacuum drying, assuming that there is no temperature gradient at the end of drying, and the final temperature is the saturation temperature at the ambient pressure. The principle of energy conservation is used to calculate the maximum amount of moisture removal during one cycle of vacuum drying. It is assumed that the amount of moisture to be removed in a cycle is M_r. From basic physics, the total energy (E_{mv}) required to evaporate moisture M_r is:

$$E_{mv}=M_r\times q.....7.1$$

where q is the heat of water vaporization.

At the beginning of a vacuum drying cycle, lumber is heated to the temperature T_b. T_f is the temperature at the end of the cycle. So, the change of energy (E_c) is:

$$E_c=C_m\times M_m\times(T_b-T_f)+\int_{T_f}^{T_b}C_w M_w dT.....7.2$$

where C_m and C_w are the specific heats of water and oven-dry wood respectively; M_m is the amount of water in the wood at the beginning of the cycle; M_w is the weight of oven-dry wood.

The moisture content (MC_b) at the beginning of this cycle is:

$$MC_b = \frac{M_m}{M_w} \times 100\% \text{.....7.3}$$

From energy balance consideration: $E_{mv}=E_e$, i.e. the evaporation energy is equal to the energy change in the wood. Combining equations 7.1 and 7.2,

$$M_r \times q = C_m \times M_m \times (T_b - T_f) + \int_{T_f}^{T_b} C_w M_w dT \text{.....7.4}$$

The amount of water removed during a cycle is:

$$M_r = \frac{C_m \times M_m \times (T_b - T_f) + \int_{T_f}^{T_b} C_w M_w dT}{q} \text{.....7.5}$$

where the saturation temperature (T_f) is determined by the ambient pressure p (equation 3.2).

The specific heat of dry wood varies with temperature (equation 3.5). Substituting equation 3.5 into equation 7.5 and integrating between T_b and T_f, gives:

$$M_r = \frac{(C_m \times M_m + 0.266 \times M_w) \times (T_b - T_f) + 0.00058 \times M_w \times (T_b^2 - T_f^2)}{q} \text{.....7.6}$$

From above analysis, the amount of moisture removal in a given cycle is determined

the temperature of wood at the beginning and end of drying.

The corresponding MC drop (MC_d) in a cycle is given by combining equations 7.3 and 7.6.

$$MC_d = \frac{M_r}{M_w} \times 100\% = \frac{(0.266 + 0.01MC) \times (T_b - T_f) + 0.00058 \times (T_b^2 - T_f^2)}{2370.7/4.18} \times 100\% \quad \text{.....7.7}$$

Based on this formulas, the maximum MC drop in a cycle can be calculated for the different ambient pressures and the temperatures T_b and T_f, . The result is presented in Figure 7.1.

For example, the lumber at the beginning of drying is heated to 60°C. The initial MC of lumber is 71%. The latent heat of water is not significantly affected by the temperature range used in this calculation. The latent heat at the mean temperature of 40°C is 2370.7 J/g. For temperature of 60°C and the MC of 71%, T_f is about 23°C, then the maximum MC drop for one cycle is about 6%.

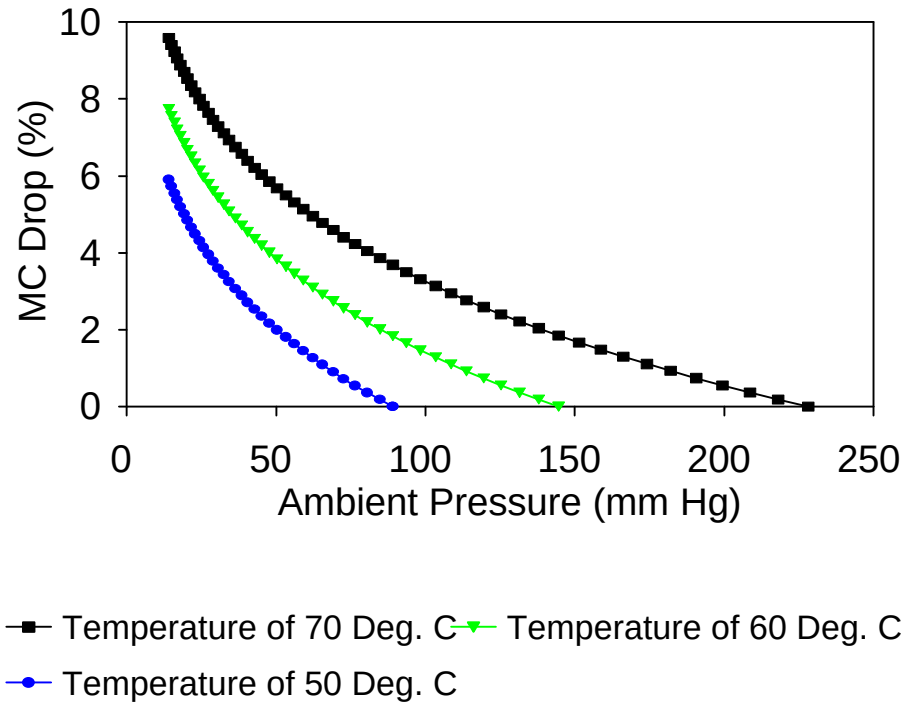

Figure 7.1 Calculated Theoretical Maximum Moisture Content Drop in a Cycle in Cyclic Vacuum Drying for MCs above FSP

8. Modeling the Cyclic Vacuum Drying Process

8.1. Objective

The objective of this phase is to develop the heat and mass transfer equations by using present vacuum drying knowledge, together with certain assumptions. By using the equations developed, the drying curve, temperature, pressure MC distribution can be determined.

8.2. Statement and Mathematical Formulation of the Problem

The mechanism of vacuum drying depends on the pressure inside the vacuum dryer and the physical properties of the wood. In the case of cyclic vacuum drying, the lumber is heated to a given temperature, and then a vacuum is pulled. It is well known that at any fixed pressure there exists a temperature at which water boils. Boiling occurs in the wood because the lumber temperature is higher than the saturation temperature inside the vacuum dryer. At the beginning, boiling occurs on the surface, then the boiling front retreats inward. The moving boiling front divides the system into two regions, namely, the boiling region and non-boiling region. In the boiling region, moisture occurs in the form of mixed vapor and liquid. In the non-boiling region, the moisture is in liquid form if the small amount of water vapor contained in the air trapped in the lumen is neglected (Bramhall 1979b).

Most vacuum drying models do not consider the pressure distribution and the boiling phenomena; instead, they consider the mechanism as diffusion (Moyne and Degoivanni 1995). As discussed in Chapter 4, diffusion is relatively small, and can be neglected.

The following model is for one cycle in the cyclic vacuum process. The typical cyclic drying chamber is equipped with heating coils and ventilators. The lumber is stacked in the conventional way. Heating is done by circulating air within the chamber. Once the temperature of the lumber reaches the required temperature, the vacuum phase is initiated and the drying process starts.

For the purpose of formulating the cyclic vacuum drying model, the following assumptions are made.

I) Two-dimensional (longitudinal and transverse) heat and mass transfer is considered, since

there is little difference between radial and tangential permeability values, and lumber width is much larger than its thickness.

ii) At the beginning of drying, the lumber is initially at a uniform temperature, pressure, and MC.

iii) The rate of evaporation from the lumber surface is very high. The lumber surface reaches equilibrium with the surrounding atmosphere when evaporation starts (Vergnaud 1982).

iv) Heat convection, and radiation to the surface of the lumber, thermal expansion, shrinkage of lumber, and Soret effects are all assumed to be small and therefore negligible (Vergnaud 1982).

v) The lumber is dried by maintaining the drying chamber at constant vacuum pressure and temperature.

vi) The differential heat of sorption is considerably smaller than the heat of water vaporization and is neglected (Vergnaud 1982).

8.2.1. Governing Equations

The problem of heat and mass transfer during cyclic vacuum drying is to obtain a simultaneous solution of coupled heat and mass transfer with a moving boiling front which separates the boiling and non-boiling regions (Figure 8.1).

In the non-boiling region, heat conduction is described by Fourier's equation:

$$\lambda \frac{\partial T}{\partial t} = \kappa_l \times \frac{\partial^2 T}{\partial x^2} + \kappa_t \times \frac{\partial^2 T}{\partial y^2} \quad \text{.....8.1}$$

where κ_t and κ_l are the thermal conductivities of wood in the transverse and longitudinal directions; $\lambda = c \times \rho$; c and ρ are the specific heat and density of wood respectively.

Similarly, the pressure distribution can be characterized by the equation (Siau 1984):

$$\alpha \frac{\partial P}{\partial t} = \kappa_{gl} \times \frac{\partial^2 P}{\partial x^2} + \kappa_{gt} \times \frac{\partial^2 P}{\partial y^2} \text{.....8.2}$$

where κ_{gl} and κ_{gt} are the gas permeability values of wood in the longitudinal and transverse directions. $\kappa_g = K/\eta$, where K is the specific permeability and η is the viscosity; term α can be expressed:

$$\alpha = \frac{V_a}{\rho_g RT} = \frac{V_a}{P} \text{.....8.3}$$

where V_a is the void fraction or porosity of wood; R is the gas constant, ρ_g is density of gas.

In the boiling region, the effect of mass transfer on heat transfer will be also considered. According to the first law of thermodynamic for a control volume, the energy equation can be written as follows:

$$\frac{dE}{dt} + h_e \dot{m}_e - h_i \dot{m}_i = \dot{Q}_i - \dot{Q}_e \text{.....8.4}$$

where, h is the enthalpy, $\dot{m}$ is the mass flow rate, dE/dt is the rate of energy change inside the control volume, and the subscript of e and i represents the flow out and into the control volume which include the free water and water vapor, $\dot{Q}$ is conduction heat transfer (see Appendix B).

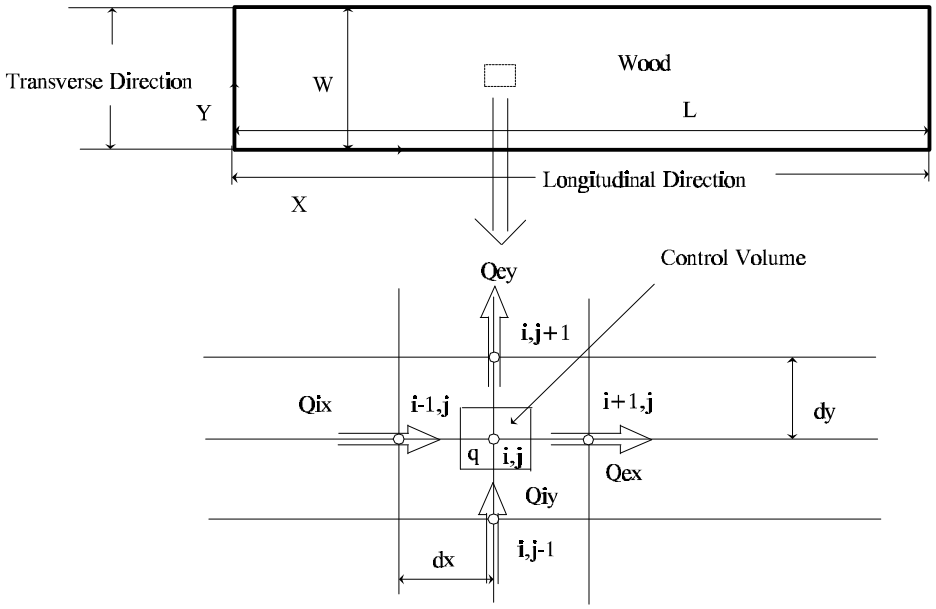

Figure 8.1 Schematic Diagram of Two Dimentional Transfer in Wood

It requires heat to evaporate water. The amount of water evaporated is assumed to be the same as the water vapor removed from the control volume. Equation can be rewritten as following partial equation (see Appendix B) :

$$\lambda\frac{\partial T}{\partial t}=\kappa_l\times\frac{\partial^2 T}{\partial x^2}+\kappa_t\times\frac{\partial^2 T}{\partial y^2}-\frac{dmu}{dtdxdy}-\frac{h_e\dot{m}_e-h_i\dot{m}_i}{dxdy}\text{.....8.5}$$

where u is the internal energy of water in liquid form, h is the evaporation heat and dm is the weight loss in the dt time interval. And the dm/dt is the drying rate.

The thermodynamic relationship between saturated pressure and temperature is given by equation 3.2. When drying starts, the pressure decreases in the lumber. The pressure on the surface decreases first, and water on the surface rapidly evaporates (Jones 1991). As drying continues, the pressure inside the wood is lowered because both moisture content and temperature decrease. When the pressure is equal to or less than the saturated pressure at the local temperature, water inside the lumber boils. The region where the pressure is equal to or less than the saturated pressure at the local temperature is considered to be the boiling region.

8.2.2. Boundary Conditions

Because of the low atmospheric pressure in the vacuum chamber, heat convection inside the kiln is small and can be neglected. The mass transfer coefficient is very high due to rapid water evaporation from the surface of the lumber (Jones 1991). Therefore, the surface pressure is close to the environmental pressure in the chamber.

The boundary conditions in the lumber are expressed in the following formulas (see Figure 8.2):$P_{(X=L/2 \text{ or } Y=W/2)}$=Po, $dT/dx_{(X=L/2)}$=0 and $dT/dy_{(y=w/2)}$=0, $dP/dx_{(x=0)}$ and $dT/dx_{(x=0)}$=0, $dP/dy_{(y=0)}$ and $dT/dy_{(y=0)}$=0

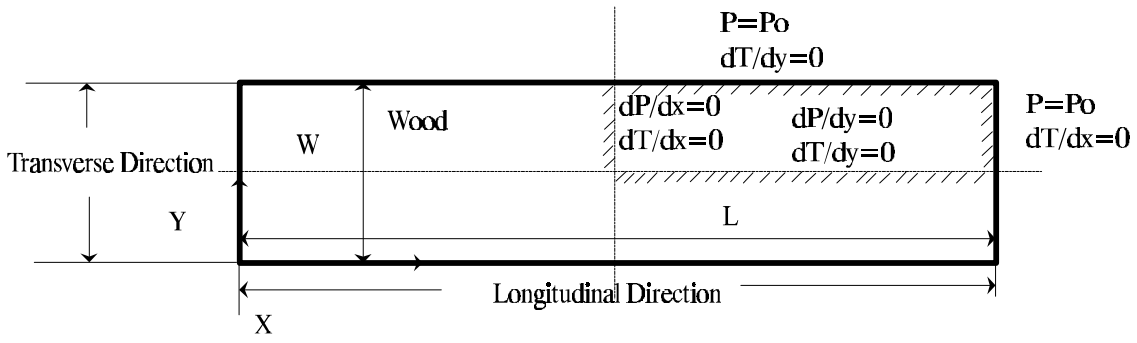

Figure 8.2 Schematic Diagram of Boundary Conditions

8.2.3. Physical Properties of Wood and Thermodynamic Relationship .

The relationship between thermal conductivity and MC has been developed empirically (Siau, 1984). The thermal conductivity for wood in the longitudinal direction is given by equation s 3.3 and 3.4. Thermal conductivity of wood in the tangential direction is related to that in the longitudinal directions by:

$$\kappa_t = 2.5 \times \kappa_l \text{.....8.6}$$

The porosity of wood is given by the empirical equation 4.6. The relation between the specific heat of wood and its MC is given in equation 3.6. The density of wood is as following: $\rho = G \times (1 + 0.01 \times MC) \times \rho_{w,}$ where ρ_w is density of water.

The zero enthalpy reference state is chosen to be 0°C and 1 atmosphere pressure. The enthalpy of water vapor is then a function of temperature only.

The relation of enthalpy (h) (J/g) with temperature T (°C) is as (Stanish et al 1986):

$$h = 1650 + 4020 \times (273 + T) - 0.00343 \times (273 + T)^2 \text{.....8.7}$$

The air viscosity η_{ga} (dyne/cm^2) is:

$$\eta_{ga} = 4.06 \times 10^{(-7)} T + 6.36 \times 10^{(-5)} \text{.....8.8}$$

The viscosity of saturated steam η_{gv} (dyne/cm^2) is:

$$\eta_{gv}=3.8\times10^{(-7)}T-1.57\times10^{(-5)}.....8.9$$

If there is free water, the gas phase at any point is assumed to be saturated at the local temperature. The saturated water vapor density for steam tables over the temperature range T of 27 to 200 °C is as following (Stanish et al 1986):

$$\rho_v=10^{-3}\times Exp(-46.49+0.26179\times T-5.0104\times10^{-4}\times T^2+3.4712\times10^{-7}\times T^3).....8.10$$

ρ_v is the vapor density in g/cm^3. T is temperature , °C

The gas and liquid permeability of wood will vary with MC, as discussed in Chapter 4. The longitudinal gas permeability of dry red oak is 59 darcy, and the liquid permeability of saturated red oak is 139 darcy (Choong and Tesoro 1974). For white oak, these two values are 0.712 and 0.604 darcy respectively (Choong and Tesoro 1974). For red oak, the ratio of longitudinal to radial permeability is 4.9×10^8 according to Eaton and hale (1993).

In this model, the size of the board is 8 feet long (244 cm) and 2 inches thick (5.08 cm). The width of board is neglected. A quarter of this size is 122 by 2.54 cm. The quarter size board will be solved in the computer program.

The empirical constants which are used in the calculations are listed in the table below.

Table 8.1 Empirical Constants in the Model

SG of Red Oak	0.56	SG of White Oak	0.60
Initial MC	71 (%)	Initial Temperature	70°C
Initial Pressure	101325 (pa)	Ambient Pressure	7330 (pa)
Internal Energy of Water	250.91 (j/g)		

8.3. Solution of the Problem

The governing equations of temperature and pressure in both the boiling region and in the non- boiling regions are second order partial derivative equations. Patankar (1981) developed a computer program called CONDUCT that can be used to solve such second order equations. This program is designed for isotropic materials. It was slightly modified to be used for an anisotropic material such as wood. A subroutine (see Appendix A) was written in order to adapt this program to our problem. In the boiling region, there is a heat sink, that is, the energy is required to evaporate the water from wood. CONDUCT has been successfully used in solving problems of heat transfer and viscous incompressible flows (Sparrow et. al. 1978, Karki and Patankar 1988). The finite-difference form on the spatial derivatives developed in CONDUCT has also been used in wood drying models (Stanish et al. 1986). The grid number is 20 and time step is 10^{-6} hr.

8.4. Result of Modeling

The computational results of the computer program provide the pressure, temperature and MC distribution data. From these, the drying rate and boiling front information can be obtained.

8.4.1. Temperature, Pressure, and Moisture Content Distributions

For red oak, the pressure, temperature and MC distributions are presented in Figures 8.2 to 8.4. The X axis is the distance from the center measured along the longitudinal direction. Similar curves were found for white oak. The temperature, pressure and MC distributions are in the

longitudinal direction at different times of the lumber drying. There are no appreciable temperature, and pressure differences in the transverse direction.

Pressure inside the wood is lowered due to mass loss during drying. At the beginning, the mass loss is mostly air. When the pressure is lower than saturated pressure, water boils. In the non-boiling region temperature distribution is affected by heat conduction only, the pressure and temperature distributions are essentially parabolic. In the boiling region, the pressure and temperature distribution are related. The pressure is saturated at the local temperature when the MC is above FSP. In the absence of free water, the total pressure is assumed to be at equilibrium with the local temperature and MC, and pressure is less than the saturation pressure. Generally the temperature gradient is small due to the relatively large thermal conductivity (Figure 8.3).

MC distribution is affected by FWBF when a moisture gradient is presented. However, the moisture gradient is relatively small due to the large FWBF. White oak is a less permeable species in which case the MC gradient is larger than for red oak. Also its drying rate is smaller than for red oak.

8.4.2. Movement of the Boiling Front

Figure 8.5 shows the movement of the boiling front along the longitudinal direction for red oak and white oak respectively. When the pressure is lower or equal to the saturated pressure at the local temperature, water boils. This happens during vacuum drying. At first, boiling occurs on the surface. The boiling front then moves toward the center of wood as drying continues leaving a boiling region behind. At the beginning of drying, because the temperature of the lumber is higher than the saturation temperature, moisture in the surface evaporates and transfers out. As moisture flows from the lumber, the pressure decreases and boiling occurs in the inner layers, and the boiling front moves toward the center in the longitudinal direction. From the boiling front to the center, the local pressure is higher than the saturated pressure at the local temperature; therefore, boiling does not occur. From the result of the CONDUCT program , the boiling extends into the whole board very rapidly for red oak (permeable wood). It takes less than one half of minute when FWBF is considered (Figure 8.5). However for less permeable woods, such as white oak, it takes longer. In

this situation, it takes almost 15 minutes. The retreating speed of the boiling front strongly depends on the longitudinal permeability of the wood.

8.4.3. Drying Curve Analysis

The drying curves calculated by the computer program for red oak and white oak are presented in Figure 8.6. Vacuum drying curves look similar to conventional kiln drying curves. Wood dries faster at the beginning and more slowly later. This is due to the reduction in pressure difference as vacuum drying continues (Figure 8.2). As expected, it takes longer to dry white oak than red oak due to the difference in their permeability values. The drying rate is related to the permeability but not linearly.

8.4.4. Conclusion of Modeling

The following conclusions can be made from this modeling. In vacuum drying, the drying rate is controlled by water vapor bulk flow, unlike the situation in conventional kiln drying which is controlled by diffusion rates. Drying speed depends on the wood temperature, vacuum pressure, and the properties of the wood (mainly permeability).

There is a boiling front, which retreats toward the center of the board as drying proceeds, and the retreating speed depends on the permeability. Pressure inside the wood is maintained by rapid vapor generation. There are little heat and moisture losses through the sides of board due to the lower permeability in the transverse direction. Most moisture loss is through the end grain during vacuum drying. Drying rate, movement of the boiling front, and MC distribution are strongly depended on the permeability.

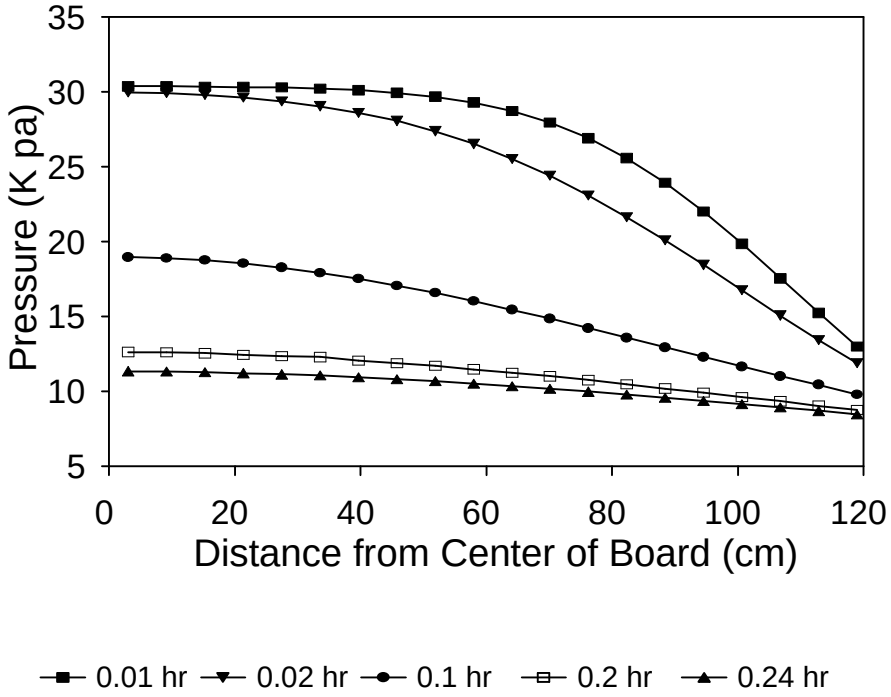

Figure 8.3 Calculated Pressure Distribution from the Vacuum Drying Model for Red Oak

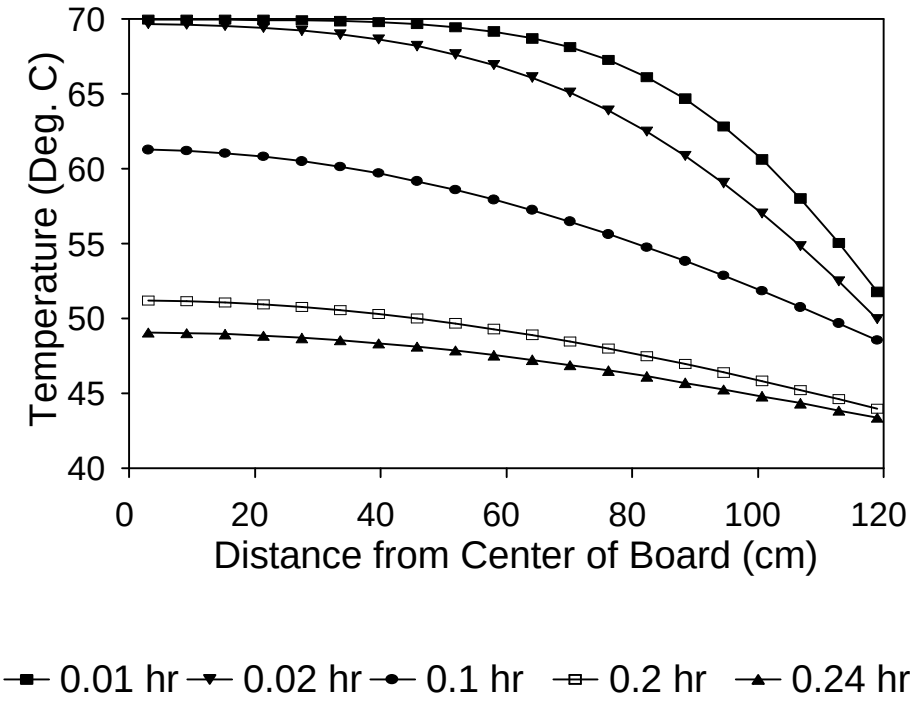

Figure 8.4 Calculated Temperature Distribution from the Vacuum Drying Model for Red Oak

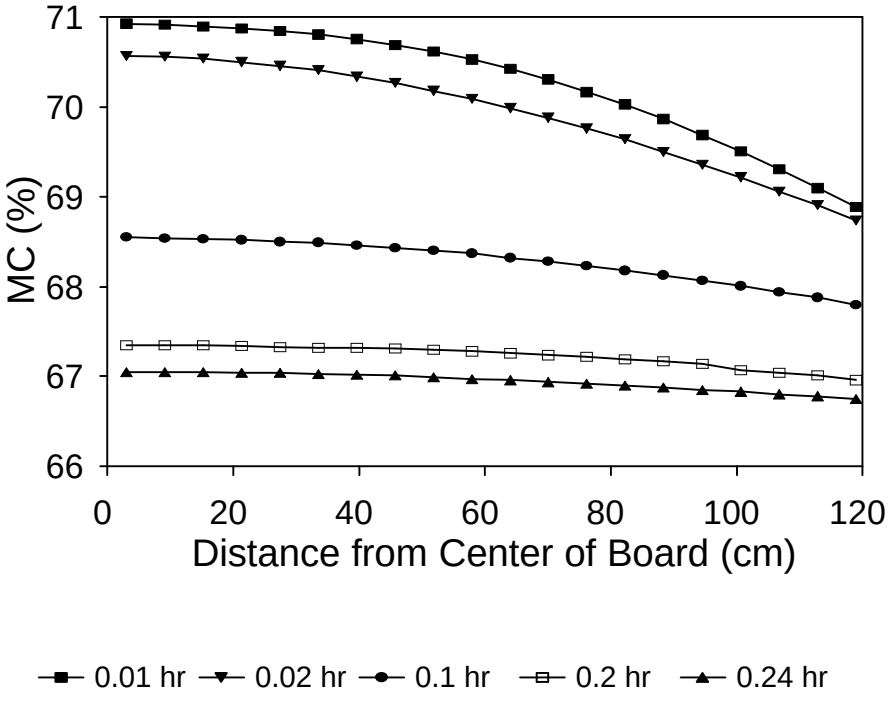

Figure 8.5 Calculated MC Distribution from the Vacuum Drying Model for Red Oak

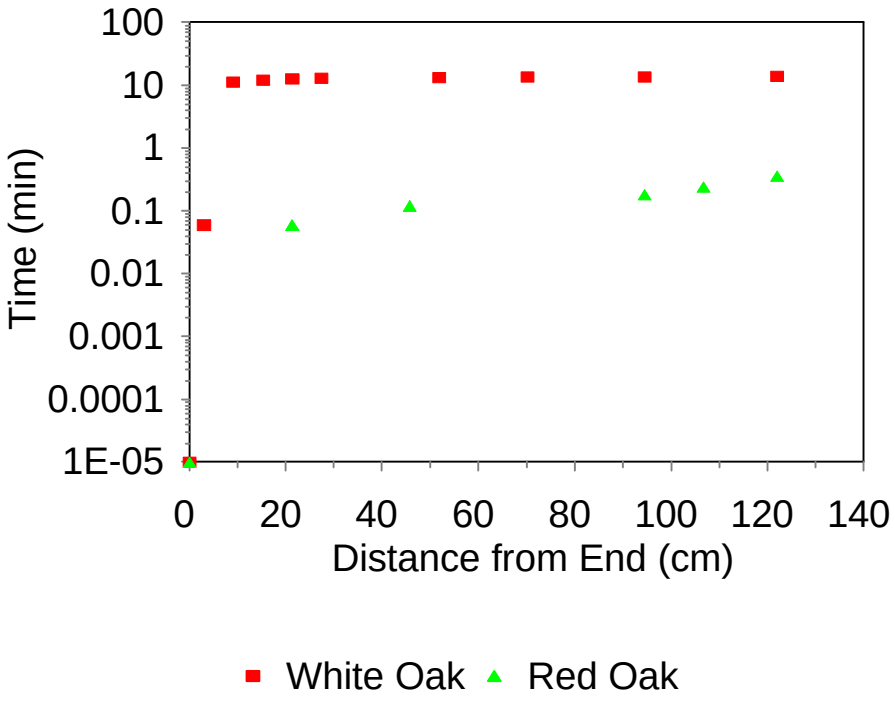

Figure 8.6 Locations of Calculated Boiling Front for Red and White Oaks from Vacuum Drying Model

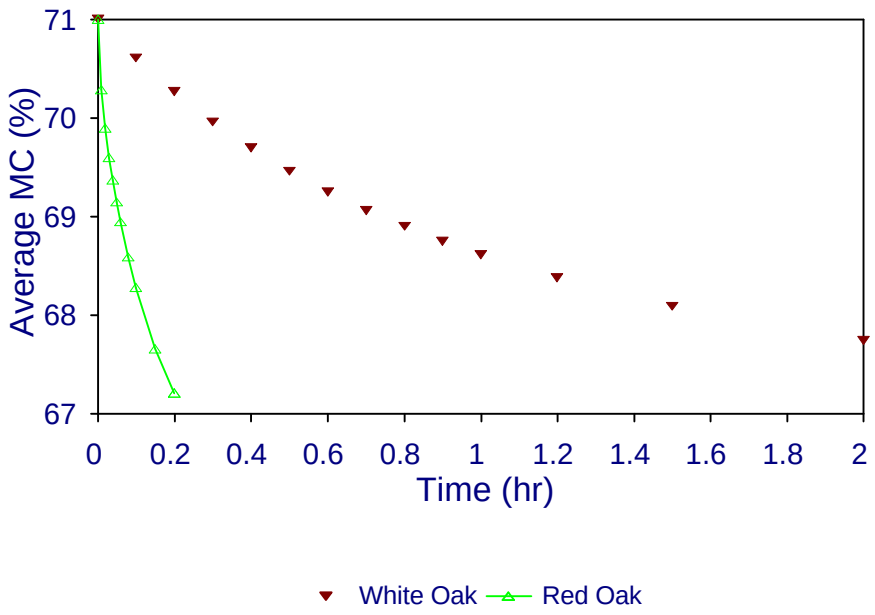

Figure 8.7 Calculated Drying Curves for Oaks from Vacuum Drying Model

9. Experimental Equipment and Materials

From the proceeding theoretical development, most of the water moves along the longitudinal direction in vacuum drying because the total pressure difference inside the wood acts as the primary driving force. As a result, a moisture gradient develops along the length. Generally, the longitudinal permeability of wood is large, and the small differences in total pressure inside the wood causes water vapor and/or air to move out of the wood. Boiling occurs inside the wood during vacuum drying when the pressure inside the wood is lower than saturation pressure. A boiling front retreats towards the center of specimen as drying proceeds. Even at low temperatures, the water evaporation rate is very large under vacuum conditions, which makes room temperature drying possible. The following experiments are used to test these theoretical consideration.

The experimental system consisted of a vacuum oven, vacuum pump, and cooling system. A Napco vacuum oven (model 5861) was used having the inside dimensions 46 (deep) by 61 (high) by 46 (wide) cm (Figure 9.1). A electrical heating device, located on the bottom and two sides, controls temperature inside the vacuum oven. The oven is rated to maintain an absolute pressure near 0 mm Hg. All pressures later referred to are absolute pressures. A Busch oil sealed pump (model RA 0025-A005-1001) was connected to the vacuum oven and is capable of pulling a vacuum to 15 mm Hg. A water cooled Neslab cooling system (model CC-70W) was used to provide the low temperature needed for the vapor freezing traps. The pressure-time performance of this system is shown in Figure 9.2, using an empty chamber. The curve shows the figure to pull vacuum on the empty chamber. A conventional drying oven (model 3-100, Scientific Equipment MFG Corp.) was used to heat the sample to the required temperature for the cyclic vacuum drying.

During the experiments, temperatures were measured with a resistance temperature device (RTD) having an accuracy of ±0.1 C. The pressures were measured using pressure transducers (model # PX213-015A5V, Omega Co.) having an accuracy of ±2 mm Hg. Weights were measured by a load cell (model # LC601-5 Omega Co.) with a capacity of five pounds (Figure 9.3).

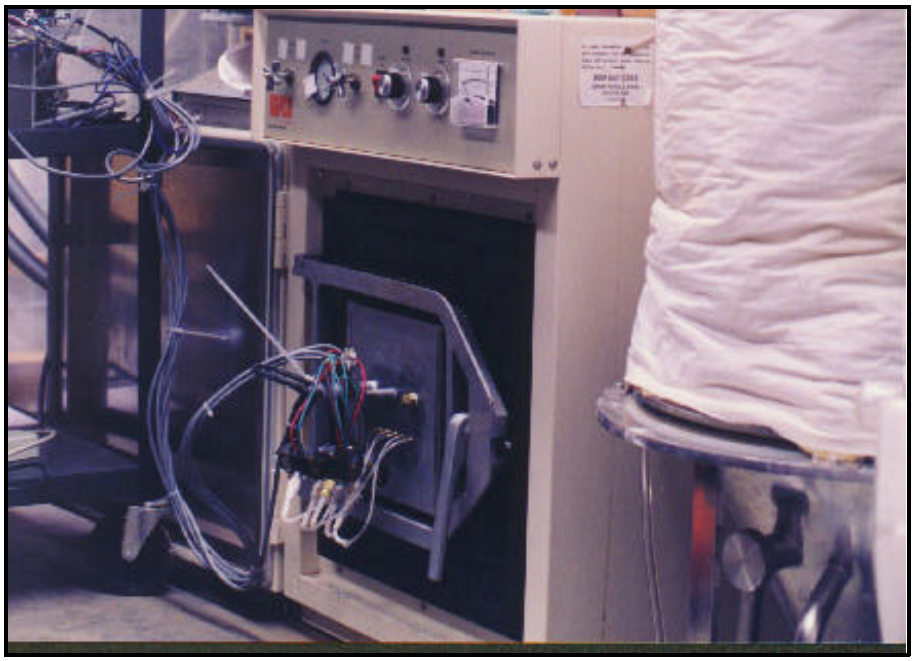

Figure 9.1 Vacuum Oven Used in Experiment

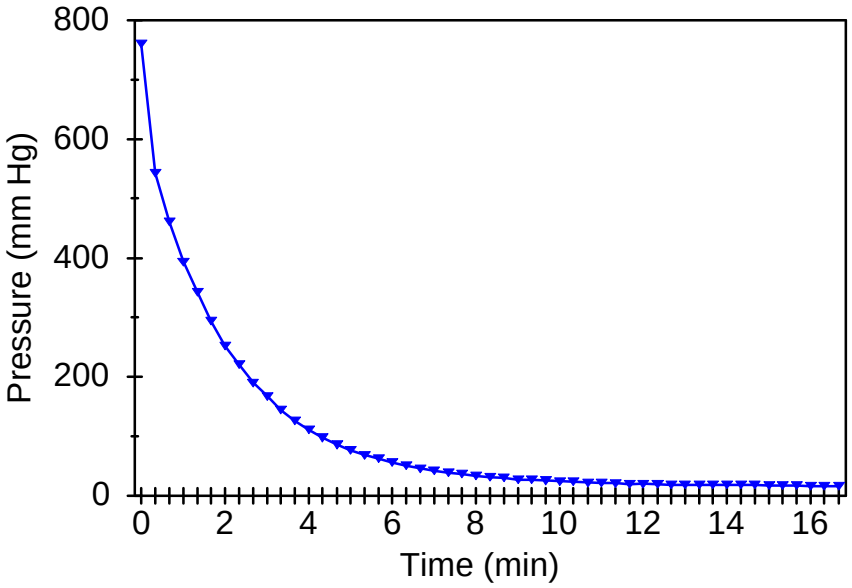

Figure 9.2 Performance Chart of Experimental Vacuum System

Data were recorded by the data acquisition system (Figure 9.4). The data acquisition system consists of computer with 12-bit, 16-channel analog-digital conversion board operating under program control EG. This program provides sequencing, scanning and mathematical conversion to engineering units.

The wood samples used in all experiments were selected from red oak or white oak heartwood. The 8.5-foot long log of white oak and 11.5-foot long logs of red oak were obtained from the local area. The small end diameters of the red oak and white oak log were 12 and 10 inches, respectively. Flatsawn boards were cut from these logs in the sawmill at Virginia Tech. The boards, other than those used immediately after sawing, were wrapped in plastic and stored in a cold room (0°C) to prevent decay and moisture loss prior to drying.

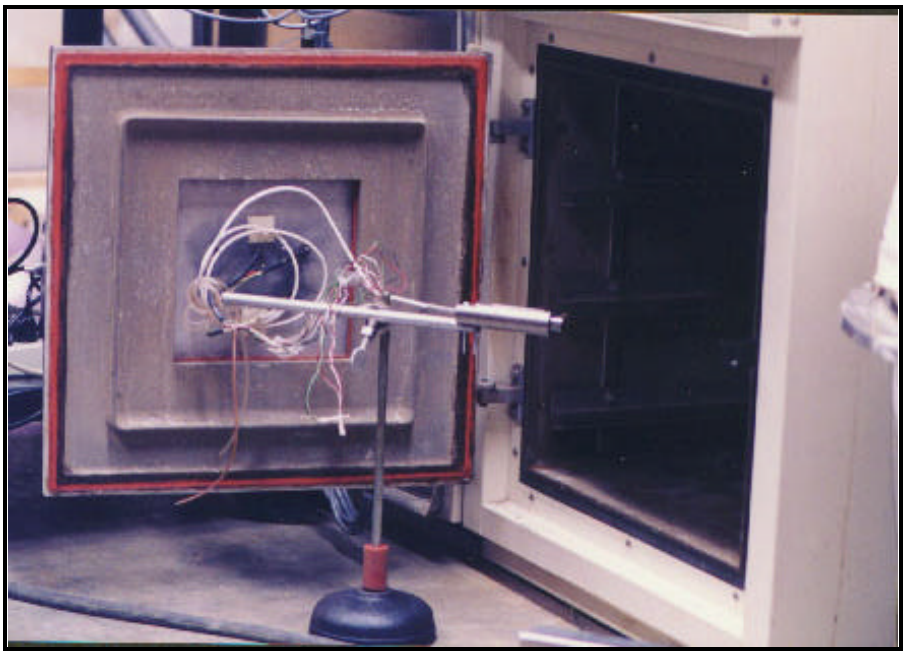

Figure 9.3 Load Cell Used to Measure Weight

Figure 9.4 Data Acquisition System

10. Effect of Specimen Size on Drying Rate

As in all other wood drying systems, energy is also required to evaporate the water in vacuum drying. In cyclic vacuum drying, the specimens are usually heated to the required temperature and then a vacuum is pulled. Most vacuum studies have been done with the heating and vacuum processes occurring in the same oven so that the ambient temperature was kept high during the vacuum phase (Zhao 1988). After the vacuum was pulled, the wood temperature decreased rapidly and became lower than the ambient temperature due to the evaporation and removal of water from the specimen. As a result, there was some heat transfer between the ambient environment inside the chamber and the wood during the vacuum phase in most studies. If the ambient temperature is high, there is a potential for significant heat transfer which will affect the drying process, especially, the drying rate and drying quality. In order to reduce the heat transfer between the wood and the surroundings, the specimens were heated in an oven and then transferred to and dried in a vacuum oven at room temperature. This allowed the wood to dry at or near room temperatures, in contrast to other studies.

The wood permeability in the longitudinal direction is more than ten thousand times higher than in the transverse direction. The permeability values for red oak and white oak in the longitudinal direction are 60 and 0.7 darcies respectively. The permeability values for red oak and white oak in transverse direction are 0.004 and 0.0004 darcies respectively (Choong and Tesoro 1974). If WVBF controlled by permeability is dominant in vacuum drying, it is expected that most of water would move in the longitudinal direction. If this is so, the width and the thickness of specimen should not significantly affect the drying rate. On the other hand, the drying rate should be related to specimen length.

10.1. Objective

The objective of this phase of the experiment was to explore how the thickness and length of the specimen affect the vacuum drying rate. In order words, it was to explore whether specimens

with different thicknesses and the different lengths have different vacuum drying rates. Both cyclic and continuous vacuum drying was investigated.

10.2. Experimental Procedure

Specimens were cut from green heartwood of the flatsawn red oak boards. Ten inches (254 mm) sections were cut from both ends of boards and discarded (Figure 10.1). One-inch (25.4 mm) moisture sections from both ends were cut to measure the initial MC of board. In order to examine the relationship between thickness and drying rate, four different sizes of specimens were used: 1 inch (25.4 mm) square, 1.5 inches (38.1 mm) square, 2 inches (50.8 mm) square and 2.5 inches (63.5 mm) square in cross-section, all with a length of 10 inches (254 mm). In order to examine the relationship between the length and drying rate, specimen lengths of 5 inches (127 mm), 10 inches (254 mm) and 15 inches (381 mm), all specimens having cross-section of 1.5 inches (38.1 mm) square were used. The maximum length of specimen was limited by size of the vacuum oven. The drying information on ten inches long specimens in study of effect of the length on drying rate was obtained in the experiment on the effect of thickness on the drying rate since the specimens were the same size. One specimen in each drying load was used to measure temperature. In this specimen, a 1/8 inches (3.715 mm) diameter hole was drilled about half way through the thickness in the center of the specimen to allow the measurement of center temperature. This method to measure center temperatures was used for all experiments.

In order to separate those factors, such as heat supply from the environment, which may affect the drying rate in cyclic vacuum drying, two ovens were used. A conventional heating oven was used to heat specimens to the required temperature, while the vacuum oven was maintained at room temperature (around 20°C). The temperature in the heating oven was set at 60°C. In order to avoid losing moisture during heating, the specimens were wrapped in plastic film and sealed in plastic bags. Before specimens were wrapped, they were weighed. The center temperature of one specimen in the heating oven was determined using a K-type thermocouple. When the temperature reached 60°C, the specimens were removed from the heating oven, the plastic removed, and the specimens were

Unit: mm

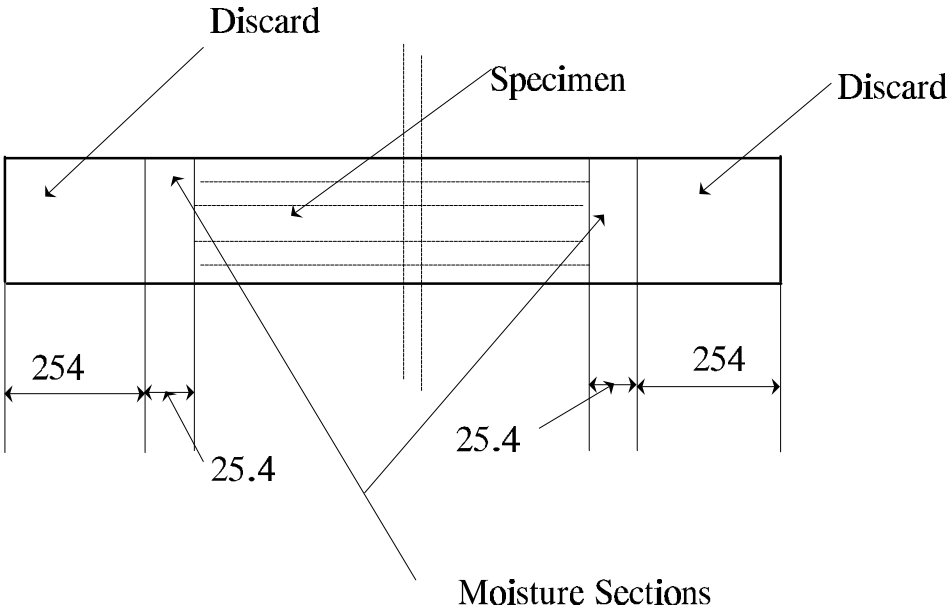

Figure 10.1 Schematic Diagram of Specimen Preparation

inserted into the vacuum oven. The RTD elements were attached to specific locations of one specimen in order to read temperatures during vacuum drying.

In order to have ambient pressure inside the chamber (which may affect the drying rate) as similar as possible for each drying load, the total weight of the specimens in each drying load was controlled at about 2000 grams for various thicknesses and lengths. In order to have better resolution on the weight measurement, several the specimens were bound together to make weight change easily detected by load cell in each drying load. Other specimens were put on the rack inside the oven during drying. The numbers of specimens on the load cell and in each drying load was listed in Table 10.1.

Table 10.1 Number of Specimen on the Load Cell and Total Number in Each Drying Load

Size (inch)	Total Number of Specimens in Each Drying Load	Number of Specimens on Load Cell
1×1×10	11	4
1.5×1.5×10	5	2
2×2×10	3	1
2.5×2.5×10	2	1
1.5×1.5×5	10	4
1.5×1.5×15	4	1

A vacuum was pulled to the maximum vacuum and the pump kept running during the drying process. The temperatures, weights and ambient pressures were recorded every minute by the data acquisition system. The temperatures recorded were center temperature, end surface temperature, and ambient temperature. The vacuum phase lasted about 140 minutes. Then, the specimens were removed from the oven and weighed. After this cycle of vacuum drying, all specimens were continuously dried under vacuum for another four hours. This is referred to as continuous vacuum

drying and will be discussed in section 10.6. After the continuous vacuum drying, the specimens were oven-dried to obtain the oven-dry weight used to calculate MC.

Data collected during the cyclic vacuum drying includes weights, MCs, temperatures, and pressures. The drying quality of all specimens was observed and recorded.

10.3. Effect of Thickness on Cyclic Drying Rate

For cyclic drying, the average drying rate per cycle is calculated as the difference in MC before heating and after 140-min of vacuum drying, divided by 140 min. The mean drying rate of specimens of various thicknesses is presented in Table 10.2. Because of different statistical sample sizes, t-tests were performed among the specimens. The p-values are shown in Table 10.2 between the specimens with various thickness. P-value is probability value when it is less than or equal to significant level α, it is very unlikely to accept the statistical hypothesis that means of two groups of data are equal.

The statistical results show that there are no significant differences in drying rates among the specimens of different thicknesses, because the p-values are always larger than 0.05. This means that the cyclic vacuum drying rate is not significantly affected by the thickness of the specimen. If any significant moisture transfer occurred from the side surface, then the drying rate would be affected by thickness, because the moisture loss and amount of heat transfer should be directly proportional to the surface area. Table 10.3 shows the different ratios of side surface and end surface to volume for various specimen thicknesses.

The following provides a discussion to highlight the fact that moisture is mainly transferred through the longitudinal direction and escapes from the end grain. If mass transfer occurs with the same mass transfer coefficient in the side surface for each thickness, the specimen with larger ratio of side surface to the volume (thinner specimen) will dry faster. This means the thinner specimens would dry fast. However, this does not apply to the end surface. In contrast, no matter what the area of the cross-section, the ratio of end surface area to volume stays the same. Thus, this would result

in the same drying rate for various thickness if the moisture is lost mostly from the end surface. This appears to be the case in cyclic vacuum drying.

Table 10.2. Mean Drying Rates and p-values for Various Thicknesses

Size	(inch)	1×1×10	1.5×1.5×10	2×2×10	2.5×2.5×10
Drying	Rate (%/hr)	2.77	2.761	2.901	2.728
St.	Dev.	0.281	0.296	0.232	0.184
Initial	MC (%)	62.82	60.31	63.42	61.98
Ending	MC (%)	56.35	53.86	56.65	55.61
P-values	1×1×10	-	0.95	0.28	0.75
	1.5×1.5×10	0.95	-	0.27	0.80
	2×2×10	0.28	0.27	-	0.19
	2.5×2.5×10	0.75	0.80	0.19	-

10.4. Effect of Length on Cyclic Drying Rate

The mean drying rates for specimens of various lengths were calculated and presented in Table 10.4. T-tests were performed among the specimens of various lengths to observe any significant difference among their drying rates. P-values were tabulated in Table 10.4.

T-test results showed that there are significant differences among the drying rates for the various specimen lengths. The shorter specimens dry faster than the longer specimens. Thus, the cyclic vacuum drying rate is affected by the specimen length. This is one more example to show that moisture moves primarily along the length during cyclic vacuum drying.

10.5. Analysis of Cyclic Vacuum Drying Curve

After drying, the drying curves of the specimens on the load cell were calculated for various specimen sizes. All drying curves showed a similar pattern. The MC, temperature and pressure curves for 2×2×10 inches specimen are presented in Figures 10.2 to 10.4, respectively.

The drying curve consists two parts. A fast drying segment follows by slow drying segment. There is a transition point which separates the two segments. This transition point is approximately 10 to 20 minutes after drying starts.

Table 10.3. Ratio of Surface Area to the Volume

Specimen Size (inch)	Volume (cm^3)	Side Surface Area (cm^2)	End Surface Area (cm^2)	Ratio of Side Surface Area to Volume (1/cm)	Ratio of End Surface Area to Volume (1/cm)
1× 1 ×10	163.87	258.06	12.90	1.575	0.079
1.5×1.5 × 10	368.71	387.1	25.04	1.050	0.079
2×2×10	655.48	516.12	51.74	0.787	0.079
2.5×2.5×10	1024.19	645.16	80.64	0.630	0.079

The fast drying period results from the transfer of moisture due to the sensible heat energy being consumed to evaporate the water. At the beginning of drying the temperature difference between the wood interior and the ambient environment is large. As a result of this difference, drying is fast.

The slow drying rate period is the results of at least two factors. One of them is that there is no significant temperature difference between the wood and ambient environment, resulting in low heat transfer to the specimen. The second factor is that cause of the high permeability of wood and the large amount of water removed in a short period of time by the WVBF, the pressure inside the wood decreases rapidly at the beginning. During the slow drying period, the pressure inside the wood is close to ambient pressure and the water vapor flow becomes small. This continues since the difference in the pressures inside and outside the wood may get smaller as drying proceeds.

Three alternative explanations are used to define the transition point. There are, (1) boiling on the end surface, (2) end surface temperature, (3) saturation pressure of the end surface.

Table 10.4. Mean Drying Rate and p-values for Various Lengths

Size (inch)		1.5×1.5×5	1.5×1.5×10	1.5×1.5×15
Drying Rate (%/hr)		3.002	2.761	2.441
St. Dev.		0.328	0.296	0.222
Initial MC (%)		63.07	60.31	60.21
Ending MC (%)		56.06	53.86	54.47
P-value	1.5×1.5×5	-	0.041	0
	1.5×1.5×10	0.041	-	0.019
	1.5×1.5×15	0	0.019	-

Boiling on the end surface. Boiling is determined by comparing the pressure and the calculated saturation pressure corresponding to the local temperature. When the calculated saturation pressure is equal to or higher than the local pressure, water boils. When the pressure curves were analyzed, boiling occurred on the surface for most drying tests for the first 20 minutes (Figure 10.5). When a vacuum is pulled, ambient pressure decreases, gradually becoming less than the saturation pressure corresponding to the end surface temperature. When the surface water boils, the temperature, and the saturation pressure are reduced significantly. Subsequently, saturation pressure again becomes less than the ambient pressure and boiling ends. The fast drying period ends when the boiling stops. This analysis works very well on most saturation pressure curves. However, boiling was not detected in one or two of the saturation pressure curves first measured, probably due to procedural difficulties.

End surface temperature. The fast drying period ends when the end surface temperature is the same as the ambient temperature. When a vacuum was pulled, the end surface temperature always decreased rapidly and approached the ambient temperature. However, in the larger specimens, end surface temperatures required much longer time to reach the ambient temperature as

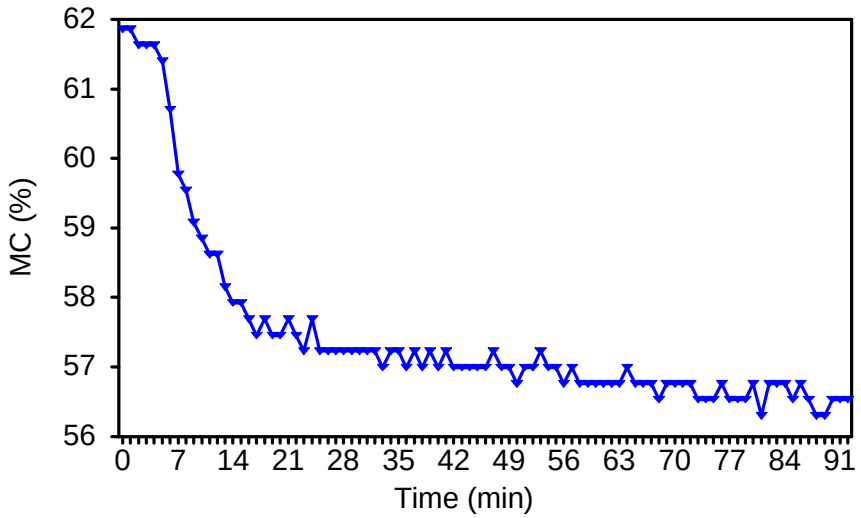

Figure 10.2 Moisture Curve for high MC Red Oak Specimen of 2 ×2 ×10 inches in Cyclic Vacuum Drying

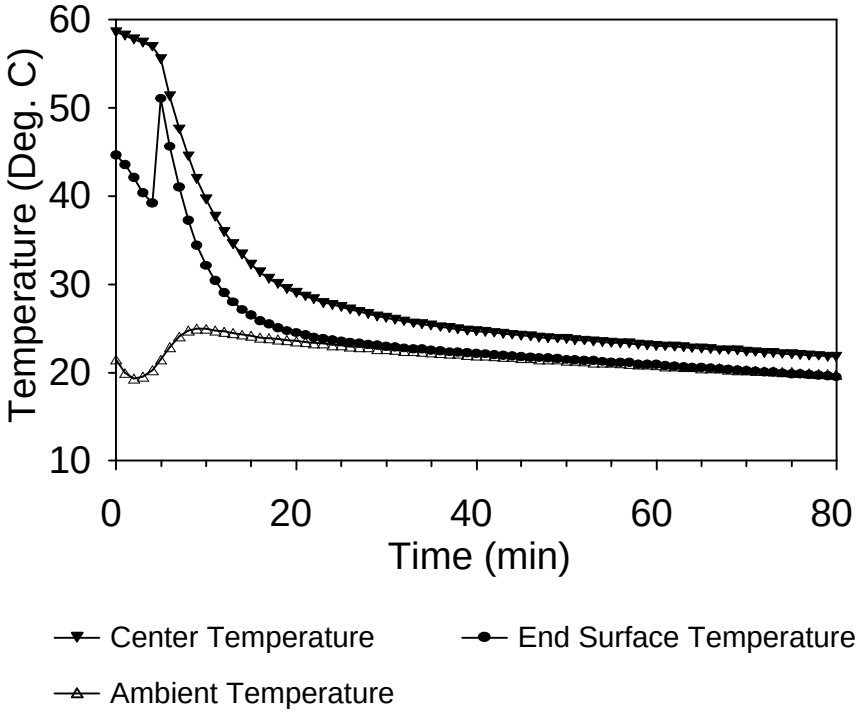

Figure 10.3 Temperature Curve for high MC Red Oak Specimen of 2 ×2 ×10 inches in Cyclic Vacuum Drying

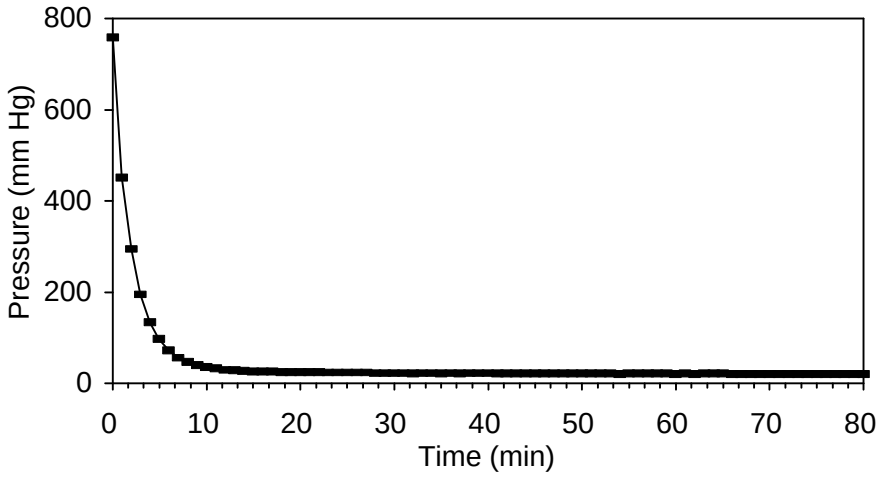

Figure 10.4 Pressure Curve for high MC Red Oak Specimen of 2 ×2 ×10 inches in Cyclic Vacuum Drying

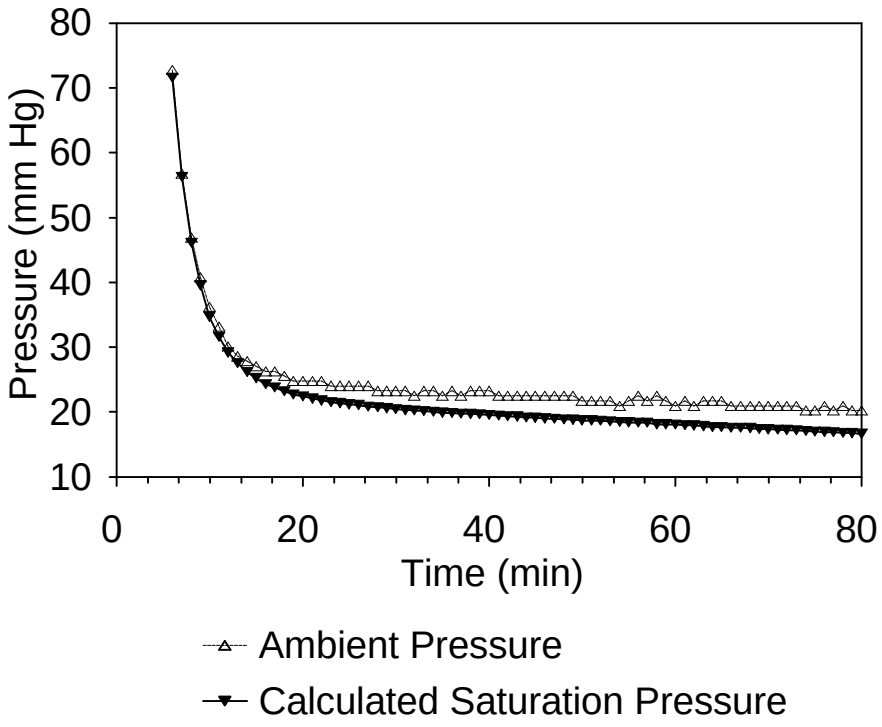

Figure 10.5 Saturation Pressure Curve for high MC Red Oak Specimen of 2 ×2 ×10 inches in Cyclic Vacuum Drying

shown in Figure 10.3. In these cases, heat transfer by convection was relatively small, and temperature decreased more slowly.

Saturation pressure of the end surface. This method compares the ambient pressure with the calculated saturation pressure corresponding to the end surface temperature. At the beginning of drying, the ambient pressure approached the saturation pressure. The difference between ambient pressure and saturation pressure became smaller and smaller as drying proceeded. It reached the smallest value and then began to increase. The transition point is the time when the smallest value is reached. The fast drying period ended when the difference between the two pressures began to increase. Based on this method, the transition time or end of the fast drying period is presented in Table 10.5. The average drying rates during fast drying and slow drying period were calculated and listed in Table 10.5. The fast drying rates are defined as the moisture loss divided by transition time. Most water removed from the specimen during the fast drying period.

In cyclic vacuum drying, the sensible energy stored in the specimen is used to evaporate the water. Theoretically, in vacuum drying, when the center and the surface temperatures are equal to the ambient temperature, there is no moisture loss and drying terminates. However, drying did not stop in all experiments. The surface temperature continued to decrease below the ambient temperature. In this situation, there probably was heat transfer from the ambient environment to the specimen. After a period of time, temperature difference between the surface and ambient environment is very large. For example, the surface temperature in drying the 1×1×10 inch specimen was about 7.5°C lower than ambient temperature after 140 minutes of vacuum drying.

Referring to the temperature curve (Figure 10.3), in the beginning of drying, the center temperature was high and end surface temperature was low. Both temperatures quickly approached the ambient temperature as vacuum drying started, and the end surface temperature was even below the ambient temperature. The rapidly decreasing temperature is attributed to water evaporation and moisture was removed from the wood. In the end surface temperature curve, there was a temperature increase about 3 to 4 minutes after vacuum was applied. This can be explained by the fact that the end surface temperature at the beginning of drying was lower due to the heat convection

and evaporation which cooled the surface. When the vacuum increased, the heat convection was significantly reduced and heat conduction and mass transfer from the center to the surface resulted in an increase in the end surface temperature.

Table 10.5 Transition Time and Drying Rates of Fast and Slow Drying Periods

Size (inch)	Transition Time (min)	Fast Drying Rate (%/min)	Slow Drying Rate (%/min)
1×1× 10	13	0.132	0.0285
1.5×1.5× 10	11	0.224	0.0257
2×2× 10	10	0.139	0.0598
2.5×2.5× 10	11	0.235	0.0312
1.5×1.5× 5	11	0.467	0.0207
1.5×1.5× 15	10	0.163	0.0272

To explore drying curves at MC below FSP, 2×2×10 inches specimens were dried to a MC of about 20%. Then they were cyclic vacuum dried to observe any differences between the cyclic vacuum drying of high MC (Figure 10.2) and low MC (Figure 10.6) specimens. The drying rate was smaller for the low MC specimen for which the temperatures decreased slowly as shown in Figure 10.7. This is due to the fact that less moisture is available near the end surface. More time is needed and some energy is transferred to the ambient environment by heat convection. The specimens were then weighed and oven dried.

The same size specimens at 0% MC were heated to 60°C and put into the vacuum oven to observe the temperature change. The temperature curves is presented in Figure 10.8. Specimen temperatures were never below the ambient temperature because there was no evaporation. However, temperatures slowly decreased as a result of convection heat transfer.

10.6. Effect of Specimen Size on Continuous Vacuum Drying

Continuous vacuum drying was conducted on the same specimens after the cyclic vacuum drying test. After each cyclic vacuum drying test, the specimens were weighed and put into the vacuum oven. The heating system in the vacuum oven was turned on and the ambient temperature was controlled to 60°C. The vacuum was pulled to a maximum and the vacuum pump kept running for four hours under this condition. Weights, ambient pressures, center, surface, and ambient temperatures were recorded every five minutes. When drying terminated, specimens were weighed and oven dried.

The drying rate was calculated as the difference between the MC before and after drying, divided by the time (4 hours). The drying rates for each specimen size were calculated and are presented in Table 10.6. T-test was performed and p-values are presented in Table 10.6.

From the discussion in section 10.3, the difference in the ratio of the surface to the volume will affect the amount of heat transfer per unit volume to the specimen. Different amounts of heat transfer cause differences in drying rates. Thus, there are different drying rate for different thicknesses in continuous vacuum drying, that is, the continuous vacuum drying rate is affected by the thickness mainly due to the amount of heat transfer. A thinner specimen will absorb more heat energy per unit volume. As a result, a thinner specimen will dry faster than a thicker specimen. This is shown in the data given in Table 10.6. The one inch thick specimens had the average highest drying rate of 5.08 %/hr, and the 2.5 inch thick specimens had the lowest average drying rate of 3.462 %/hr.

Figures 10.9 and 10.10 represent MC and temperature curves for continuous vacuum drying of a 2×2×10 inch specimen. The drying curve is almost linear and specimens of every thickness show a similar shape. R^2 values for MC vs time are higher than 0.95 in all cases (Table 10.6). This means that a constant drying rate occurs during the drying process. Because heat is required to evaporate the water, the amount of heat transfer determines the amount of water evaporation that occurred during drying period. Because there is small difference (Figure 10.10) in the peak and valley temperatures between the end surface and ambient environment during drying, the amount of the heat transfer is almost the same in the process.

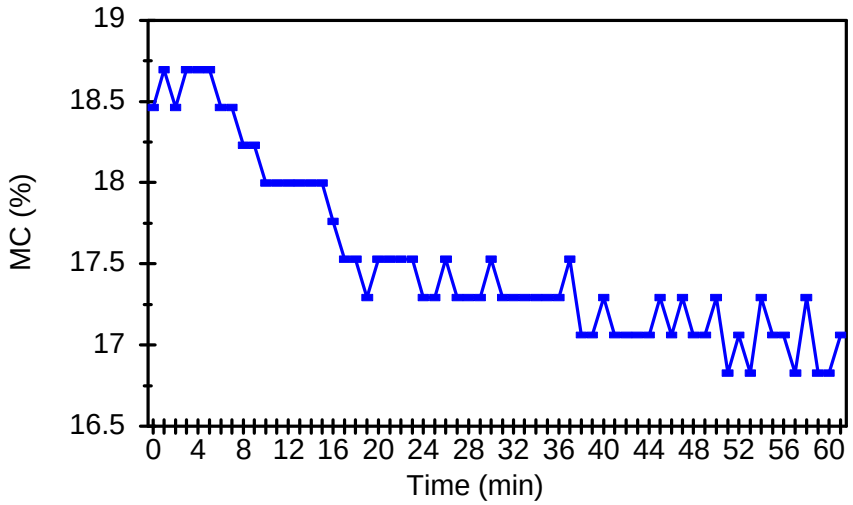

Figure 10.6 Moisture Curve for low MC Red Oak Specimen of 2 ×2 ×10 inches in Cyclic Vacuum Drying

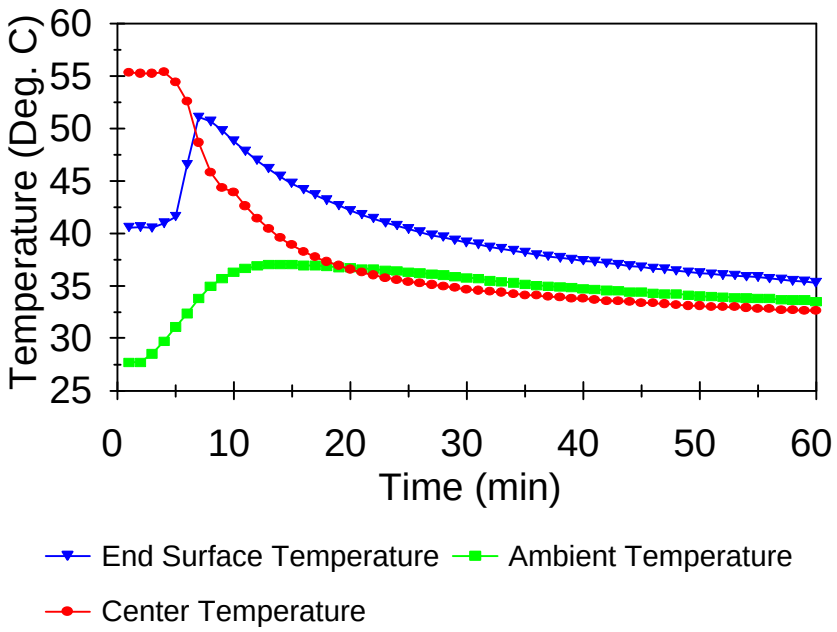

Figure 10.7 Temperature Curve for high MC Red Oak Specimen of 2 ×2 ×10 inches in Cyclic Vacuum Drying

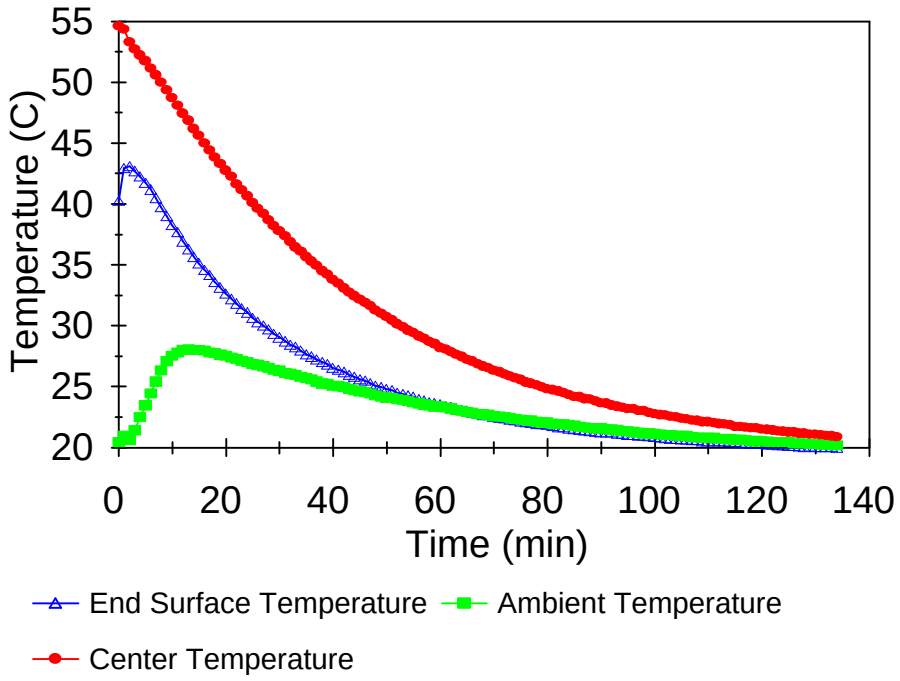

Figure 10.8 Temperature Curve for Oven-dry Red Oak Specimen of 2 ×2 ×10 inches In Cyclic Vacuum Drying

Table 10.6 Drying Rate and p-values of Continuous Vavuum Drying

Size (inch)		1×1×10	1.5×1.5×10	2×2×10	2.5×2.5×10	1.5×1.5×5	1.5×1.5×15
Drying	Rate (%/hr)	5.08	4.562	3.872	3.462	4.27	4.01
St.	Dev.	1.3	0.827	0.45	0.198	1.35	0.398
Initial	MC (%)	56.31	53.5	56.65	53.98	56.06	54.47
Final	MC (%)	36.00	35.25	41.16	40.13	38.99	38.43
R^2		0.991	0.970	0.962	0.981	0.965	0.986
P-value	1×1×10	-	0.29	0.014	0.0022		
	1.5×1.5×10	0.29	-	0.038	0.0024	0.47	0.086
	2×2×10	0.014	0.038	-	0.046		
	2.5×2.5×10	0.0022	0.0024	0.046	-		
	1.5×1.5×5		0.47			-	0.45
	1.5×1.5×15		0.086			0.45	-

End check was found in the continuous vacuum drying specimen, but no surface and internal checks (Figure 10.11). The end check occurs because of the large moisture gradient along the length. When the MC near the end surface is below FSP, wood shrinks. While center with MC above FSP restrains the shrinkage, then the end check occurs as shown in Figure 10.11.

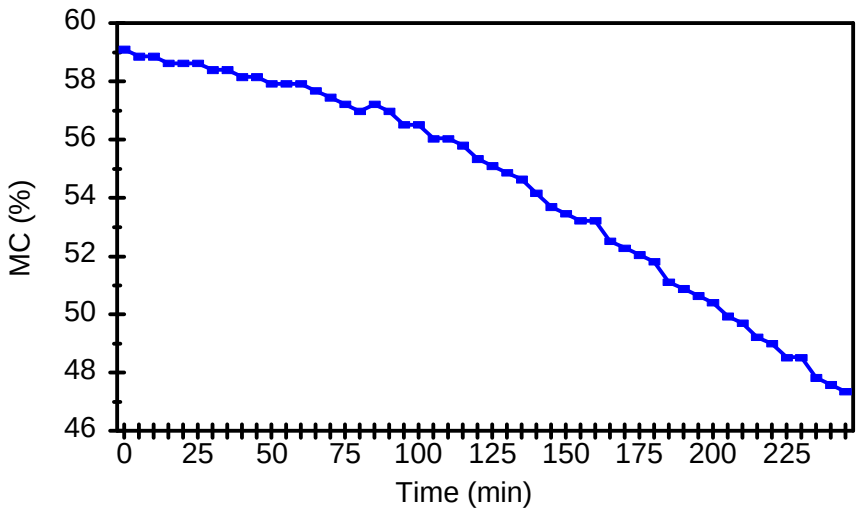

Figure 10.9 Moisture Curve for high MC Red Oak Specimen of 2 ×2 ×10 inches in Continuous Vacuum Drying

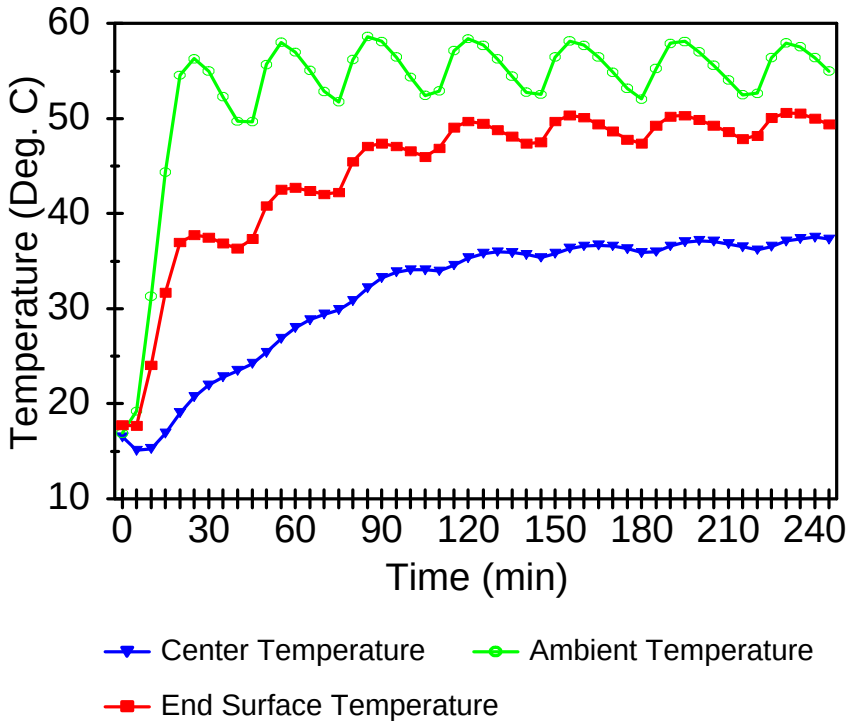

Figure 10.10 Temperature Curve for high MC Red Oak Specimen of 2 ×2 ×10 inches in Continuous Vacuum Drying

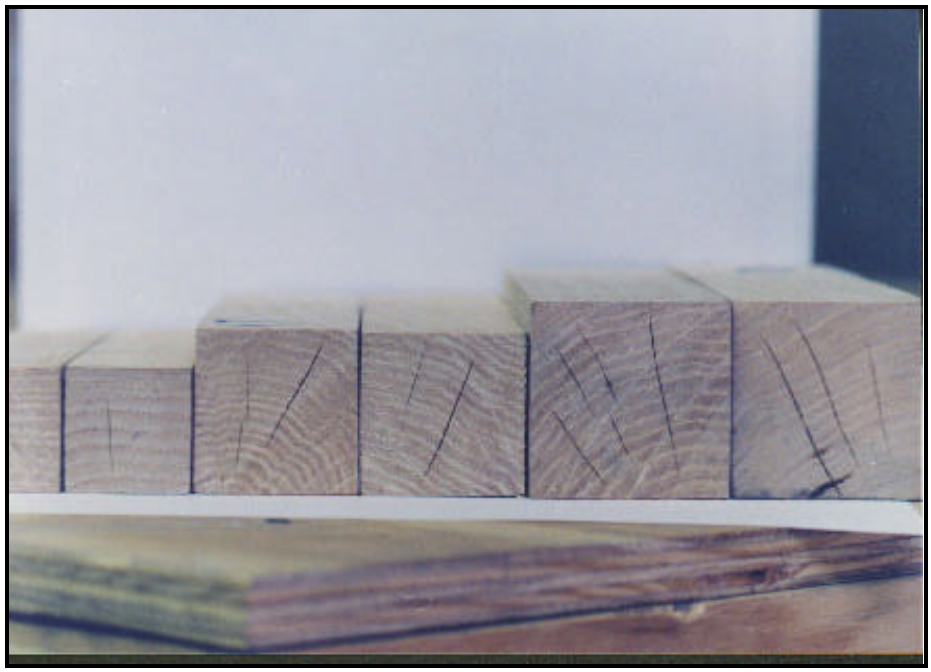

Figure 10.11 End Check in Red Oak Occurring in Continuous Vacuum Drying

11. Effect of End Grain on Vacuum Drying

If moisture transfer is governed by WVBF, moisture is essentially transferred in the longitudinal direction because of its higher permeability, and wood can be dried from the end grain only. The objective of this experiment is to explore the effect of end grain on vacuum drying by sealing the four side surfaces of specimens with paraffin wax, plastic films and butyl rubber tubes. Therefore, moisture movement will be entirely along the grain. The end grain drying rates of both red oak and white oak will be compared for both cyclic and continuous vacuum drying.

11.1. Effectiveness of Specimen Sealing

The purpose of this experiment is to determine the effectiveness of the sealing procedure. The sealing should prevent any significant loss of moisture from the specimen at a drying temperature of about 60°C in a high vacuum condition.

A preliminary study showed that wax alone was not sufficient to prevent moisture loss. For this experiment, the specimen size 1 by 1 by 6 inches red oak. The specimens were prepared as shown in Figure 10.1. After the specimens were cut, they were weighed and dipped into the melted wax to coat all six surfaces. The melting temperature of paraffin wax was 80°C. The specimens were then wrapped with plastic film on the four side surfaces. The end grain surfaces were also covered with plastic film. Finally, the specimens with wax and plastic film were inserted into the butyl rubber tube with an inside diameter of 28.31 mm and outside diameter of 29.83 mm (Figure 11.1). Seven specimens were tested by this process.

The specimens were heated in a heating oven at temperature of 60°C for three hours. They were removed, and weighed, and put into vacuum oven. A vacuum was pulled and maintained at 16 mm Hg for three hours. After this procedure, the specimens were removed from the vacuum oven and weighed. The data are presented in Table 11.1.

The total specimen weight of all seven specimens before sealing was 746.0 grams and the initial MC was 63.16%. The estimated oven-dry weight of the specimens was 457.67 grams. The

total weight loss during heating was about 0.9 gram for a MC drop of 0.20%. The weight loss during vacuum exposure was 1.2 grams for a MC drop of 0.26%. Total MC loss in the entire process was 0.46%. Based on this result, this sealing method was assumed to be effective, and this method of sealing was used in these experiments.

Table 11.1 Effectiveness of the Sealing

Specimen	Weight before Heating (g)	Weight after Heating at Atmospheric Pressure (g)	Weight after 3 hours in Vacuum (g)
A	128.2	128.1	128.1
B	125.5	125.3	124.7
C	127.8	127.7	127.7
D	123.9	123.7	123.7
E	132.8	132.7	132.1
F	120.3	120.2	120.2
G	123.1	123.0	123.0

11.2. Comparison of Cyclic Vacuum Drying Rates of Side-sealed Red Oak and White Oak

The moisture sections and ten specimens 1×1×10 inches were cut from the red oak and white oak green board as shown (Figure 10.1). Based on these moisture sections, the initial MC was calculated, and the oven-dry weights of specimens were estimated. Specimens were sealed on the four side surfaces using the procedure described in section 11.1. The end grain was not sealed. After sealing, the specimens were weighed.

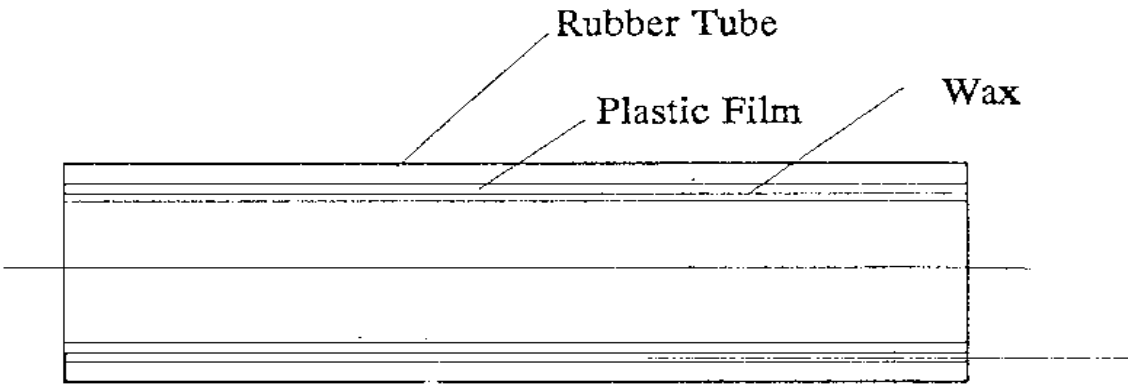

Figure 11.1 Schematic Diagram of Specimen Sealing

There were five specimens in each drying load. The specimens were heated to 60°C and dried in vacuum for 140 minutes as in section 10.2. After this vacuum process, the specimens were reweighed. This sequence is one cycle of drying. After this cycle of drying, the specimens were reheated to 60°C and dried again, for a total of four vacuum cycles. One specimen in each load was used for measuring temperature and the other four specimens were used to measure the weight changes. The ambient pressure was measured by the pressure transducer. Data of temperature, pressure and weight were recorded every minute during vacuum drying. The drying, temperature, and pressure curve were plotted from the data.

The drying rates of the specimens are presented in Table 11.2. T-tests were performed on the drying rates of both red and white oak and the p-values are also shown in Table 11.2.

Statistical comparison (with p-value greater than 0.05) concludes that there is no significant difference in the drying rates of red oak and white oak for 3 of 4 cycles of vacuum drying. However, for the 3rd cycle, the red oak dried significantly faster than white oak. It is believed that this may be due to experimental error in this cycle.

In the analysis of cyclic vacuum drying curve in section 10.5, the fast drying period usually lasted only a very short time (10 to 20 minutes) for red oak. Therefore, another comparison between the drying rates after twenty minutes of drying were done for sealed red oak and white oak. The twenty specimens of red oak and white oak were cut and dried using a single cyclic vacuum procedure. The experimental procedure was the same as above except that the drying time was limited to 20 minutes. The drying rates and p-values are listed in Table 11.3.

The p-value is 0.058, indicating that there is no significant difference in the drying rates of red oak and white oak at the 5% significance level. This may be because both red and white oaks are sufficiently permeable that permeability is not the limiting factor in this case. Furthermore, there are variations of permeability within the same species and even within the same tree. The standard deviations in the drying rates are sufficient large to cause no significant difference in the statistical sense. On the other hand, the p-value is only slightly more than 0.05. If α is chosen as 10%, then there would be a significant difference in the drying rates.

Table 11.2 Drying Rates for Red Oak and White Oak in Each drying Cycle

Specimen	Red Oak		White Oak		P-value
	Mean	St. Dev.	Mean	St. Dev.	
Initial MC (%)	52.30		56.87		
MC after 1st cycle (%)	45.96		49.89		
Drying Rate of 1st Cycle (%/hr)	2.718	0.588	2.993	0.567	0.36
MC after 2nd cycle (%)	39.81		43.77		
Drying Rate of 2nd Cycle (%/hr)	2.636	0.211	2.621	0.537	0.94
MC after 3rd cycle (%)	33.89		39.16		
Drying Rate of 3rd Cycle (%/hr)	2.535	0.120	1.976	0.376	0.004
MC after 4th cycle (%)	29.46		34.81		
Drying Rate of 4th Cycle (%/hr)	1.898	0.503	1.862	0.110	0.85

11.3. Comparison of Cyclic Vacuum Drying of Sealed and Unsealed Specimens

11.3.1. Comparison of the Drying Rates of Sealed and Unsealed Specimens

Cyclic vacuum drying rates of sealed (four side surfaces sealed) red oak and unsealed red oak were compared in order to confirm that most water is lost through the end grain surfaces. The drying rate data of unsealed 1×1×10 inches red oak specimens were taken from the experiment in section 10.3. The drying rate data of sealed red oak were taken from the first cycle in section 11.2 so that

both the sealed specimens and unsealed specimens were MC. These cyclic drying rates of sealed and unsealed specimens are was presented in Table 11.4, with corresponding statistical values.

Table 11.3 Drying Rates of Red Oak and White Oak in Twenty Minutes of Cyclic Vacuum Drying

	Red Oak	Red Oak	White Oak	White Oak
	Initial MC (%)	Drying Rate (%/min)	Initial MC (%)	Drying Rate (%/min)
Mean	46.10	0.2443	45.91	0.2152
St. Dev.		0.0369		0.0552
P-value	0.058			

Table 11.4 shows that the there is no significant difference in the drying rates of sealed and unsealed specimens. This indicates that there is no significant moisture loss from the side surfaces of the unsealed specimens during vacuum drying. It should be also noted that drying rates for the sealed specimens are large. Due to the limitation of specimen size by the equipment, most of the sizes are 1 by 1 by 10 inches. This size is similar to the real size of lumber 14.4 inches by 14.4 inches by 12 feet long. It should not be difficult to dry this size of lumber as it can be predicted from the modeling.

11.3.2. Comparison of Drying Curves of Sealed and Unsealed Specimens

The MC and temperature curves of the sealed red oak specimens are shown in Figures 11.2 and 11.3. The curves for the sealed specimens have the same shape as those of the unsealed vacuum drying curves (see Figure 10.2). Figure 11.2 also shows two parts corresponding to the fast and slow drying rates. The similar curves result from the insignificant moisture loss from the side surfaces during vacuum drying. It should be noted that the drying curves of sealed white oak specimens are similar to that of side sealed red oak specimens. The ambient pressure curves were also identical for the sealed and unsealed specimens.

Table 11.4 Comparison of Drying Rates of Sealed and Unsealed Specimen

Specimen	Unsealed (%/hr)	Sealed (%/hr)
Initial MC (%)	62.82	52.30
Ending MC (%)	56.35	45.96
Mean	2.77	2.718
St. Dev.	0.281	0.588
P-value	0.82	

11.4. Comparison of Continuous Vacuum Drying Rates of Sealed Red Oak and White Oak

The objective of this experiment was to compare the continuous vacuum drying rates of sealed red oak with those of sealed white oak. Ten pieces of white and red oak specimens (1×1×10 inches) were tested in continuous vacuum drying as described in section 10.2. The specimens were sealed on the four side surfaces. Two continuous drying loads were done with five red oak and five white oak specimens in each load. The weight of each specimen was measured every 90 minutes when the vacuum was relieved for about one minute (Figure 11.4). The mean drying rates were compared after 9 hours and 22 hours of drying. The statistical results are presented in Table 11.5. There is a significant difference between the drying rates of continuous vacuum dried red oak and white oak. The red oak dries faster due to its larger permeability.

More heat energy was consumed by the red oak specimens than the white oak specimen in order to maintain the larger drying rate. The red oak specimens were always than the white oak specimens (Table 11.6). Apparently, red oak absorbs more energy than white oak from the ambient environment because it dries faster. A moisture gradient developed along the length as will be discussed in the section 11.7.

Table 11.5 Continuous Vacuum Drying Rates of Red Oak and White Oak

Specimen	Red Oak		White Oak		P-value
	Mean	St. Dev.	Mean	St. Dev	
Initial MC (%)	56.41		53.18		
MC after 9 hrs of drying (%)	26.35		29.01		
Drying Rate after First 9 Hours (%/hr)	3.34	0.32	2.686	0.351	0.0004
MC after 22 hrs of drying (%)	4.4		10.61		
Drying Rate in 22 Hours (%/hr)	2.364	0.116	1.935	0.241	0.0003

11.5. Moisture Loss from the Side Surfaces during Cyclic Vacuum Drying

The objective of this experiment was to determine the amount of water is removed from the side surfaces during cyclic vacuum drying. Twelve 4×4×4 inch specimens of red oak were cut from the sample boards. Specimens were separated into two groups: six pieces sealed in the four side surfaces and six pieces left unsealed. They were dried under cyclic conditions. There were two vacuum cycles of one hour each. The results are shown in Table 11.7. The initial MC was based on unsealed specimens.

The moisture loss from the side surfaces is small for cyclic vacuum drying (less than 5% in weight for both cycles). Statistical test results show that there is no significant difference in drying rates between sealed and unsealed specimens during cyclic vacuum drying.

11.6. Moisture Gradient through Thickness

The objective of this experiment was to investigate the moisture gradient through the thickness of specimens. Five specimens of 2.5×1.5×10 inches were prepared (Figure 10.1). The specimens were completely sealed including the end grain, except for a one inch strip in the center

of specimen (Figure 11.5). Specimens were then continuously vacuum dried at a vacuum level of 18 mm Hg and temperature of 60°C for three hours. The unsealed one inch strips were cut from the specimens. They were then sliced into seven layers through the thickness as shown in Figure 11.6. The moisture content of these layers were used to calculate moisture gradient.

The average moisture gradient from the five specimens is presented in Figure 11.7. It is clearly seen that the moisture gradient is very steep near surface of the specimens, indicating that there is little transverse moisture movement from the center to the surface. This steep moisture gradient was also found in RFV drying wood (Kanagawa and Yisujima 1993, Avramidis et al. 1986).

11.7. Moisture Gradient along Length

Data of cyclic vacuum drying for this section came from those sealed specimens of cyclic vacuum drying discussed in section 11.2. Data for continuous vacuum drying came from those sealed specimens of continuous vacuum drying discussed in section 11.4. In order to determine the longitudinal moisture distribution after vacuum drying, the specimens were first ripped on four side surfaces to remove the coating as shown in Figure 11.8. They were then cross-cut into small segments (Figure 11.8). The lengthwise moisture distribution curves for cyclic and continuous vacuum drying are presented in Figure 11.9 and Figure 11.10. The moisture gradients along the length were found for both cyclic and continuous vacuum drying. Avramidis et al. (1996) also found the moisture gradient along the length in the RFV material. The results indicates the most of the moisture movement occurs along the length.

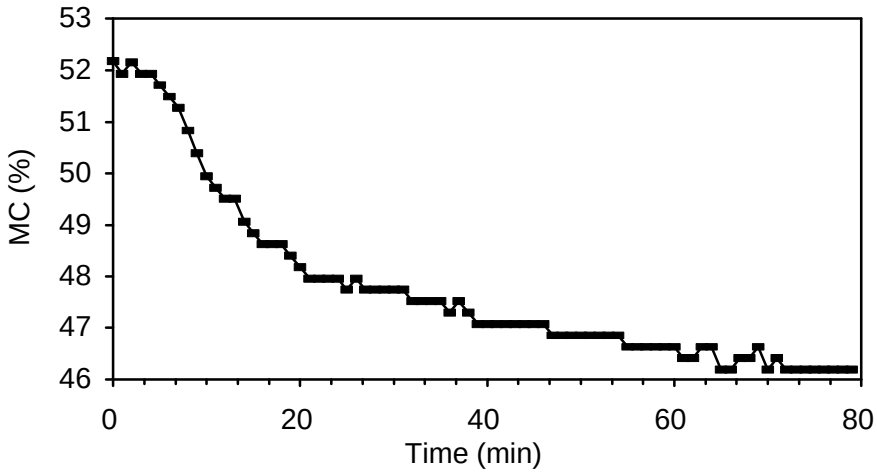

Figure 11.2 Moisture Curve of Cyclic Vacuum Drying of Sealed Red Oak Specimen

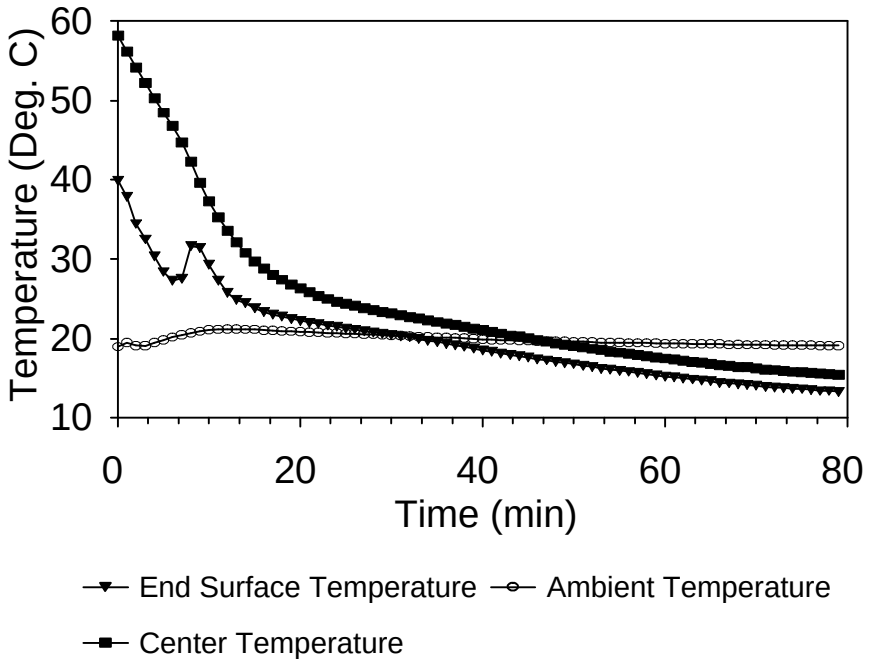

Figure 11.3 Temperature Curve of Cyclic Vacuum Drying of Sealed Red Oak Specimen

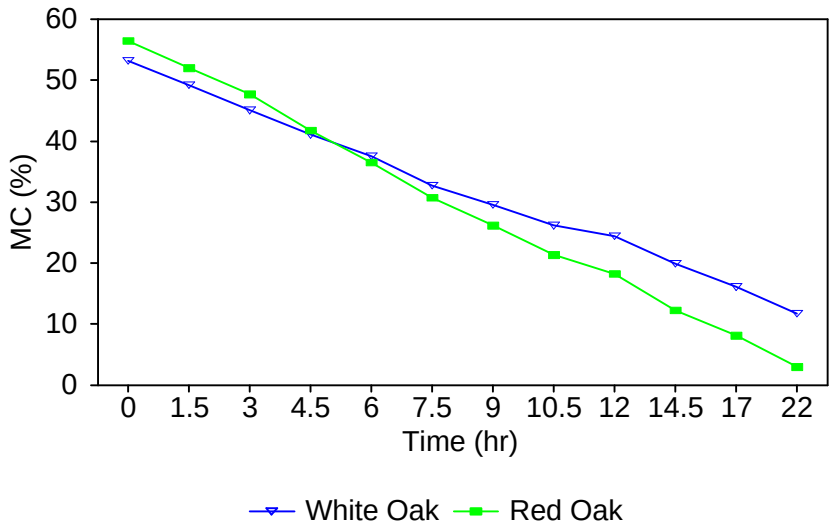

Figure 11.4 Moisture Curve of Continuous Vacuum Drying of Sealed Red Oak and White Oak

Table 11.6 Temperatures of Red Oak and White Oak During Continuous Vacuum Drying

Drying Time	Red Oak		White Oak	
(h)	MC (%)	Temperature (˚C)	MC (%)	Temperature (˚C)
1.5	51.3	34.9	47.9	35.6
3	46.3	36.9	42.9	37.8
4.5	40.5	37.2	38.7	37.5
6	35.0	37.4	34.9	39.6
7.5	30.0	37.3	31.8	40.3
9	26.0	39.2	28.5	43.8
20	7.2	54.8	10.7	61.6

11.7 Weight Loss of Sealed and Unsealed Specimens

	Specimen	Sealed	Unsealed	Difference	P-value
First Cycle	Initial MC (%)	46.04	42.69		
	Ending MC (%)	41.74	38.44		
	Drying Rate (%/hr)	4.30	4.25		0.78
	Weight Loss (g)	146.7	151.98	5.28	
Second Cycle	Initial MC (%)	40.96	37.11		
	Final MC (%)	36.89	33.22		
	Drying Rate (%/hr)	4.07	3.89		0.62
	Weight Loss (g)	138.3	139.2	0.9	

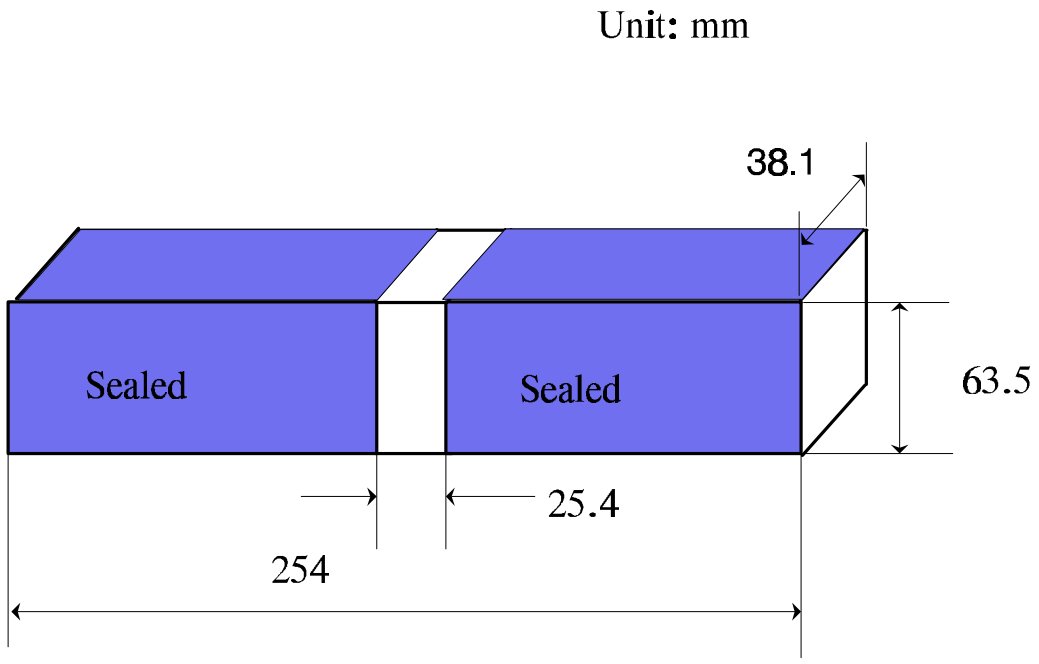

Figure 11.5 Schematic Diagram of Sealed Specimen for the Study of Moisture Loss from Side Surface

Unit: mm

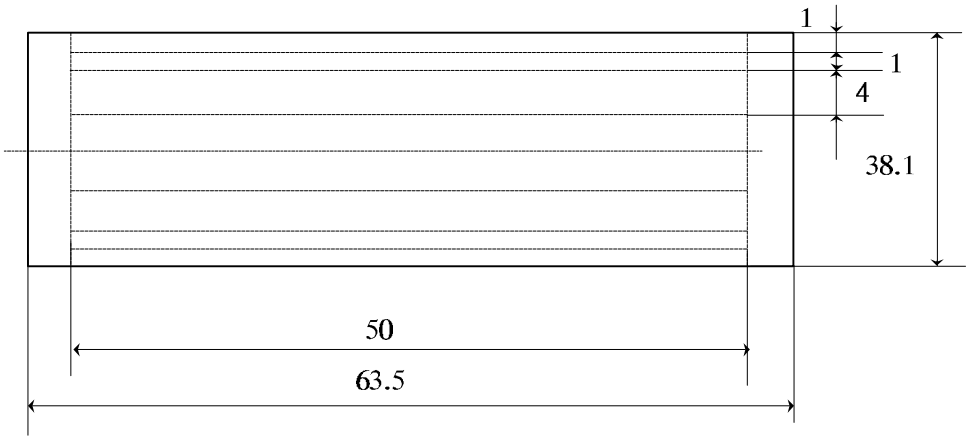

Figure 11.6 Schematic Diagram for Measuring the Moisture Gradient in Thickness

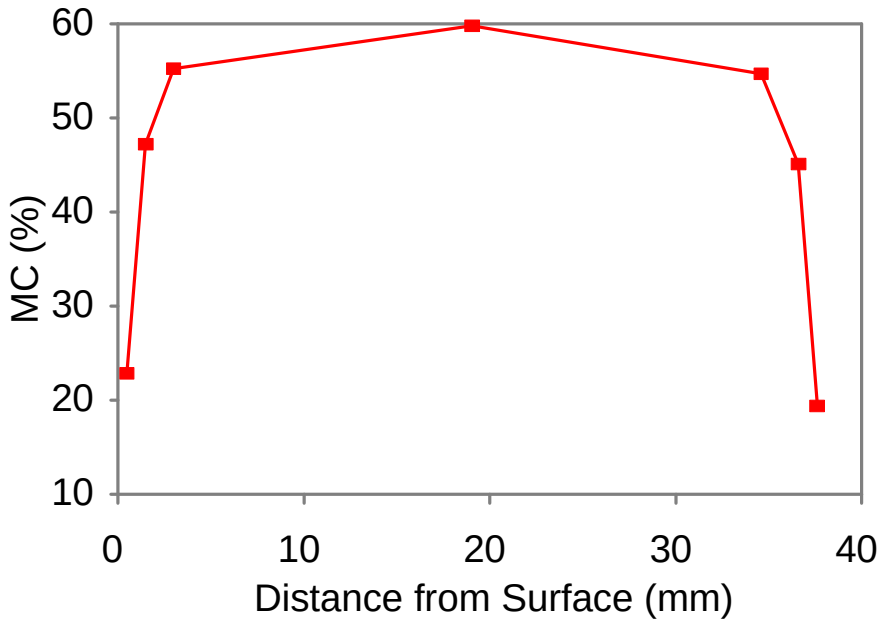

Figure 11.7 Moisture Gradient through Thickness in Continuous Vacuum Drying of Red Oak Specimens

Unit: mm

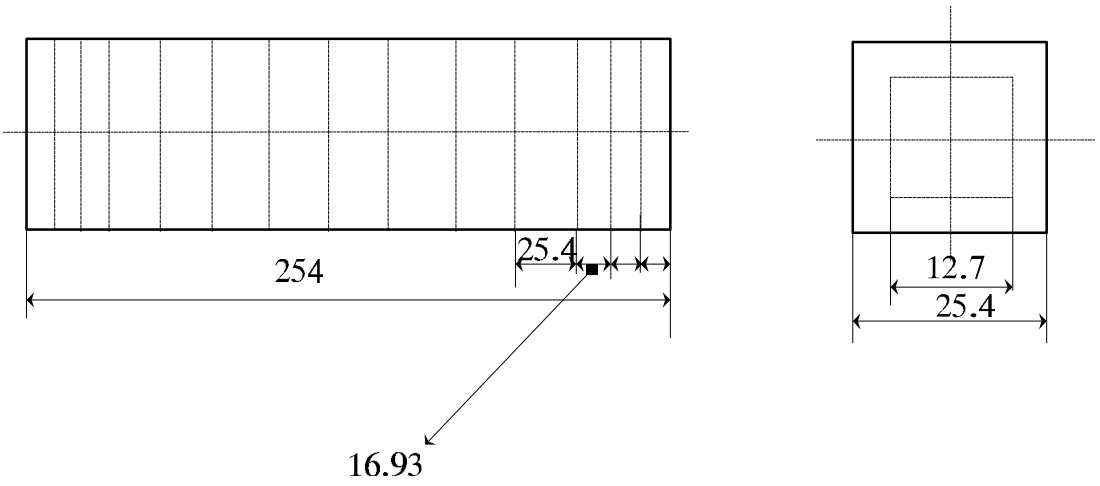

Figure 11.8 Schematic Diagram for Measuring Moisture Gradient along the Length

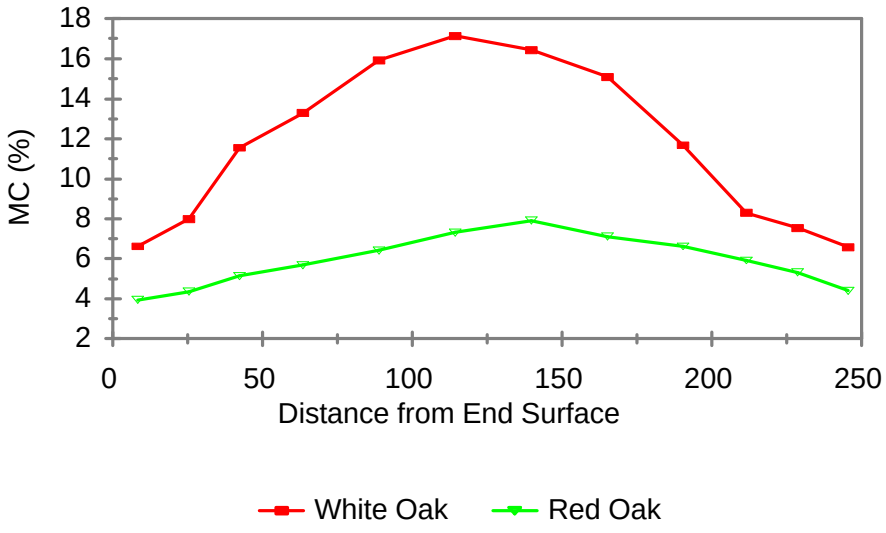

Figure 11.9 Moisture Gradient along the Length in Continuous Vacuum Drying in Sealed White Oak and Red Oak Specimens

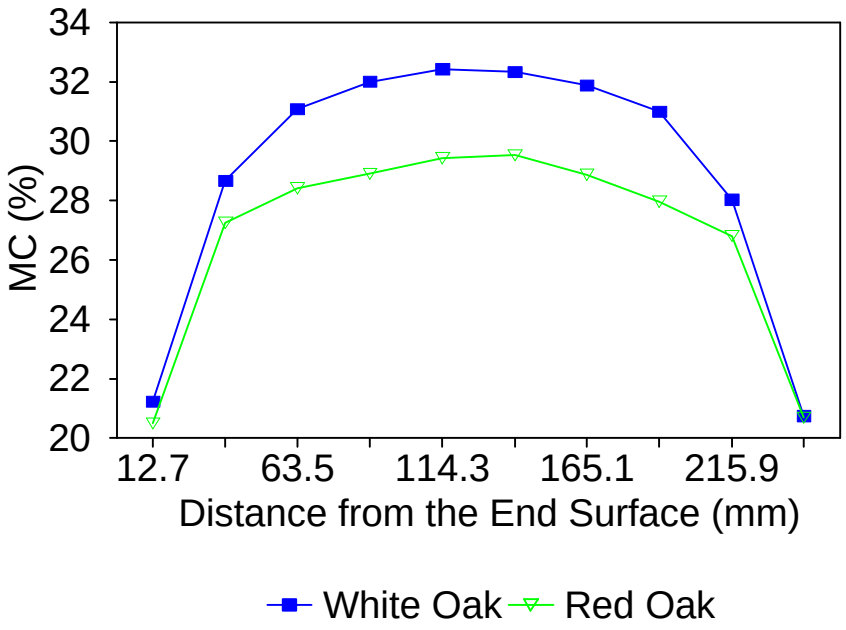

Figure 11.10 Moisture Gradient along the Length in Cyclic Vacuum Drying in Sealed White Oak and Red Oak Specimens

12. Boiling Front During Vacuum Drying

When the pressure is lower than saturated pressure, water boils. Most research supports the concept that moisture inside wood is boiling as the boiling temperature is lowered in a vacuum. In RFV, the temperature of wood reaches the boiling temperature in a very short time (Avramidis et al. 1994). However, Neumann et al. (1992) simultaneously measured temperatures and pressures at the different depths of beech boards during convective vacuum drying in superheated steam at 2×10^4 Pa (0.2 bar). They found that the pressures at different depths were always higher than the saturation pressures corresponding to the local temperatures. They concluded that water was not boiling in the wood and the faster drying in vacuum drying may not be attributed to the boiling phenomena as most researchers supposed. The boiling front concept has been proposed by Chen and Lamb (1995a), who suggested that not only is water boiling inside the wood, but also there is boiling front. From the boiling front to wood surface, the boiling temperature is lower than the wood temperature, and moisture in this region boils. From the boiling front to the center of the wood, there is no boiling due to the fact that the pressure inside the wood is higher than the vapor saturation pressure. The boiling front retreats from the surface to the center as drying process proceeds. The retreating speed depends on the heat energy supply and the properties of the wood, such as permeability and thermal conductivity. The objective of this experiment was to investigate the boiling phenomena and the boiling front during continuous and cyclic vacuum drying. The MC at the boiling front was also explored.

12.1. Boiling Front Determination

From theoretical considerations (Chapter 8), there is a boiling front and it retreats to the center of a board as drying proceeds. The emphasis of this experiment is on detecting boiling phenomenon and characterizing the boiling front movement.

Specimens used in the experiments were prepared as discussed in section 10.2 as shown in Figure 10.1. The specimens were 2.5×1.5×10 inches. Some specimens were green, and others were air dried to about 10% MC.

Two pairs of 1/8 inches (3.175 mm) holes were drilled in each specimen (see Figure 12.1). They are designated as locations "1" and "2". In each pair of holes, the hole closest to the edge was used for the pressure probe and other for the temperature probe.

Experiments were conducted for the high MC (above FSP) and low MC (around 10%) specimens. Six experimental runs are discussed here. The A and B values (Figure 12.1) from the designated locations on the specimen in relationship to the end grain are presented in Table 12.1.

Glass tubes with outside diameter of 1.727 mm and inside diameter of 1.27 mm were inserted into the holes and sealed with epoxy. Rubber tubes with an inside diameter of 1.27 mm and outside diameter of 3.3 mm were then used to connect the glass tubes to the pressure transducers (Figure 12.2).

Both cyclic and continuous vacuum drying were investigated using procedure described in section 10.2. One specimen was dried at a time.

In cyclic vacuum drying, the temperature probes were inserted into the holes after heating. The rubber tube were then connected to the glass tube to measure the pressure. Then the specimen was hung on the load cell and vacuum drying started. The end surface temperatures, ambient temperatures, and temperatures at locations “1" and “2" were measured. Ambient pressures and pressures at locations “1" and “2" were measured. The weight, pressure and temperature readings were recorded during the drying every thirty second for specimen of low initial MC and every minute for specimen of high initial MC. When the temperature of wood was lower than the ambient temperature, cyclic drying was stopped.

For continuous vacuum drying, the data were recorded every minute for specimens of low initial MC and every five minutes for specimen of high initial MC. When the temperatures in the designated locations were higher than the saturated temperature, drying was stopped.

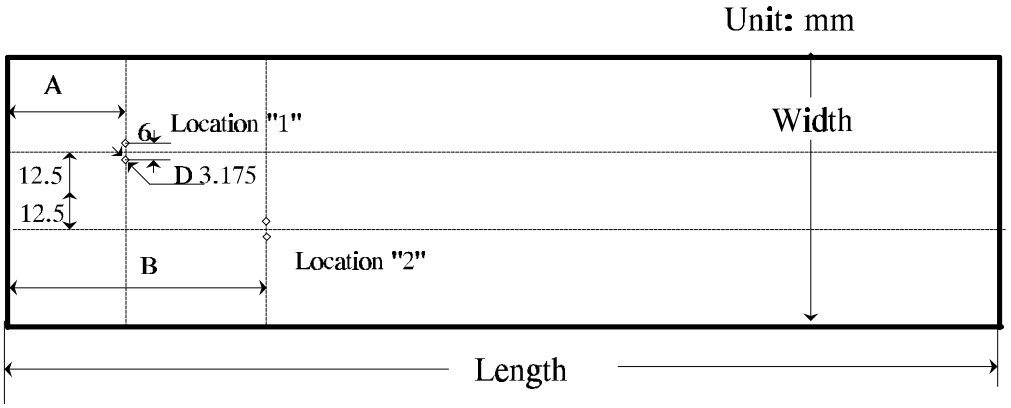

Figure 12.1 Longitudinal Locations on Specimen for Measuring Pressure and Temperature

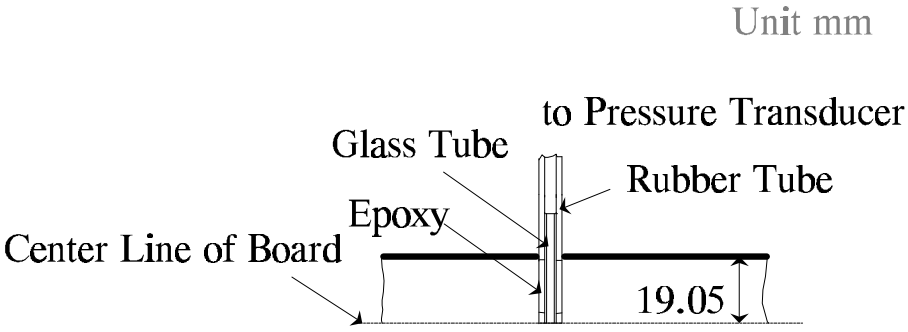

Figure 12.2 Connection to Measure the Pressure in the Specimen

Table 12.1 Two Locations in the Specimens for Measuring Pressures and Temperatures

	Run	Initial MC (%)	A Distance (mm)*	B Distance (mm)*
Continuous Drying	#1	77.59	38.1	76.2
	#2	44.88	12.7	38.1
	#3	38.36	25.4	50.8
	#4	8.83	8	25.4
Cyclic Drying	#5	50.92	8	25.4
	#6	9.89	8	25.4

* see Figure 12.1.

The experimental results are shown as MC, temperature and pressure curves versus time. They are presented in Figures 12.3 to 12.5 for continuous vacuum drying and Figures 12.6 and 12.7 for cyclic vacuum drying. The temperature curves represent ambient temperature, surface temperature and temperatures at locations “1" and “2". There are three pressures, the ambient pressure and the pressures at locations “1" and “2". Thus, there are four calculated saturation pressures shown in Figures 12.4, 12.5 and 12.7, corresponding to the four local temperatures.

The calculated saturation pressures were compared with the measured pressures at the same times and locations. If the calculated saturation pressure was higher than the corresponding measured pressure, boiling is assumed to occur at this location. From Figures 12.5 and 12.7, it is clearly seen that there was boiling during vacuum drying and that the boiling front moved towards the center as drying proceeded. The time required to reach the boiling condition at each location is presented in Table 12.2, for both cyclic and continuous vacuum drying.

It takes less time for the boiling front to retreat to the center of a specimen in continuous vacuum drying for lower MC specimens. This is because it takes energy to boil the water and the heat supply is almost the same for specimens of high MC and low initial MC, and specimens having low MC simply have less water to boil. Thus, the temperature increased more rapidly to reach the

boiling condition inside the wood. The temperature inside the specimens of lower MC increased faster during drying, since the temperature inside the wood is related inversely to the MC. If the temperature is uniform in the entire specimen, the pressure gradient only can be built up when the MC is lower than FSP and also there is a MC gradient as discussed in Chapter 6. The high MC specimens require more heat supply to boil the water in the surface first in order to build up the pressure difference to move the moisture from the interior to the surface. The boiling front then slowly retreated to the center of the specimen.

Table 12.2 Time for Each Location to Reach the Boiling Condition

Drying Method	Run	Ambient (min)	Surface (min)	Location "1" * (min)	Location "2"* (min)
Continuous Drying	#1	5	30	65	730
	#2	10	25	35	190
	#3	10	15	325	645
	#4	8	11	12	48
Cyclic Drying	#5	Non-Boiling	9	Non-Boiling	Non-Boiling
	#6	Non-Boiling	7	8.5	5

* Distance to location from end grain surface (see Figure 12.1).

In continuous vacuum drying, the boiling front should be located at the point in the wood which is at FSP in specimens whose initial MCs exceed FSP. This is true because the temperature near the surface is higher than in the center and the saturated pressure is higher in the surface than in the center. Therefore, the surface approaches the boiling condition first because the pressure decreases there first. According to sorption theory, only when MC is below FSP can the pressure be lower than saturation pressure. From the boiling front to the center of a specimen, the MC is higher than FSP, the pressure is higher than saturation pressure. Therefore it is not boiling. Due to the high permeability of wood, when the MC is above FSP, there is no large pressure gradient built

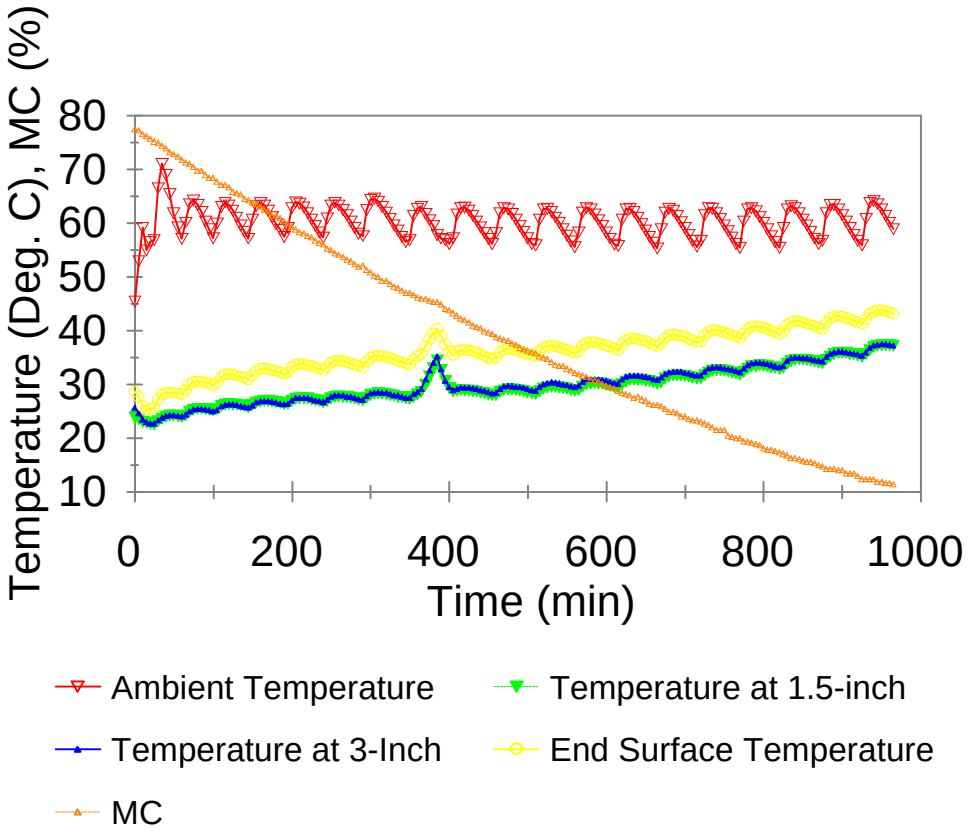

Figure 12.3 MC and Temperature Curves at Different Locations in Red Oak Specimen in Continuous Vacuum Drying

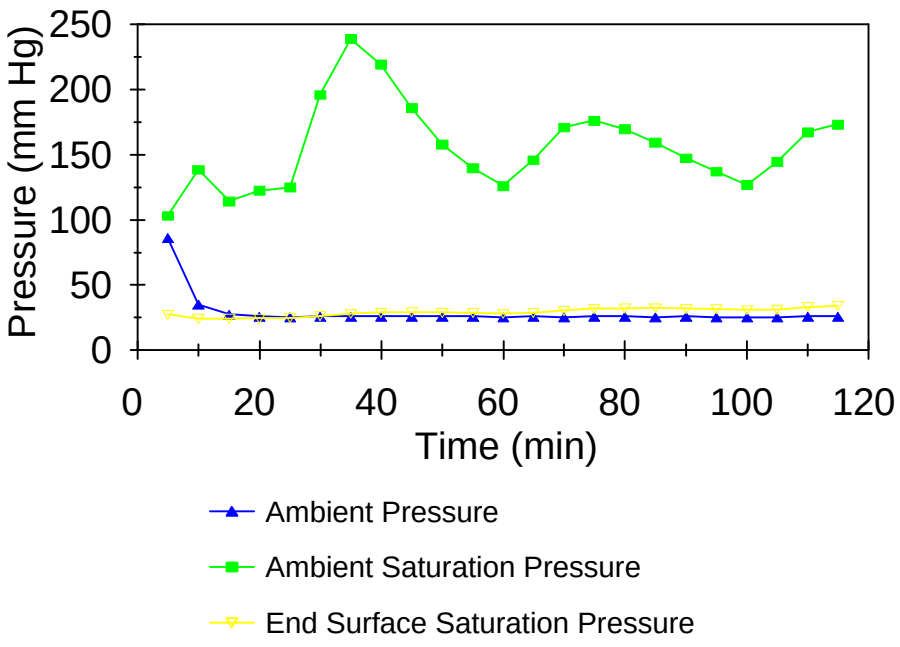

Figure 12.4 Pressure and Saturation Pressure Curves of Ambient Environment and End Surface in Continuous Vacuum Drying of Red Oak Specimen

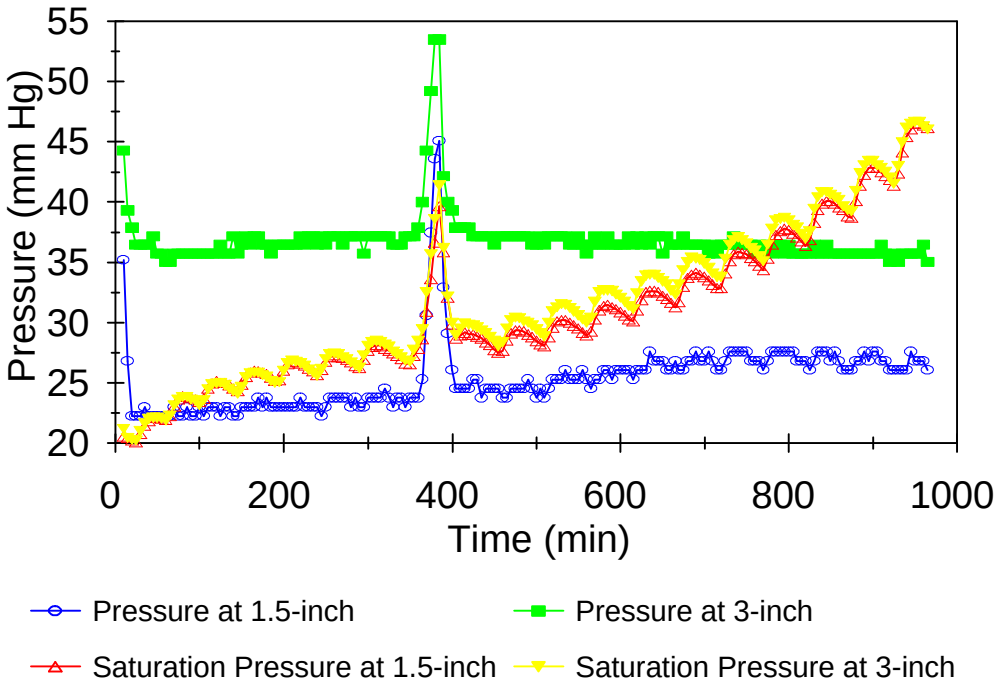

Figure 12.5 Pressure and Saturation Pressure Curves at Different Locations in Red Oak Specimen in Continuous Vacuum Drying

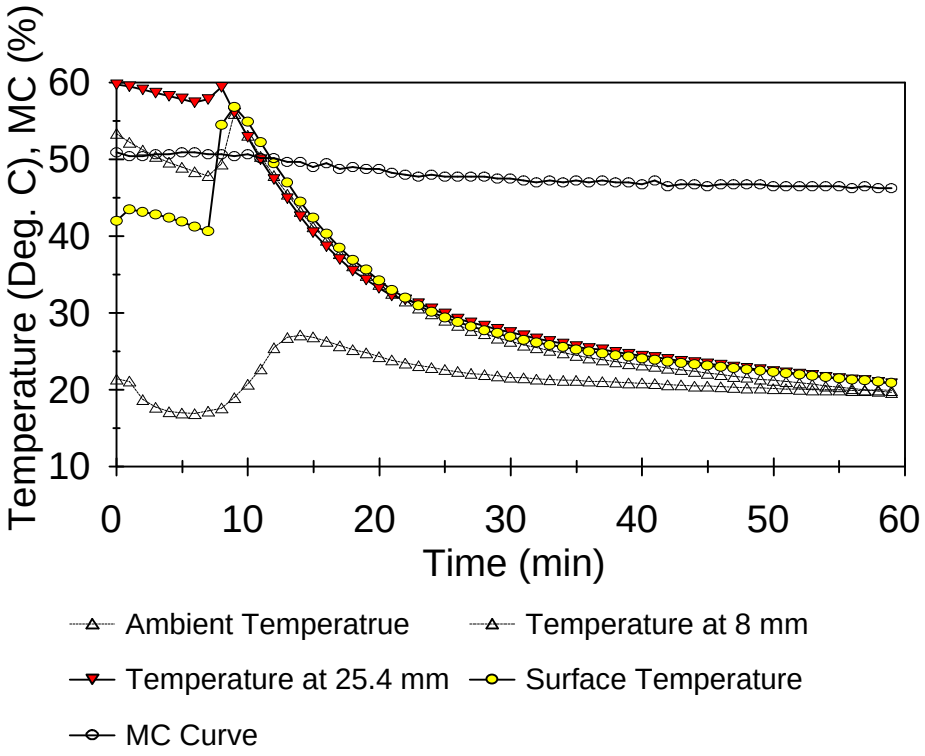

Figure 12.6 MC and Temperature Curves at Different Locations in Red Oak Specimen in Cyclic Vacuum Drying

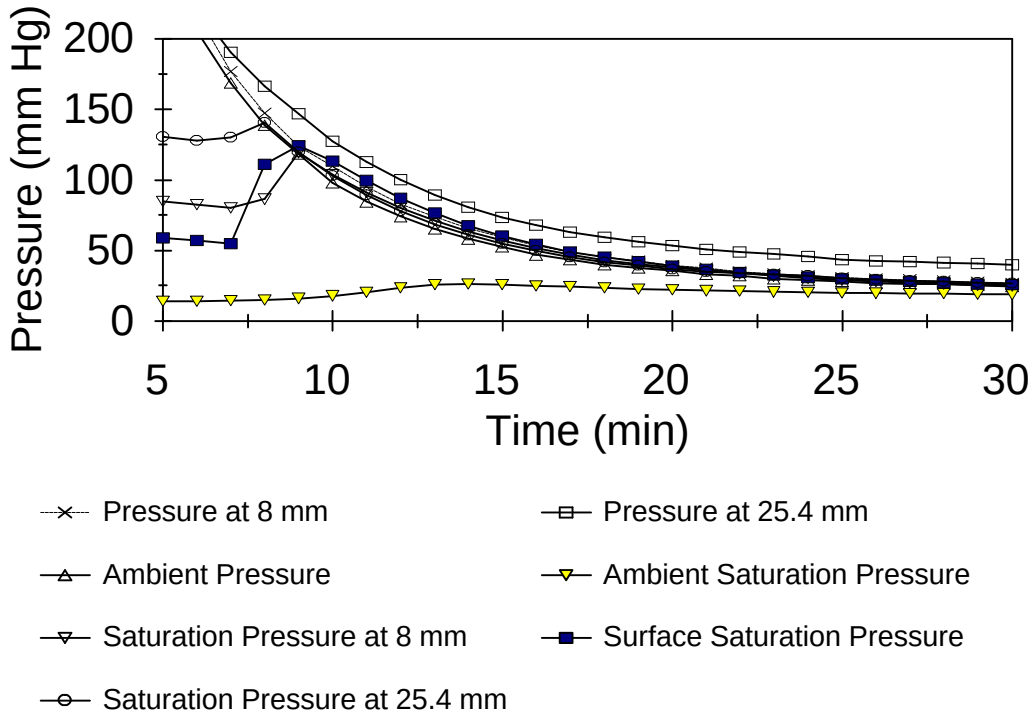

Figure 12.7 Pressure and Saturation Pressure Curves for Red Oak Specimen in Cyclic Vacuum Drying

up in this zone. Therefore, there is not significant moisture transfer by WVBF. However, this zone (Figure 12.5) still loses a significant amount of moisture due to large FWBF (capillary flow).

In cyclic vacuum drying, due to experimental procedures after heating and before applying a vacuum, surface temperatures tend to be lower than those in the center when a vacuum is applied. After the vacuum is applied, there is not much difference in pressure between the surface and interior of the wood. Under these conditions, boiling may occur inside the specimen first because of the higher interior temperature. This is the situation which occurred in the low initial MC specimens (Run #6). If at the beginning of the drying, there had not been a temperature gradient, boiling would have occurred at the surface first.

For the higher initial MC specimens, due to limited heat supply, locations inside the specimens did not reach the boiling condition. The boiling condition inside the wood was almost reached, but the local saturation pressure was not sufficient. The surface reached the boiling condition first. Regarding the center temperature, the decreasing temperature may be attributed to heat conduction from center to the surface as the surface was cooled because of the boiling or heat convection loss. This decreasing temperature reduced the chance for the wood near the center to reach the boiling condition. Regarding the pressure, when boiling occurred on the surface, the pressure inside the specimen did not decrease sufficiently to reach the boiling condition.

For the high initial MC specimens, more water was available to evaporate near the end surface. The boiling may have occurred near the surface (Run #5). The pressure near the surface could not be measured. Some boiling may have occurred inside the wood not far from the end surface.

Due to the relatively high permeability of wood, the pressures inside the specimens decreased rapidly after the vacuum was applied, but before boiling occurred on the end surface (Figure 12.5). According Figure 12.5, there was pressure gradient along the length. This occurred in every specimen. The pressure was lower at the location closest to the end grain and higher toward the center of the specimen. When boiling occurred on the surface of a specimen, the pressure in the location near the center of the specimen decreased more slowly. This can be clearly seen in Figure

12.5 in which the pressure at location "2" did not decrease significantly after boiling occurred at the end surface. On the other hand, there was still moisture transport due to the pressure difference. However, water vapor was continuously supplied by evaporation which kept the pressure almost steady at this location.

Figures 12.3 and 12.6 show that temperature increased gradually for continuous vacuum drying and decreased gradually for cyclic vacuum drying. This is because the ambient temperature was larger than the wood temperature in continuous vacuum drying and the opposite is true in cyclic vacuum drying. It is interesting to observe that in the high MC continuous vacuum drying, the temperature at the location "1" was lower than the temperature at the location "2" (Figure 12.3). This may be due to the fact that boiling occurred in location "1" not at location “2". Energy is consumed to evaporate water. Therefore, the wood in location "1" was cooled. For cyclic vacuum drying, temperatures at locations near the end surface were always lower than temperatures at the locations further from the end grain surface. However, the temperature difference between these two locations were very small.

12.2. Moisture Content at the Boiling Front

From the results of the previous section, in continuous vacuum drying the pressures decreased rapidly at first and remained generally unchanged after that (Figure 12.5). The temperature however kept increasing, as did the saturation pressure. When the saturation pressure is higher than local pressure, water boils. From preceding discussion, it seems that the temperature inside the wood is closely related to the MC. The objective of this experiment is to investigate the MC at the boiling front location.

Specimens were prepared the same way as shown in Figure 10.1. The specimens were is 2.5×1.5×10 inches in size and all have MCs above FSP. After a specimen was cut, one pair of holes was drilled in the center of the specimen as was done in section 12.1. The holes were located about 50 mm from the end surface. One hole was used to measure pressure, and other to measure temperature (Figure 12.8). There were nine experimental runs. The specimens were dried by

continuous vacuum drying. The same methodology as in section 12.1 was applied here to measure temperature and pressure.

When the saturation pressure was greater than the measured pressure, drying was stopped. At the conclusion of drying, the specimens were cut into five sections (Figure 12.8). The sections were oven-dried to constant weight. The MCs of these sections for one run are shown in Figure 12.9. This figure clearly shows that there was a moisture gradient along the length.

The relationship between the final MC and local temperature is presented in Figure 12.10, which includes results from nine experiments. There is one saturation temperature corresponding to each pressure. The pressures measured during vacuum drying were about 19 to 20 mm Hg. The saturation temperatures corresponding to this pressure range is about 22 to 23°C. In Figure 12.10, the first five points are at temperatures which are at or near these saturation temperatures. It is considered that boiling occurred in these five experiments and the boiling front is at these locations. All five of these MCs were all greater than FSP. The conclusion can be drawn that the moisture content at the boiling front is above FSP. The other four points have temperatures greater than the saturation temperatures. It is assumed that boiling occurred in each of these cases, but there was no longer a boiling front. The correlation between MC and temperature in the nine experimental runs was calculated to be 0.903. There appears to be a relationship between the MC and temperature during continuous vacuum drying.

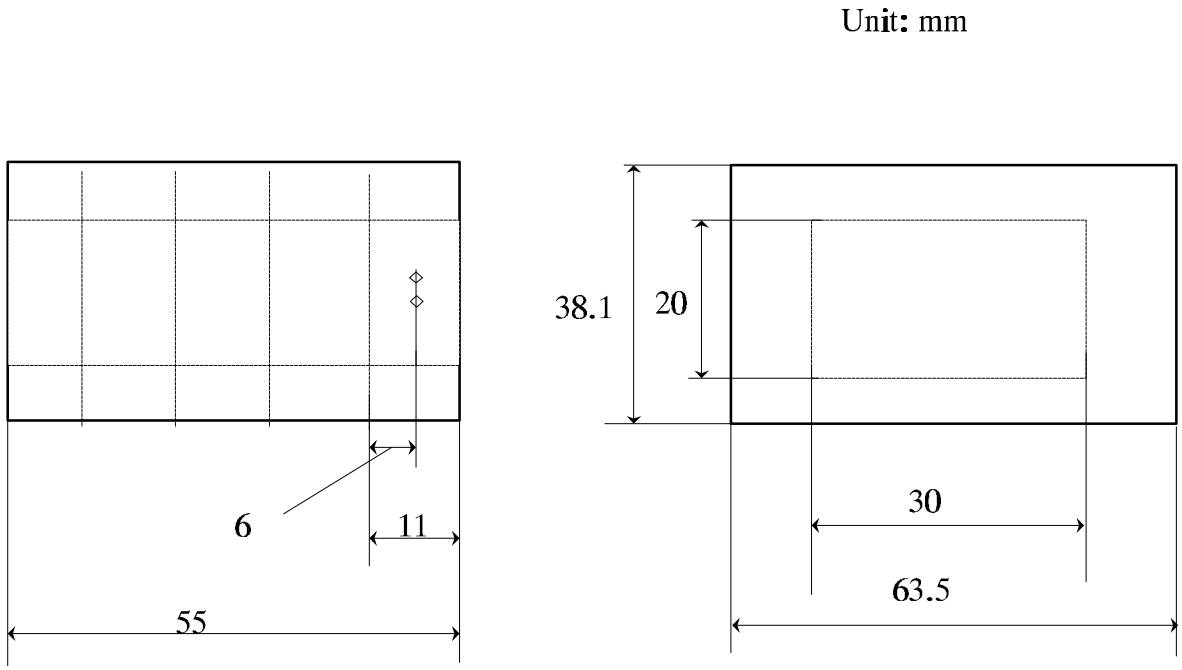

Figure 12.8 Schematic Diagram of Locations to Measure MC at Boiling Front

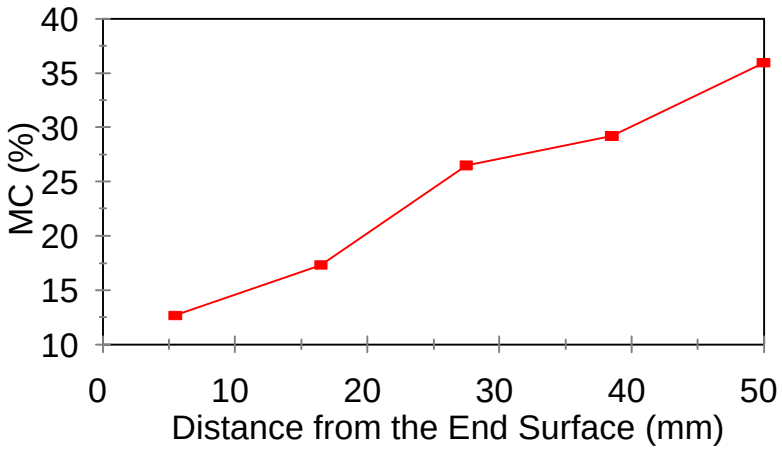

Figure 12.9 Moisture Gradient along the Length From Boiling Front to End Surface for Red Oak during Continuous Vacuum Drying

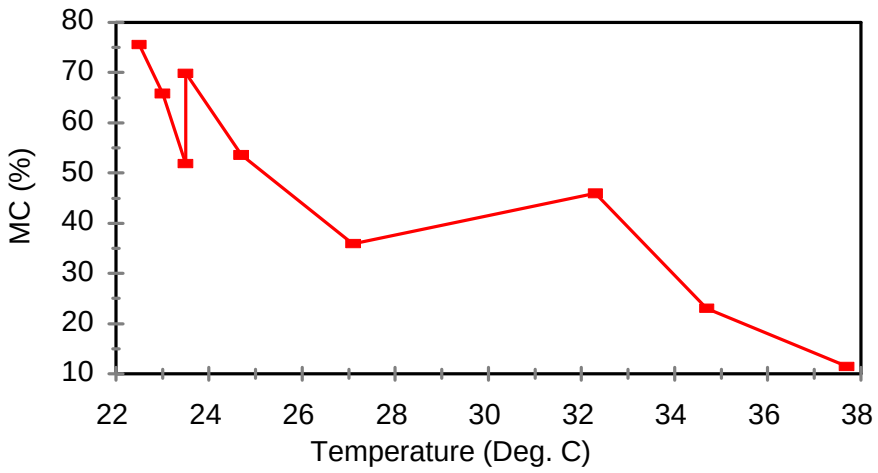

Figure 12.10 Relationship between the MC and Temperature in Continuous Vacuum Drying of Red Oak Specimens

13. Room Temperature Vacuum Drying

Vacuum drying of wood is fast, especially at high temperatures and high levels of vacuum, as can be seen in the previous chapters. Red oak has been dried in 22 hours from 56% to 5% MC at 60°C (see section 11.4). The drying rates are reduced if the drying temperatures are lowered. The objective of this experiment is to explore the possibility of drying red oak under vacuum by lowering the drying temperature to about room temperature. In previous experiments, drying did not stop even when the specimen temperature was lower than ambient temperature (Figure 10.3). Even at this low temperature, wood still dried at a reasonable drying rate.

Every drying process involves the supply of energy and removal of water. Theoretically vacuum drying at room temperature is possible. As discussed in the theoretical section (section 4.4), the evaporation rate is very high even at low temperatures at 0 mm Hg pressure. For example, the evaporation rate is about 0.25 g/cm^2 s at a temperature of 20°C in a perfect vacuum, even though the specimen temperature is lower than ambient temperature, as can be seen in Figure 10.3. This shows that the surface temperature is lower than the ambient temperature soon after drying. For drying of 1×1×10 inches specimen, the difference between the ambient and surface temperature reached 7.5°C after 140 minutes of cyclic vacuum drying. That means that there is certain amount of heat transfer by radiation and/or convection from the environment to the specimen providing energy to dry the wood. Heat convection is related to the density of medium. There is some heat convection even in vacuum drying because of the trace of water vapor in the chamber. Radiation is emitted from a body as a result of vibrational and rotational movements of molecular, atomic, and subatomic particles. Thermal radiation is transferred by electromagnetic wave and does not require a medium for its transfer as in the heat conduction and convection. The radiation heat transfer rates are proportional to the fourth power of the difference in temperature (Hewitt et al. 1997).

The specimens were prepared according to the procedure described in section 10.2 (Figure 10.1). The specimens were free of visible defects, such as knots and decay, etc. Three specimen sizes were used. In each drying run, the total weight of each specimen size was controlled to ca. 2000 grams. The size and the number of specimens are listed in Table 13.1. Several specimens were hung from the load cell and the others were put on the rack to dry in the oven. One specimen in each size was used to measure temperatures. The weights were recorded every five minutes. The pump was

stopped every 10 to 12 hours for 10 minutes for necessary maintenance.

Table 13.1 Number of Specimens on the Load Cell for Different Sizes

Size (inch)	Number of Specimen in Each Drying Load	Number of the Specimen on Load Cell
1×1×10	11	2
1.5×1.5×10	5	1
1×1×15	8	3

Figures 13.1 to 13.3 show the MC, temperature and pressure curves of the room temperature vacuum drying for the size of 1×1×15 inches. The drying (MC) curves for the other two sizes are shown in Figure 13.1. The spikes in figure 13.3 correspond to the time when pressures were relieved due to the maintenance requirement. Average drying rates for three different specimen sizes are presented in Table 13.2.

Table 13.2 Room Temperature Drying Rates

Size (inch)	Initial MC (%)	Final MC (%)	Drying Time (h)	Dry Rate (%/h)	R^2
1.5 × 1.5 × 10	49.82	14.71	110	0.319	1.00
1 × 1 × 10	81.42	24.19	70.67	0.810	0.97
1 × 1 × 15	79.64	11.92	115.5	0.587	1.00

By comparing the drying rates of the three specimen sizes, statistical results showed significant differences between the drying rates. This result is consistent among all tests (see sections 10.6 and 11.4). Specimens of 1×1×10 inches dried the fastest. Specimens of 1×1×15 inches dried slower and 1.5×1.5×10 inches the slowest.

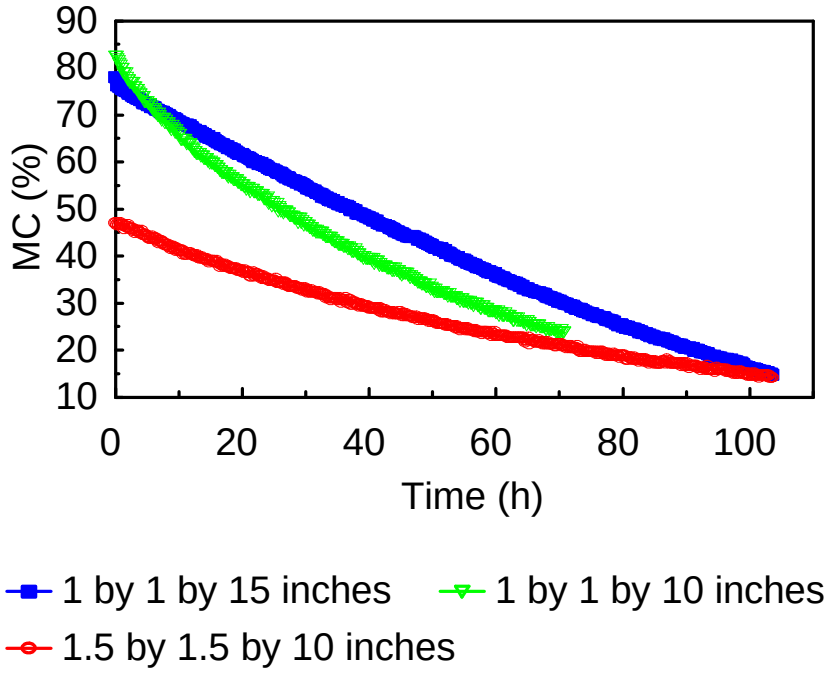

Figure 13.1 Moisture Content Curve of Room Temperature Vacuum Drying of Red Oak

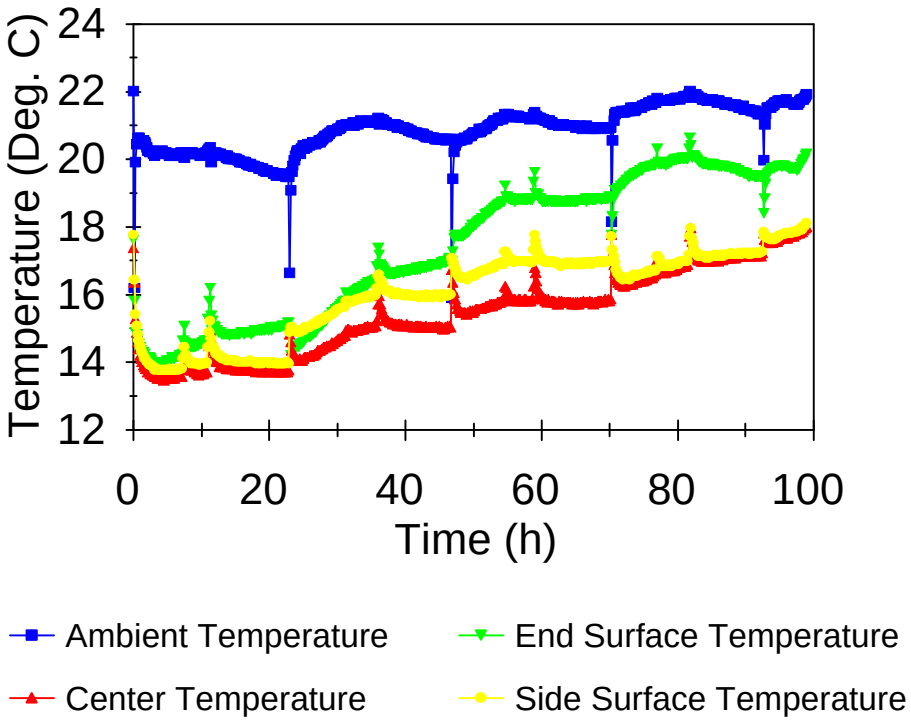

Figure 13.2 Temperature Curves of Room Temperature Vacuum Drying of Red Oak of 1×1×15 inches Specimens

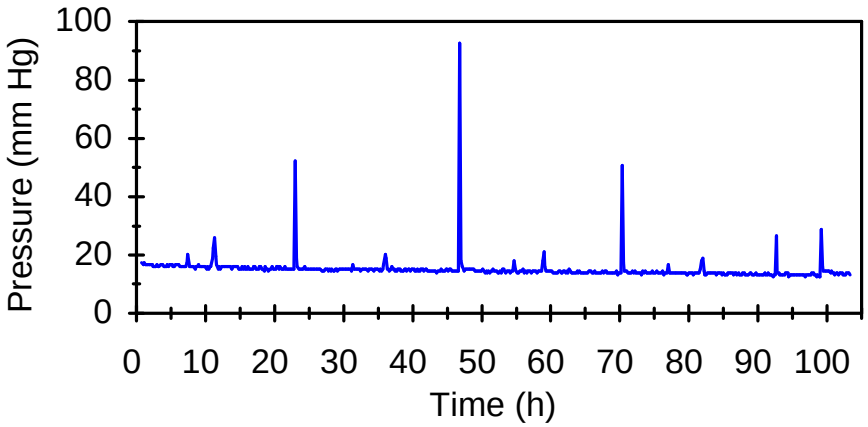

Figure 13.3 Pressure Curve of Room Temperature Vacuum Drying of Red Oak of 1×1×15 inches Specimens (the initial pressure of 760 mm Hg is not shown because of scale consideration)

The MC curves are more linear than most conventional drying curves (Salin 1991). Wood is dried at almost a constant rate. R^2 values presented in Table 13.2 are also close to unity. The MC curve is nearly linear. The drying rate was determined primarily by the heat supply from the ambient environment. The temperature difference between the specimen and the environment was almost constant over time and the ambient pressure was constant. Therefore, the amount of water removal was almost the same which resulted in a practically constant drying rate. The temperature (Figure 13.2) curve shows that at the very beginning the surface temperature was reduced, because the sensible heat energy stored in the wood was consumed to evaporate the water initially.

It was observed that the drying quality was good with no color change during drying, nor were there is any visible drying defects. This experiment indicates that it is possible to dry red oak at room temperature condition with reasonable drying rates.

14. Summary and Conclusions

14.1. Summary

The primary objective of this study, based on both theory and experimentation was to prove that the total pressure difference is the primary driving force during vacuum drying. Several theoretical aspects related to the vacuum drying process were investigated. First, the effects of various driving forces on vacuum drying were discussed. The theoretical drying rates for diffusion, FWBF and WVBF were calculated and compared. Then, using the Hailwood and Horrobin sorption theory, the concept of EMC in the absence of air was developed. Finally, the theoretical maximum MC drop in one cycle of cyclic vacuum drying was calculated using energy balance considerations. A model, using the above theoretical results, was developed for vacuum drying to describe the mechanism of cyclic vacuum drying, including the concept of a boiling front and its movement.

The experimental tests were conducted in a vacuum system capable of pulling the vacuum to 15 mm Hg. Temperatures were measured with RTD and pressures were measured with pressure transducers. Weights were measured by a load cell located inside the vacuum oven. Red oak and white oak were used due to the large differences in their permeability values.

To evaluate the effect of specimen size on the drying rate, four different thicknesses (1, 1.5, 2, 2.5 inches) and three different lengths (5, 10, 15 inches) were used. The specimens were dried under both continuous and cyclic vacuum drying procedures. In cyclic vacuum drying, the specimens were heated to 60°C in a heating oven. They were then transferred to the vacuum oven. A vacuum was pulled to about 18 mm Hg, and the vacuum was continually for 140 minutes. In continuous vacuum drying, a temperature of 60°C was maintained in the vacuum oven. The vacuum pump pulled a vacuum to 18 mm Hg which was maintained for four hours.

For cyclic vacuum drying, the results showed that the drying rate was not affected by specimen thickness. However, it was affected by specimen length, since the shorter material dried faster. The cyclic drying curve consisted of two distinct parts, a fast and slow-drying period. The fast drying period which occurred at the beginning of drying lasted about 10 to 20 minutes. The slow drying period began when the specimen cooled to a temperature close to the ambient temperature.

In continuous vacuum drying, the drying rate was affected by both the specimen length and

thickness. The shorter and thinner specimens dried faster. The continuous vacuum drying curves was almost linear.

In order to analyze the drying rates from the end grain surfaces, specimens were coated with wax, wrapped in a plastic film and inserted into a rubber tube to prevent the moisture loss from the side surfaces during vacuum drying. The specimen size was 1×1×10 inches (25.4×25.4×254 mm) and the inner diameter of the rubber tube was 28.31 mm. Red oak specimen were sealed and dried by both the cyclic and continuous vacuum drying procedures. This indicates that side-sealed specimens dried almost as fast as unsealed specimen. Both had the same drying curve pattern. The results showed that there was little moisture loss from the side surfaces; most of the moisture loss was through the end grain. White oak was sealed and dried in both cyclic and continuous vacuum drying. The drying rates of sealed white oak and red oak are compared. There was no significant difference in the cyclic vacuum drying rate of the sealed red oak and sealed white oak specimens at the 5% significant level. However, they were significantly different at 10% significant level. In contrast, however, there was a significant difference between the two species for the continuous vacuum drying. Red oak dried faster than white oak.

There was a moisture gradient along the specimen length in both cyclic and continuous vacuum drying procedures. A very steep moisture gradient through the thickness occurred in the side surface during continuous vacuum drying.

In order to characterize boiling front during the vacuum drying, red oak specimens of 2.5×1.5×10 inches were used. The specimens were drilled in two designated locations with 3.175 mm diameter holes. There were two pairs of holes in each specimen. One hole in each pair was used to measure the pressure in the wood and the other hole was used to measure the temperature. Glass tubes with outside diameter of 1.7272 mm and inside diameter of 1.27 mm were inserted into the hole and sealed with epoxy resin. Rubber tubes were then used to connect the glass tubes to the pressure transducers. Both cyclic and continuous vacuum drying were used. The experimental results showed that boiling occurred during drying and that the boiling front retreated from the ends toward the center of wood as drying proceeded. The retreating speed depended on the heat supply and the permeability. The MC of wood was closely related to the local temperature.

Continuous vacuum drying at room temperature was investigated. Three sizes (1×1×10,

1.5×1.5 ×10, and 1×1×15 inches) of red oak specimens were used. The specimens were dried at 20°C and a pressure of about 18 mm Hg. The results showed that wood can be vacuum dried at room temperature with little or no degrade at reasonable drying rates.

14.2. Conclusions

The objectives of this research are to show: (1) Total pressure difference is the major driving force which controls the vacuum drying rate. (2) Moisture is removed mainly in the longitudinal direction and moisture moves in steam form. (3) Boiling occurs inside the wood. There is a boiling front and the boiling front moves toward the center of the lumber as drying proceeds.

Objective #1 is: Total pressure difference is a major driving force which controls the vacuum drying rate.

In vacuum drying, the ambient pressure is lowered, which creates total pressure differences inside the wood. According to Darcy's law, moisture is transferred due to a total pressure difference and the amount of moisture transferred is directly proportional related to the permeability, which is an important factor affecting the drying rate. The continuous vacuum drying rate of red oak is larger than that of white oak due to its higher permeability.

Theoretical comparison of several forms of moisture movement inside the wood showed that moisture movement under a total pressure difference is the dominant mechanism during vacuum drying. It was shown that diffusion is not a major moisture transport mechanism in vacuum drying as it is in conventional kiln drying. This is further reaffirmed in the room temperature vacuum drying, because diffusion is related to temperature and at the room temperatures, the diffusion rate is small. However, the vacuum drying rate at room temperature was still reasonably high. Because of this, diffusion is not considered to be a major factor in moisture movement during vacuum drying.

Using drying curve analysis, it was shown that a cyclic vacuum drying curve had two distinct parts. The fast drying period corresponded to the period of fast water vapor movement due to the large pressure difference in the early stages of drying. The slow drying period occurred when the pressure difference decreased.

Objective #2: Moisture is removed mainly in the longitudinal direction and moisture moves in steam form.

At room temperature, the theoretical evaporation rate is large which allows the possibility of converting liquid water to water vapor which can be transferred under a total pressure difference in which water moves in steam form. Through the vacuum drying model development and analyses, it was shown that the moisture movement is in steam form and most water is transferred in the longitudinal direction. This conclusion was also tested and confirmed in the various laboratory experiments.

Based on theoretical calculation, most moisture is removed in the longitudinal direction. The experimental tests showed that the cyclic vacuum drying rate was not affected by the specimen thickness but it was affected by the specimen length. This showed that moisture moved in the longitudinal direction. In end grain vacuum drying, the drying rate of sealed specimens was not significantly different from that of unsealed specimens. Little moisture transfer through the side surface was found in the experiment. A moisture gradient was found along the length. A moisture gradient through the thickness was steep and occurred in a very shallow surface. These facts further enhance the conclusion that the moisture is transferred primarily in the longitudinal direction.

Objective #3: The boiling occurs inside the wood. There is a boiling front and the boiling front moves from the ends toward the center of wood as drying proceeds.

Under vacuum drying, the pressure inside the wood is reduced due to the low ambient pressure. When the pressure is lower than the saturation pressure, water boils. At the beginning, boiling occurs on the surface and the boiling front retreats to the center of the wood as drying proceeds. This phenomenon was found in the theoretical calculation and was shown to exist in the experimental tests.

The following general conclusions can be drawn from this research. Total pressure difference is a major driving force during vacuum drying. Most moisture moves and transfers from the wood along the longitudinal direction. Boiling occurs during vacuum drying. Therefore a boiling front exists and it moves towards the center of lumber along the grain as drying proceeds.

15. Literature Cited

Alder, H.A. 1995. Hardwoods of North America. General Technical Report FPL-GTR-83. Forest Products Laboratory, Madison, WI. pp136.

Adesanya, B. A., A. K. Nanda, and J. N. Beard. 1988. Drying rates of high temperature drying of yellow poplar. Drying Technology 6(1):95-112.

Avramidis, S., and R.L. Zwick. 1992. Exploratory radio-frequency/vacuum drying of three B.C. coastal softwoods. Forest Products Journal 42(7/8):17-24.

_____, M. Liu, and B.J. Neilson. 1994. Radio-frequency/vacuum drying of softwoods: drying of thick western red cedar with constant electrode voltage. Forest Products Journal. 44(1):41-47.

_____, L. Zhang, and S.G. Hatzikiriakos. 1996. Moisture transfer characteristics in wood during radio frequency vacuum drying. P125-p133. In: proceedings of 5th international IUFRO wood drying conference. Quebec City. Canada.

Benet, J. C., and P. Jouanna. 1983. Non-equilibrium thermodynamic in non-saturated porous media with phase change. Int. J. Heat and Mass Transfer 26(11):1585-1595.

Bramhall, G. 1979a. Mathematical model for lumber drying. I. Principles involved. Wood Sci. 12(1):14-21.

_____. 1979b. Mathematical model for lumber drying. II. The Model. Wood Sci. 12(1):22-31.

Bolton, A.J., and J.A. Petty. 1978. A model describing axial flow of liquids through conifer wood. Wood Science and Technology 12(1):37-48.

Bruin, S., and K. C. Luyben. 1980. Drying of food materials: A review of recent developments. P155-215. In Mujumdar, A.S., (ed). Advances in Drying. Volume 1. Hemisphere, Publishing Corp. N.Y.

Chen, Z., and F. M. Lamb. 1995a. The concept of boiling front in vacuum drying. Vacuum Drying of Wood '95. Slovakia. p110-116.

_____, and _____ 1995b. The internal conditions in vacuum drying of wood. Vacuum Drying of Wood '95. Slovakia. p45-53.

Cho, S. H. 1975. An exact solution of the coupled phase-change problem in a porous medium.

Int. J. Heat and mass /transfer 18(10):1139-1142.

Choong, E.T., and F.O. Tesoro. 1974. Permeability of twenty two small diameter hardwoods growing on southern pine sites. Wood and Fiber 6(1):91-101.

Cloutier, A., Y. Fortin, and G. Dhatt. 1992. A wood drying finite element model based on the water potential concept. Drying Technology 10(5):1151-1181.

Comstock, G.L., and W.A. Cote, Jr. 1968. Factors affecting permeability and pit aspiration in coniferous sapwood. Wood Science and Technology 2(3):279-291.

Cote, W.A.Jr. 1963. Structural factors affecting permeability of wood. Journal of Polymer Science, Part C. No. 2:231-242.

Cross, M., R.E. Gibson, and R. W. Young, 1979. Pressure generation during the drying of a porous half-space. Int. J. Heat and Mass Transfer 22(1):47-50.

Dayan, A., and E.L. Gluekler. 1982. Heat and mass transfer within intensively heated concrete slab. Int. J. Heat and Mass Transfer 25(10):1461-1467.

Degroot, S. R., and P. Mazur, 1962. Non-equilibrium Thermodynamics. North Holland Publishing Co. N.Y. pp510.

Droin, A., J.L.Taverdet, and J. M. Vergnaud. 1988. Modeling the kinetics of moisture adsorption by wood. Wood Science and Technology 22(1):11-20.

_____. 1989a. Modeling the process of moisture absorption in three dimensions by wood samples of various shapes: cubic, parallelepedic. Wood Science and Technology 23(3):299-310.

_____. 1989b. Modeling of moisture absorption within a section of parallelepipedic sample of wood by considering longitudinal and transversal diffusion. Holzforschung. 43(5):297-302.

Eaton, R.A. and M.D.C. Hale. 1993. Wood: Decay, Pests, and Protection. Chapman and Hall, N. Y. pp546.

Erickson, H.D. 1970. Permeability of southern pine. Wood Science 2(3):149-157.

Forest Products Laboratory. 1990. Wood Engineering Handbook. Prentice Hall, Eaglewood Cliff, NJ. pp438.

Fortes, M., and M.R. Okos. 1981. A non-equilibrium thermodynamics approach to transport

phenomena in capillary porous media. Trans, ASAE 24(3):756-760.

Furguson W. J., and I. W. Turner. 1994. A two-dimensional numerical simulation of drying of pine at high temperature. In: Proceedings of 4th IUFRO wood drying conference. Rotorua, New Zealand.

Guilmain, C., O. Baixeras, and W. Jomaa. 1996. Discontinuous and convective vacuum drying of oak. 5th IUFRO Wood Drying Conference. Quebec City, Canada. pp 559.

Gupta, L. N. 1974. An approximate solution of the generalized Stefan's problem in a porous medium. Int. J. Heat and Mass Transfer 17(2):313-321

Hamano Y., and S. Nishio. 1986. High frequency electric power-vacuum drying of wood (3). Wood Industry 41(8):376-380.

Harris, R.A., and M.A. Taras. 1984. Comparison of moisture content distribution, stress distribution, and shrinkage of red oak lumber dried by a radio frequency/vacuum drying process and a conventional kiln. Forest Products Journal 34(1):44-54.

Hayashi, K., Y. Kanagawa, and M. Yasujima. 1993. Change of dry ability under vacuum drying by improvement of permeability of wood. Vacuum Drying of Wood' 93. Slovakia. pp292.

_____, and _____ . 1995. Experimental evidence of an importance of permeability in RF/Vacuum drying. Vacuum Drying of Wood '95. Slovakia. pp295.

Haygreen, J.G., and J. L.Bowyer. 1996. Forest Products and Wood Science: An Introduction. Iowa State University Press, Iowa. pp484.

Hewitt, G.F., G.L. Shires, and Y.V. Poleshaev. 1997. Heat and Mass Transfer. CRC Press. N.Y. pp1312.

Hillel, D. 1971. Soil and Water. Academic Press. N.Y. pp288.

Hougen, O. A., H.J. McCauley, and W.R. Marshall 1940. Limitations of diffusion equations in drying. AIChE Transaction. 36(2):183-206.

Jones, F.E. 1991, Evaporation of Water. Lewis Publisher. Chelsea, Mich. pp188.

Kamke, F A., and M. Vanek 1994. Comparison of wood drying model. p1-21. In: proceedings of 4th IUFRO wood drying conference. Rotorua, New Zealand.

_____, and _____ . 1996. Computer models for wood drying. In: Drying Pacific Northwest Species for Quality Markets. Proceedings of a conference sponsored

by the Forest Products Society. Oct. 30-Nov. 1, 1995. Washington.

Kanagawa, Y., and M. Yasujima. 1993. Effect of heat sources on drying time in vacuum drying of wood. Vacuum Drying of Wood'93. Slovakia, pp292.

Karki, K.C., and S. V. Patankar. 1988. Calculation procedure for viscous impressible flows in complex geometries. Num. Heat Transfer 14(3):295-317.

Kawabe, J., and M. Mori. 1984, Vacuum drying of wood with high frequency heating (I) On the drying rate, compared with the kiln drying. Bulletin of the Kyushu University Forests 54:125-135.

Kollmann, F.F.P., and W.A. Cote. 1968. Principle of Wood Science and Technology. I. Solid Wood. Springer-Verlag. N.Y. pp592.

Koppleman, E. 1976. Process and apparatus for seasoning wood. US. Patent #3986268.

Kozlowski, T.T., and S.G. Pallardy. 1997. Physiology of Woody Plants. Academic Press. N.Y. pp411.

Lamb, F.M., and E.M. Wengert. 1993. Comparison of lumber drying quality between two vacuum drying systems and a conventional predryer and dry kiln system. Vacuum Drying of Wood, 93.Slovakia. pp292.

Lee, A.W.C., and R.A. Harris. 1984. Properties of red oak lumber dried by a radio frequency/vacuum process and dehumidification process. Forest Products Journal. 34(5):56-58.

Lin, S. 1982. An exact solution of the sublimation problem in a porous medium. With an unknown temperature and vapor concentration at the moving sublimation front. Trans. ASME J. Heat Transfer 104(4):808-811.

Liu, J. Y. 1990. Lumber drying in a medium with variable potentials. In: General Papers: Phase change and convective heat transfer: Proceedings of AIAA/ASME Thermophysics and heat transfer conference. pp149-156.

Luikov, A.V. 1975. Systems of differential equations of heat and mass transfer in capillary porous bodies. Int. J. Heat Mass Transfer 18(1):1-14.

MacLean, J.D. 1941. Thermal conductivity of wood. Heating, Piping, and Air Conditioning. 13(6):380-391.

Massey, B. S. 1986. Mechanics of Fluid. 6th edition. Reinhold Co. Van Nostrand, London. pp508.

Mikhailov, Y. 1976. Exact solution for freezing of humid porous half space. Int. J. Heat and Mass Transfer 19(5):651-655.

Moldrup, S., and B. Moldrup, 1992. Drying of timber under vacuum in an atmosphere of super-heated steam. Understanding the Wood Drying Process: A synthesis of theory and practice. 3rd IUFRO international wood drying conference. Vienna, Austria.

Moyne, C., and A. Degiovanni. 1985. Importance of gas phase momentum equation in drying above the boiling point of water p109-115. In: Mujumda, A.S., and R. Toei (Ed). Drying'85, Hemisphere Publishing Corp., Washington D. C.

_____, and M. Martin, 1982. Influence of a total pressure gradient in gaseous phase on drying with particular reference to wood. International Heat and Mass Transfer 25(12):1839-1845.

Nelson, R. M. Jr. 1986a. Diffusion of bound water in wood. Part 1: The drying force. Wood Sci. Technol. 20(2):125-135.

_____ 1986b. Diffusion of bound water in wood. Part 2: a model for isothermal diffusion. Wood Sci. Technol. 20(3):235-251.

_____1986c. Diffusion of bound water in wood. Part 3: A model for nonisothermal diffusion. Wood Sci. Technol. 20(4):309-328.

Neumann R, A. Mielke, and G. Böhner. 1992. Comparison of conventional and convective vacuum drying of beech. Understanding the Wood Drying Process: A synthesis of theory and practice. 3rd IUFRO international wood drying conference. Vienna, Austria.

Noack, D. 1965. Sonderverfahren der Holztrocknung Holzwirtschaftliches Jahrbuch Nr. 15, Holztrocknung. DRW-verlags-gmbh Stuttgart.

Pagnozzi, E.G. 1983. Vacuum Drying of Wood: Possibilities and Limitations. Modeling. No. 98 Vol.II, 688-703. Paper presented at Jubila symposia of thefaculty of forestry university of Stellenbosch.

Patankar, S. V. 1991. Computation of conduction and Duct Flow. Heat Transfer Innovative Research Inc. Maple Grove, MN. pp354.

Peng, S. W., and G.Q. Chen. 1993. Exact solution of coupled heat and mass transfer with double moving interfaces in a porous half-space. Int. J. of Energy Research. 17(3):193-202.

Perre, P., and S. Mosnier. 1995. Vacuum drying with radiative heating. Vacuum Drying of Wood '95.

Plumb, O.A., G.A. Spolek, and B. A. Olmstead. 1985. Heat and mass transfer in wood during drying. Int. J. Heat Mass Transfer 28(9):1669-1678.

Ressel, J.B. 1994. State of art on the vacuum drying of timber. In: 4th IUFRO Wood Drying Conference. Rotorua, New Zealand. pp472.

Salin, J. 1991. Modeling of wood drying. Drying Technology 9(3):775-793.

Salisbury, F.B. and C.W. Ross. 1992. Plant physiology. Wadsworth Publish Co. CA. pp682.

Sasaki, K., J. Kawabe, and M. Mori. 1987. Vacuum drying of wood with high frequency heating (II), The pressure within lumber during evacuation and drying. Bulletin of the Kyushu University Forests 57:245-265.

Siau, J.F. 1983. A proposed theory for nonisothermal unsteady-state transport of moisture in wood. Wood Sci, Technol. 17(1):75-77.

_____.1984. Transport Process in Wood. Springer-verlag, N.Y. pp218.

Simpson, W.T. 1971. Equilibrium moisture content prediction for wood. Forest Products Journal. 21(5):48-49.

_____. 1973. Predicting equilibrium moisture content of wood by mathematical models. Wood and Fiber Science 5(1):41-49.

_____. 1984. Drying wood: A review. Drying Technology 2(3):353-368.

_____.1987. Vacuum drying northern red oak. Forest Products Journal. 37(1):35-38.

_____, and H. N. Rosen. 1981. Equilibrium moisture content of wood at high temperatures. Wood and Fiber 13(3):150-158.

Sidiropoulos, E., and C. Tzimopoulos. 1983. Sensitivity analysis of a coupled heat an mass transfer model in unsaturated porous media. Journal Of Hydrology 64(1-4):281-298.

Skaar, C. 1972. Water in Wood. Syracuse Univ. Press, Syracuse, N.Y. pp218.

Smith, D.N., and E. Lee. 1958. The longitudinal permeability of some hardwoods and softwoods.

For. Prod. Res. Spec. Report No. 13. Dept. Of Sci and Indust. Res., London, England. pp13.

Sparrow, E.M. S.V. Patankar. and H. Shahrestani. 1978. Laminar heat transfer in a pipe subjected to a circumferentially varying enteral heat transfer coefficient. Num. Heat Transfer 1(1):117-127.

Spolek, G., and O. A. Plumb. 1981. Capillary pressure of woods. Wood Sci. Tech. 15(3):109-100.

Stanish, M. A., G. S. Schajer, and F. Kayihan. 1986. A mathematical model of drying for hygroscopic porous media. AIChE J. 32(8):1301-1311.

Stefan, H.S., and J. C. Jaeger. 1959. Heat Conduction in Solids. Clarendon Press, Oxford. pp 296.

Taniguchi, Y., and S. Nishio. 1991. High frequency power vacuum drying of wood. IV. Comparison of physical and mechanical properties of lumber dried by several drying methods. J. Japanese Wood Res. Soc. 37(5):405-414.

Tesoro, F.O., E.T. Choong, and O.K. Kimbler. 1974. Relative permeability and the gross pore structure of wood. Wood and Fiber 6(3):226-236.

Thomas, H.R., K. Morgan, and R.W. Lewis. 1980. A fully nonlinear analysis of heat and mass transfer problems in porous bodies. Int. J. For Num. Meth. In Eng. 15(5):1381-1393.

Trebula, P., and A. Dekret. 1984. Vacuum drying hornbeam wood. Holztechnologie 25(1):20-22.

Trofatter, G., R.A. Harris, J. Schroeder, and M.A. Taras. 1986. Comparison of moisture content variation in red oak lumber dried by a radio-frequency/vacuum process and a conventional kiln. Forest Products Journal 16(5):25-28.

Tuttle, F. 1925. A mathematical theory of the during of wood. Journal of the Franklin Institute 200(5):609-614.

Vergnaud, J. M. 1982. Drying of Polymeric and Solid Materials. Springer-Verlag. N.Y. pp336.

Voigt, H., O .U. Krischer, and H. Schauss. 1940. Special technique for wood drying. Holz als Roh-Werkstoff 11(9):364-375.

Waananen, K.M., and M.R. Okos. 1989. Analysis of mass transfer mechanisms during drying

of extruded semolina. Proceedings of the 5th International Congress on Engineering and Food. May 28-June 3, Cologne, Germany.

_____, J.B. Litchfield, and M.R. Okos. 1993. Classification of drying models for porous solids. Drying Technology 11(1):1-40.

Walker, J.C.F. 1993. Primary Wood Processing. Chapman & Hall. N.Y. pp955.

Wangaard F.F. 1981. Wood: Its structure and Properties. Clark C. Heritage Memorial Workshop on Wood Materials Research Laboratory. Penn. State Univ. PA. pp 465.

Wengert, E.M., and F.M. Lamb. 1982. Hardwood drying test evaluates new methods. Forest Industries 109(13):21-22.

Whitaker, S. 1988. The role of irreversible thermodynamics and the Onsager relations in the analysis of the drying phenomena. Proceedings of the sixth international drying symposium, Versailles.

Zhao, S. 1988. A new approach to eliminate checking in hardwood dried by a vacuum drying method. Holz als Roh- und Werkstoff 46(9):331-334.

Zimmermann, M.H. 1983. Xylem Structure and the Ascent of Sap. Springer-Verlag, Berlin. pp143.

16. Appendix

Appendix A

Computer program

```
CCCCCCCCCCCCCCCCCCCCCCCCCCCCCCCCCCCCCCCCCCCCCCCCCCCCCCCCCCCCCCCCCCCC
      SUBROUTINE ADAPT
C=================================================
C-----MOISTURE DISTRIBUTION FOR 2-D GEOMETRY RED OAK
C---------------------------------------------------------------------
$ INCLUDE:'COMMON'
C  P  REPRESENTS THE MOISTURE CONTENT IN PERCENT, TEM TEMPERATURE
C>>>>>>>>>>>>>>>>>>>>>>>>>>>>>>>>>>>>>>>>>>>>>>>>>>>>>>>>>>>>>>>>>>>
      DIMENSION PMC (NI,NJ), TEM(NI,NJ),CMC(NI,NJ)
      DIMENSION PO(30,30),DM(30,30),PC(30,30),DML(30,30),AHV(30,30),
     1   PEG(30,30),PEL(30,30),DMC(30,30),
     2   DMV(30,30),ADV(30,30),MB(30,30)
      EQUIVALENCE (F(1,1,1), TEM(1,1)), (F(1,1,2), PMC(1,1))
C>>>>>>>>>>>>>>>>>>>>>>>>>>>>>>>>>>>>>>>>>>>>>>>>>>>>>>>>>>>>>>>>>>>
      ENTRY   GRID
      HEADER ='WOOD VACUUM DRYING PROCESS'
      PRINTF ='PRINT1'
C  CROSS-SECTION IS 122*2.54 CM AS XL AND XY
      CALL  DATA2 (XL, 122., YL,2.54)
      CALL  INTA2 (NCVLX,20, NCVLY,20)
      CALL EZGRID
      RETURN
C---------------------------------------------------------------------
      ENTRY BEGIN
      TITLE(1)='TEMPERATURE FIELD'
      TITLE(2)='PRESSURE FIELD'
      WRITE(6,*) 'ENTER IO'
```

```
      READ(6,*) IO
      CALL INTA5 (KSOLVE(2), 1, KPRINT(1), 1,KSOLVE(1),1,
     1  LAST,IO, KPRINT(2),1)
C       HE IS HEAT TRANSFER COEFFICIENT.
      CALL DATA9 (DT,0.000001, HE,SMALL, PMCO, 101325.,
     1  TEMO, 70., PE,BIG, G,0.56, AMC,71.,
     1  TINF,40., PINF,7330.)
C INF INITIALLY SURROUNDINGS
      DO  100 J=1, M1
      DO  100 I=1, L1
      PMC(I,J)=PMCO
      MB(I,J)=0
      DM(I,J)=0.
      DMC(I,J)=0.
      ADV(I,J)=0.
      PEG(I,J)=0.
      PO(I,J)=343000
      TEM(I,J)=TEMO
C ASSIGN THE INITIAL MOISTURE CONTENT 71%.
      CMC(I,J)=71
 100    CONTINUE
      DO 101 J=1, M1
      PMC(L1,J)=PINF
 101    CONTINUE
      DO 102 I=1, L1
      PMC(I,M1)=PINF
 102    CONTINUE
      RETURN
C---------------------------------------------------------------------
      ENTRY OUTPUT
      DO 210 IUNIT = IU1,IU2
CONNOR VALUE IS THE AVERAGE OF NEIGHBOR VALUES
      TEM(1,1)=(TEM(1,2)+TEM(2,1))/2.
      TEM(1,M1)=(TEM(1,M2)+TEM(2,M1))/2.
      TEM(L1,1)=(TEM(L2,1)+TEM(L1,2))/2.
```

```
      TEM(L1,M1)=(TEM(L2,M1)+TEM(L1,M2))/2.
      CMC(1,1)=(CMC(1,2)+CMC(2,1))/2.
      CMC(1,M1)=(CMC(1,M2)+CMC(2,M1))/2.
      CMC(L1,1)=(CMC(L2,1)+CMC(L1,2))/2.
      CMC(L1,M1)=(CMC(L2,M1)+CMC(L1,M2))/2.
      PMC(1,1)=(PMC(1,2)+PMC(2,1))/2.
      PMC(1,M1)=(PMC(1,M2)+PMC(2,M1))/2.
      PMC(L1,1)=(PMC(L2,1)+PMC(L1,2))/2.
      PMC(L1,M1)=(PMC(L2,M1)+PMC(L1,M2))/2.
COME HERE TO CALCULATE THE MOISTURE CONTENT OF WOOD
      DO  2011 J=1, M1
      DO  2011 I=1, L1
      PO(I,J)=101325./76*87500000*EXP(-10400/2./(TEM(I,J)
     1  +273.))
      DMC(I,J)=DMC(I,J)+DM(I,J)
COME HERE TO CALCULATE THE TOTAL MOISTURE LOSS
      TM=TM+DM(I,J)
      IF(MB(I,J).EQ.1) PMC(I,J)=PO(I,J)
      IF(CMC(I,J).LT.30.) THEN
      PMC(I,J)=PO(I,J)*(((1-1800/CMC(I,J)/
     1  (1417-9.43*(TEM(I,J)+273)+1.853/100*(TEM(I,J)+273)**2))/
     2  2/(-0.1722+4.732/1000*(TEM(I,J)+273)-5.553/1000000*
     3  (TEM(I,J)+273)**2))-(1+1800/CMC(I,J)/
     4  (1417-9.43*(TEM(I,J)+273)+1.853/100*(TEM(I,J)+273)**2))/
     5  2/(-0.1722+4.732/1000*(TEM(I,J)+273)-5.553/1000000*
     6  (TEM(I,J)+273)**2)/(-45.7+0.3216*(TEM(I,J)+273)-5.012/
     7  10000*(TEM(I,J)+273)**2)+((((1-1800/CMC(I,J)/
     8  (1417-9.43*(TEM(I,J)+273)+1.853/100*(TEM(I,J)+273)**2))/
     9  2/(-0.1722+4.732/1000*(TEM(I,J)+273)-5.553/1000000*
     1  (TEM(I,J)+273)**2))-(1+1800/CMC(I,J)/
     2  (1417-9.43*(TEM(I,J)+273)+1.853/100*(TEM(I,J)+273)**2))/
     3 2/(-0.1722+4.732/1000*(TEM(I,J)+273)-5.553/1000000*
     4  (TEM(I,J)+273)**2)/(-45.7+0.3216*(TEM(I,J)+273)-5.012/
     5  10000*(TEM(I,J)+273)**2))**2+1/(
     6  -45.7+0.3216*(TEM(I,J)+273)-5.012/10000*(TEM(I,J)+273)**2)/
```

```
     7   (-0.1722+4.732/1000*(TEM(I,J)+273)-5.553/1000000*
     8   (TEM(I,J)+273)**2)**2)**0.5)
         IF(PMC(I,J).GT.PO(I,J)) PMC(I,J)=PO(I,J)
         ENDIF
  2011    CONTINUE
         DO 212 K=0,500000, 100
         IF (K.EQ.ITER) GOTO 2155
  212     CONTINUE
         GOTO 210
COME HERE TO CALCULATE THE MC CHANGE
  2155    DO  2012 J=1, M1
         DO  2012 I=1, L1
         CMC(I,J)=CMC(I,J)+DMC(I,J)*100./G/XCV(2)/YCV(2)*DT*3600.
         DMC(I,J)=0.
  2012    CONTINUE
COME HERE TO CALCULATE THE AVERAGE MC OF THE BOARD
         AMC=AMC+TM*100/G/XL/YL*DT*3600
         TM=0.
         IF (ITER .EQ.0) WRITE (IUNIT,215)
  215     FORMAT (2X,'ITER',3X,'TIME H',4X,'TEM(22,10)', 3X,'TEM(20,10)',
     1   3X,'TEM(18,10)',3X,'TEM(16,10)', 3X,'(TEM(10,10)')
         WRITE (IUNIT,*) ITER,TIME, TEM(22,10),
     1   TEM(21,10), TEM(20,10), TEM(19,10), TEM(18,10), TEM(17,10),
     2   TEM(16,10), TEM(15,10), TEM(14,10), TEM(13,10), TEM(12,10),
     3   TEM(11,10),TEM(10,10),TEM(9,10),TEM(8,10),TEM(7,10),
     4   TEM(6,10),TEM(5,10),TEM(4,10),TEM(3,10),TEM(2,10),TEM(1,10)
         IF (ITER .EQ.0) WRITE (IUNIT,220)
  220     FORMAT (2X,'ITER', 3X,'TIME H',5X, 'PMC(22,10)', 3X,
     1   'PMC(20,10)', 3X,'PMC(18,10)',4X, 'PMC(15,10)')
         WRITE (IUNIT, *) ITER,TIME, PMC(22,10), PMC(21,10),
     1   PMC(20,10), PMC(19,10),PMC(18,10),PMC(17,10),PMC(16,10),
     2   PMC(15,10),PMC(14,10),PMC(13,10),PMC(12,10),PMC(11,10),
     3   PMC(10,10),PMC(9,10),PMC(8,10),PMC(7,10),PMC(6,10),
     4   PMC(5,10),PMC(4,10),PMC(3,10),PMC(2,10),PMC(1,10)
         IF (ITER .EQ.0) WRITE (IUNIT,277)
```

```
 277    FORMAT (2X,'ITER',3X,'TIME H',4X,'CMC(22,10)', 3X,'CMC(21,10)',
    1  3X,'CMC(18,10)',3X,'CMC(16,10)', 3X,'(CMC(10,10)')
       WRITE (IUNIT,*) ITER,TIME, CMC(22,10),
    1  CMC(21,10), CMC(20,10),  CMC(19,10), CMC(18,10), CMC(17,10),
    2  CMC(16,10), CMC(15,10),CMC(14,10), CMC(13,10),
    3  CMC(12,10), CMC(11,10),CMC(10,10),CMC(9,10), CMC(8,10),
    4  CMC(7,10), CMC(6,10),  CMC(5,10),CMC(4,10), CMC(3,10),
    5  CMC(2,10), CMC(1,10)
       WRITE(IUNIT,*) ITER, TIME,AMC
COME HERE TO OBSERVE THE BOILING FRONT
       LL=L2
       MM=M2
       DO  2015 I=1, L2
       DO  2015 J=1, M2
       IF(PO(I,J).LT.PMC(I,J)) GOTO 2015
       IF(I.LE.LL.AND.J.LE.MM) THEN
       LL=I
       MM=J
       ENDIF
 2015  CONTINUE
       WRITE (IUNIT,*) 'BOILXY IS THE NEXT',LL,MM
 210   CONTINUE
       RETURN
C-------------------------------------------------------------------     --
       ENTRY PHI
C IN THIS PROBLEM GAM AND ALAM ARE FUNCTION OF MC
       IF(NF.EQ.1) THEN
COME HERE TO CALCULATE THE CAPILLARY PRESSURE AS FUNCTION OF MC
       DO 3011 I=1,L1
       DO 3011 J=1,M1
       ADV(I,J)=EXP(-46.49+0.2618*(273+TEM(I,J))-5.0104*(273.+
    1  TEM(I,J))**2/10000.+3.4712*(273+TEM(I,J))**3/10000000.)/1000.
       IF(PO(I,J).LT.PMC(I,J)) ADV(I,J)=0
       IF(CMC(I,J).LE.38) GOTO 3002
       PC(I,J)=10000*((0.01*G*CMC(I,J)-
```

```
     1   0.3*G)/(1-G*0.967))**0.61
 3002    IF(CMC(I,J).LE.38) THEN
         PC(I,J)=10000*((0.01*G*38-
     1   0.3*G)/(1-G*0.967))**0.61
C PC IN PASCAL
         ENDIF
 3011    CONTINUE
         DO 3009 I=2,L2
         DO 3009 J=2,M2
COME HERE TO CALCULATE THE PERMEABILITY OF GAS AND LIQUID
C FOR GAS      PEG IN DARCY
         PEG(I,J)=59*(1-G*(0.667+0.01*CMC(I,J)))/(1-0.967*G)
         PEL(I,J)=139*COS(3.14/2*(0.01*G*(CMC(I,J)
     1   -30)/(1-G*0.967)-0.1)/(1-0.1))
         IF(CMC(I,J).LT.38) PEL(I,J)=0
 3009    CONTINUE
         DO 3012 I=2,L2
         DO 3012 J=2,M2
         DML(I,J)=0
         DML(I,J)=-(9.87/1000000000.*YCV(J)*100.*
     1   ((-PC(I+1,J)-(-PC(I,J)))*PEL(I,J)-
     1   ((-PC(I,J))-(-PC(I-1,J)))*PEL(I-1,J))*10/XCV(I))
         IF(I.EQ.L2) DML(I,J)=-(PEL(I-1,J)*
     1   9.87/1000000000.*YCV(J)*100.*
     1   (-((-PC(I,J))-(-PC(I-1,J))))*10./XCV(I))
 3012    CONTINUE
         DO 301 I=2,L2
         DO 301 J=2,M2
         GAMX(I,J)=(G*(4.8+0.125*CMC(I,J))+0.57)
     1   *4.18*3600
         GAMY(I,J)=GAMX(I,J)/2.5
         ALAM(I,J)=(0.01*CMC(I,J)+0.324)/(1.+0.01*CMC(I,J))
     1   *4.180*G*(1.+0.01*CMC(I,J))
         IF(PO(I,J).GE.PMC(I,J)) THEN
         MB(I,J)=1
```

```
      DMV(I,J)=-(-PEG(I,J)*9.87/9.92/10000.*ADV(I,J)*(PMC(I+1,J)-
     1  PMC(I,J))/XCV(I)*YCV(J)-PEG(I,J)/4.9/100000000*
     2  9.87/9.92/10000.*ADV(I,J)*(PMC(I,J+1)-PMC(I,J))
     3  /YCV(J)*XCV(I))+(
     4  -PEG(I,J)*9.87/9.92/10000.*ADV(I-1,J)*(PMC(I,J)-
     5  PMC(I-1,J))/XCV(I)*YCV(J)- PEG(I,J)/4.9/100000000*
     6  9.87/9.92/10000.*ADV(I,J-1)*(PMC(I,J)-PMC(I,J-1))
     7  /YCV(J)*XCV(I))
      ENDIF
      IF(I.EQ.L2) THEN
      DMV(I,J)=PEG(I,J)*9.87/9.92/10000.*ADV(I,J)*((PMC(I+1,J)-
     1  PMC(I,J))/XCV(I)*2+(-PMC(I,J)
     2  +PMC(I-1,J))/XCV(I)*YCV(J))+ PEG(I,J)/4.9/100000000*
     3  9.87/9.92/10000.*ADV(I,J)*(
     4  (PMC(I,J+1)-2.*PMC(I,J)+PMC(I,J-1)
     5  )/YCV(J)*XCV(I))
      ENDIF
      DM(I,J)=DMV(I,J)+DML(I,J)
      AHV(I,J)=1650.+4.02*(273.+TEM(I,J))-
     1  3.43*(273.+TEM(I,J))**2/1000
C AHV IS ENTHALPY IN J/G
C WE NEED TO SEPARATE THE STEAM AND WATER HOWEVER WATER ENTHOPY IS MIN
      SC(I,J)=(-DM(I,J)*250.91+DML(I,J)*4.18*TEM(I,J)
     1  +DMV(I,J)*AHV(I,J))/(XCV(I)*YCV(J))*3600.
      IF(I.EQ.L2) THEN
      SC(I,J)=(-DM(I,J)*250.91+DML(I,J)*4.18*TEM(I,J)
     1  +(DMV(I,J)-DML(I,J))*AHV(I,J))/(XCV(I)*YCV(J))*3600.
      ENDIF
 301   CONTINUE
      ENDIF
      IF (NF.EQ.2) THEN
      DO 302 I=2,L2
      DO 302 J=2,M2
C THE VISCOSITY IS AIR VISCOSITY
      GAMX(I,J)=PEG(I,J)*9.87/18100.*3600
```

```
      GAMY(I,J)=GAMX(I,J)/4.9/100000000
      ALAM(I,J)=(1-G*(0.667+0.01*CMC(I,J)))/PMC(I,J)
 302  CONTINUE
COME HERE TO CONTROL THE PRESSURE IN THE BOILING REGION.
      DO 387 I=1,L1
      DO 387 J=1,M1
      PO(I,J)=101325./76*87500000*EXP(-10400/2./(TEM(I,J)
     1 +273.))
      IF(MB(I,J).EQ.1) PMC(I,J)=PO(I,J)
 387  CONTINUE
      DO 388 I=2,L2
      DO 388 J=2,M2
      IF(PO(I,J).GE.PMC(I,J)) THEN
      PMC(I,J)=PO(I,J)
      IF(CMC(I,J).LT.30.) THEN
      PMC(I,J)=PO(I,J)*(((1-1800/CMC(I,J)/
     1 (1417-9.43*(TEM(I,J)+273)+1.853/100*(TEM(I,J)+273)**2))/
     2 2/(-0.1722+4.732/1000*(TEM(I,J)+273)-5.553/1000000*
     3 (TEM(I,J)+273)**2))-(1+1800/CMC(I,J)/
     4 (1417-9.43*(TEM(I,J)+273)+1.853/100*(TEM(I,J)+273)**2))/
     5  2/(-0.1722+4.732/1000*(TEM(I,J)+273)-5.553/1000000*
     6 (TEM(I,J)+273)**2)/(-45.7+0.3216*(TEM(I,J)+273)-5.012/
     7 10000*(TEM(I,J)+273)**2)+((((1-1800/CMC(I,J)/
     8 (1417-9.43*(TEM(I,J)+273)+1.853/100*(TEM(I,J)+273)**2))/
     9 2/(-0.1722+4.732/1000*(TEM(I,J)+273)-5.553/1000000*
     1 (TEM(I,J)+273)**2))-(1+1800/CMC(I,J)/
     2 (1417-9.43*(TEM(I,J)+273)+1.853/100*(TEM(I,J)+273)**2))/
     3  2/(-0.1722+4.732/1000*(TEM(I,J)+273)-5.553/1000000*
     4 (TEM(I,J)+273)**2)/(-45.7+0.3216*(TEM(I,J)+273)-5.012/
     5 10000*(TEM(I,J)+273)**2))**2+1/(
     6 -45.7+0.3216*(TEM(I,J)+273)-5.012/10000*(TEM(I,J)+273)**2)/
     7 (-0.1722+4.732/1000*(TEM(I,J)+273)-5.553/1000000*
     8 (TEM(I,J)+273)**2)**2)**0.5)
      ENDIF
      GAM(I,J)=10**15.
```

```
      M=10**20
      SC(I,J)=M*PMC(I,J)
      SP(I,J)=-M
      ENDIF
  388 CONTINUE
      ENDIF
COME HERE TO SPECIFY BOUNDARY CONDITION
      IF(NF.EQ.1) THEN
      DO 310 I=2,L2
      KBCJ1(I)=2
      KBCM1(I)=2
  310 CONTINUE
      DO 320 J=2,M2
      KBCI1(J)=2
      KBCL1(J)=2
  320 CONTINUE
      ENDIF
      IF (NF.EQ.2) THEN
      DO 330 I=2,L2
      KBCJ1(I)=2
      KBCM1(J)=1
      PMC(I,M1)=PINF
  330 CONTINUE
      DO 340 J=2,M2
      KBCI1(J)=2
      KBCL1(J)=1
      PMC(L1,J)=PINF
  340 CONTINUE
      ENDIF
      RETURN
      END

C=================================================
```

Nomenclature

ADV: density of vapor

AHV: enthalpy of vapor

AMC: averaged moisture content

CMC: moisture content

DM: amount of moisture removal

DMC: difference of moisture content

DML: liquid water transferred

DMV: water vapor transferred

G: specific gravity

HE: heat transfer coefficient

LL, MM: boiling front determinant

MB: boiling region indicator

PC: capillary pressure

PEG: gas permeability

PEL: liquid permeability

PINF: ambient pressure

PMC: pressure

PMCO: initial pressure

PO: saturation pressure

TEM: temperature

TEMO: initial temperature

TINF: ambient temperature

Appendix B

This appendix describes the several steps from equation 8.6 to equation 8.7. Equation 8.6 is as follow,

$$\frac{dE}{dt} + h_e \dot{m}_e - h_i \dot{m}_i = \dot{Q}_i - \dot{Q}_e \text{.....} A.1$$

where dE consists of internal energy differences of dry wood and water inside wood.

$$dE = dE_{dw} + dE_{wa} \text{.....} A.2$$

where dE_{dw} is the internal energy difference of dry wood in dt interval, dE_{wa} is the internal energy difference of water in dt interval.

$$dE_{dw} = c_{dw} \times m_{dw} \times (T_2 - T_1) \text{.....} A.3$$

where c_{dw} is specific heat of dry wood, m_{dw} is mass of dry wood. T_2 and T_1 are temperatures of water before and after dt interval.

$$dE_{wa} = m_2 \times c_w \times T_2 - m_1 \times c_w \times T_1 \text{.....} A.4$$

where m_2 and m_1 are masses of water before and after dt time, c_w specific heat of water.

$$m_2 = m_1 + dm \text{.....} A.5$$

where dm is weight loss during dt time interval.

$$dE_{wa} = m_1 \times c_w \times T_2 - m_1 \times c_w \times T_1 + c_w \times T_2 \times dm \ldots\ldots A.6$$

Let

$$u = c_w \times T_2 \ldots\ldots A.7$$

which is the internal energy of water.

Substitute equation A.3 and A.6 into equation A.1, then,

$$dE = c_{dw} \times m_{dw} \times (T_2 - T_1) + m_1 \times c_w \times T_2 - m_1 \times c_w \times T_1 + u \times dm \ldots\ldots A.8$$

which can be written as,

$$dE = c \times m \times dT + u \times dm \ldots\ldots A.9$$

where c is specific heat of moist wood and m is the mass of moist wood.

In the control volume, the weight of wood can be calculated as,

$$m = \rho \times dx \times dy \ldots\ldots A.10$$

where ρ is the density of wood.

where Q_i is energy transferred by heat conduction into the control volume. Q_{ix} and Q_{iy} are energy

$$\dot{Q}_i = \dot{Q}_{ix} + \dot{Q}_{iy} \ldots\ldots A.11$$

transferred into the control volume by through x and y directions respectively (see Figure 8.1) .

$$\dot{Q}_e = \dot{Q}_{ex} + \dot{Q}_{ey} \text{.....} A.12$$

where Q_e is energy transferred by heat conduction out of the control volume. Q_{ex} and Q_{ey} are energy transferred out of the control volume by through x and y directions respectively (see Figure 8.2).

$$\dot{Q}_{ix} = -\kappa_l \frac{dT}{dx}\Big|_x dy \text{.....} A.13$$

$$\dot{Q}_{ex} = -\kappa_l \frac{dT}{dx}\Big|_{x+dx} dy \text{.....} A.14$$

$$\dot{Q}_{iy} = -\kappa_t \frac{dT}{dy}\Big|_y dx \text{.....} A.16$$

$$\dot{Q}_{ey} = -\kappa_t \frac{dT}{dy}\Big|_{y+dy} dx \text{.....} A.17$$

so

$$\dot{Q}_i = -\kappa_l \frac{dT}{dx}\Big|_x dy - \kappa_t \frac{dT}{dy}\Big|_y dx \text{.....} A.18$$

and

$$\dot{Q}_e = -\kappa_l \frac{dT}{dx}\Big|_{x+dx} dy - \kappa_t \frac{dT}{dy}\Big|_{y+dy} dx \text{.....} A.19$$

$$\dot{Q}_i - \dot{Q}_e = \kappa_l \frac{dT}{dx}\Big|_{x+dx} dy - \kappa_l \frac{dT}{dx}\Big|_x dy + \kappa_t \frac{dT}{dy}\Big|_{y+dy} dx - \kappa_t \frac{dT}{dy}\Big|_y dx \text{.....} A.20$$

Equation A.8 and A.20 are substituted into equation A.1, then both sides of equation are divided by dxdy.

$$\lambda \frac{\partial T}{\partial t} = \kappa_l \times \frac{\partial^2 T}{\partial x^2} + \kappa_t \times \frac{\partial^2 T}{\partial y^2} - \frac{dmu}{dtdxdy} - \frac{h_e \dot{m}_e - h_i \dot{m}_i}{dxdy} \text{.....} A.21$$

17. Vita

The author, Chen Zhangjing, was born in Fujian Province, P.R. China, on October 7, 1963. After receiving a bachelor degree in Department of Forest Products of Fujian Forestry College in 1983, he worked as a technician in the Fujian Lumber Corporation. From 1985 to 1988, he was a graduate student in the Northeast Forestry University, Harbin, P.R. China, majoring in wood drying. After receiving Master Degree in 1988, he was employed as a researcher in Shanghai Wood Industry Research Institute. In 1990, he was enrolled as a graduate student at Department of Wood Science and Forest Products at Virginia Tech. He completed Master Degree in 1993 and began pursuing Ph. D. Degree since 1994.